IN-24
142844
P.102

NASA Contractor Report 191055

Geometrically Nonlinear Analysis of Laminated Elastic Structures

J.N. Reddy, K. Chandrashekhara, and W.C. Chao
Virginia Polytechnic Institute and State University
Blacksburg, Virginia

January 1993

Prepared for
Lewis Research Center
Under Grant NAG3–208

(NASA-CR-191055) GEOMETRICALLY NONLINEAR ANALYSIS OF LAMINATED ELASTIC STRUCTURES (Virginia Polytechnic Inst. and State Univ.) 102 p

N93-17924

Unclas

G3/24 0142844

National Aeronautics and Space Administration

Table of Contents

Part 1: Geometrically Nonlinear Analysis of Laminated Shells Including Transverse Shear Strains by J. N. Reddy and K. Chandrashekhara

Summary; Introduction; A Review of Governing Equations; Finite Element Model; Numerical Results; Conclusions; References; Appendix.

Part 2: Analysis of Laminated Composite Shells Using a Degenerated 3-D Element by W. C. Chao and J. N. Reddy

Summary; Introduction; Incremental, Total-Lagrangian Formulation of a Contiuous Medium; Finite Element Model; Discussion of the Numerical Results; References.

Part 3: Nonlinear Material Models for Composite Plates and Shells by K. Chandrashekhara and J. N. Reddy

Summary; Introduction; Material Model; Finite Element Formulation; Numerical Results; Conclusions; References.

PRECEDING PAGE BLANK NOT FILMED

GEOMETRICALLY NONLINEAR ANALYSIS OF LAMINATED ELASTIC STRUCTURES

J.N. Reddy, K. Chandrashekhara, and W.C. Chao
Virginia Polytechnic Institute and State University
Blacksburg, Virginia 24061

ABSTRACT

This final technical report contains three parts: Part 1 deals with the 2-D shell theory and its element formulation and applications. Part 2 deals with the 3-D degenerated element. These two parts constitute the two major tasks that were completed under the grant. Another related topic that was initiated during the present investigation is the development of a nonlinear material model. This topic is briefly discussed in Part 3. To make each part self-contained, conclusions and references are included in each part. In the interest of brevity, the discussions presented here are relatively brief. The details and additional topics are described in the references cited.

PART 1

GEOMETRICALLY NONLINEAR ANALYSIS OF LAMINATED SHELLS INCLUDING TRANSVERSE SHEAR STRAINS

J. N. Reddy and K. Chandrashekhara[+]

(A condensed version of this paper is to appear in AIAA Journal, 1984)

SUMMARY

The paper contains a description of a doubly curved shell finite element for geometrically nonlinear (in the von Karman sense) analysis of laminated (doubly-curved) composite shells. The element is based on an extension of the Sanders shell theory and accounts for the von Karman strains and transverse shear strains. The numerical accuracy and convergence characteristics of the element are further evaluated by comparing the present results for the bending of isotropic and orthotropic plates and shells with those available in the literature. The many numerical results presented here for the geomertically nonlinear analysis of laminated composite shells should serve as reference for future investigations.

INTRODUCTION

Laminated shells are finding increased application in aerospace, automobile and petrochemical industries. This is primarily due to the high stiffness to weight ratio, high strength to weight ratio, and less machining and maintenance costs associated with composite structures. However, the analysis of composite structures is more complicated when compared to metallic structures, because laminated composite structures are anisotropic and characterized by bending-stretching coupling. Further, the classical shell theories, which are based on the Kirchhoff-Love kinematic hypothesis (see Naghdi [1] and

[+] Graduate research assistant

Bert [2]) are known to yield deflections and stresses in laminated shells that are as much as 30% in error. This error is due to the neglect of transverse shear strains in the classical shell theories.

Refinements of the classical shell theories (e.g., Love's first approximation theory [3]) for shells to include transverse shear deformation have been presented by Reissner [4-6]. Sanders [7] presented modified first- and second-approximation theories that removed an inconsistency (nonvanishing of a small rigid-body rotations of the shell) existed in Love's first-approximation theory.

The first thin shell theory of laminated orthotropic composite shells is due to Ambartsumyan [8,9]. In these works Ambartsumyan assumed that the individual orthotropic layers were oriented such that the principal axes of material symmetry coincided with the principal coordinates of the shell reference surface. Dong, Pister, and Taylor [10] presented an extension of Donnell's shallow shell theory [11] to thin laminated shells. Using the asymptotic integration of the elasticity equations, Widera and Chung [12] derived a first-approximation theory for the unsymmetric deformation of nonhomogeneous, anisotropic, cylindrical shells. This theory, when specialized to isotropic materials, reduces to Donnell's shell theory.

The effects of transverse shear deformation and thermal expansion through the shell thickness were considered by Zukas and Vinson [13]. Dong and Tso [14] constructed a laminated orthotropic shell theory that includes transverse shear deformation. This theory can be regarded as an extension of Love's first-approximation theory [3] for homogeneous isotropic shells. Other refined theories, specialized to anisotropic cylindrical shells, were presented by Whitney and Sun [15], and Widera and Logan [16,17].

The finite-element analysis of layered anisotropic shells, all of which are concerned with bending, stability, or vibration of shells, can be found in the works of Schmit and Monforton [18], Panda and Natarajan [19], Shivakumar and Krishna Murty [20], Rao [21], Siede and Chang [22], Hsu, Reddy, and Bert [23], Reddy [24], and Venkatesh and Rao [25,26]. Recently, Reddy [27] extended the Sanders theory to account for the transverse shear strains, and presented exact solutions for simply supported cross-ply laminated shells. All of these studies are limited small displacement theories and static analyses.

In the present paper, an extension of the Sanders shell theory that accounts for the shear deformation and the von Karman strains in laminated anisotropic shells is used to develop a displacement finite element model for the bending analysis of laminated composite shells. The accuracy of the element is evaluated by comparing the results obtained in the present study for isotropic and orthotropic plate and shell problems with those available in the literature. Numerical results for bending analysis of cylindrical and doubly-curved shells are presented, showing the effect of radius-to-thickness ratio, loading, and boundary conditions on the deflections and stresses.

A REVIEW OF THE GOVERNING EQUATIONS

Consider a laminated shell constructed of a finite number of uniform-thickness orthotropic layers, oriented arbitrarily with respect to the shell coordinates (ξ_1,ξ_2,ζ). The orthogonal curvilinear coordinate system (ξ_1,ξ_2,ζ) is chosen such that the ξ_1- and ξ_2- curves are lines of curvature on the midsurface $\zeta=0$, and ζ-curves are straight lines perpendicular to the surface $\zeta=0$ (see Fig. 1). A line element of the shell is given by (see Reddy [27]

$$(dS)^2 = [(1 + \zeta/R_1)\alpha_1 d\xi_1]^2 + [(1 + \zeta/R_2)\alpha_2 d\xi_2]^2 + (d\zeta)^2 \qquad (1)$$

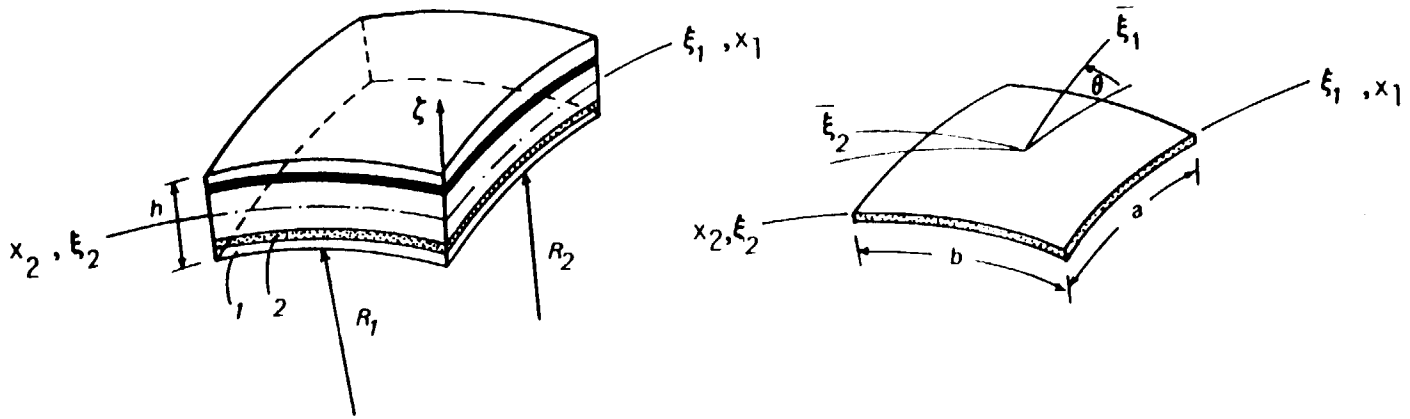

Figure 1 The geometry and notation for a laminated doubly curved shell

where α_i and R_i $(i = 1,2)$ are the surface metrics and radii of curvature, respectively. In general, α_i and R_i are functions of ξ_i only. For the doubly curved shells considered in the present theory, α_i and R_i are constant.

The strain-displacement equations of the shear deformable theory of doubly-curved shells are given by

$$\begin{aligned} \varepsilon_1 &= \varepsilon_1^0 + \zeta\kappa_1 \\ \varepsilon_2 &= \varepsilon_2^0 + \zeta\kappa_2 \\ \varepsilon_4 &= \varepsilon_4^0 \\ \varepsilon_5 &= \varepsilon_5^0 \\ \varepsilon_6 &= \varepsilon_6^0 + \zeta\kappa_6 \end{aligned} \tag{2}$$

where

$$\varepsilon_1^0 = \frac{\partial u_1}{\partial x_1} + \frac{u_3}{R_1} + \frac{1}{2}\left(\frac{\partial u_3}{\partial x_1}\right)^2 , \quad \kappa_1 = \frac{\partial \phi_1}{\partial x_1}$$

$$\varepsilon_2^0 = \frac{\partial u_2}{\partial x_2} + \frac{u_3}{R_2} + \frac{1}{2}\left(\frac{\partial u_3}{\partial x_2}\right)^2 , \quad \kappa_2 = \frac{\partial \phi_2}{\partial x_2}$$

$$\varepsilon_6^0 = \frac{\partial u_1}{\partial x_2} + \frac{\partial u_2}{\partial x_1} + \frac{\partial u_3}{\partial x_1}\frac{\partial u_3}{\partial x_2} , \quad \kappa_6 = \frac{\partial \phi_1}{\partial x_2} + \frac{\partial \phi_2}{\partial x_1} + c_o\left(\frac{\partial u_2}{\partial x_1} - \frac{\partial u_1}{\partial x_2}\right)$$

$$\varepsilon_4^0 = \phi_2 + \frac{\partial u_3}{\partial x_2} - \frac{u_2}{R_2}$$

$$\varepsilon_5^0 = \phi_1 + \frac{\partial u_3}{\partial x_1} - \frac{u_1}{R_1}$$

$$c_o = \frac{1}{2}\left(\frac{1}{R_2} - \frac{1}{R_1}\right) \tag{3}$$

Here u_i denotes the displacements of the reference surface along $\xi_i (\xi_3 = \zeta)$ axes, and ϕ_i are the rotations of the transverse normals to the reference surface. In Love's first-approximation theories the parameter c_o is taken to be zero, and it is introduced only in the Sanders theory.

The stress-strain relations, transformed to the shell coordinates, are of the form

$$\{\sigma\} = [Q]\{\varepsilon\} \tag{4}$$

where $Q_{ij}^{(k)}$ are the material properties of k-th layer.

The principle of virtual work for the present problem is given by

$$0 = \sum_{k=1}^{L} \int_{\zeta_{k-1}}^{\zeta_k} \int_{\Omega} \{\sigma_1^{(k)}\delta\varepsilon_1 + \sigma_2^{(k)}\delta\varepsilon_2 + \sigma_6^{(k)}\delta\varepsilon_6 + \sigma_4^{(k)}\delta\varepsilon_4 + \sigma_5^{(k)}\delta\varepsilon_5 - q\delta u_3\}\alpha_1\alpha_2 d\xi_1 d\xi_2 d\zeta \tag{5}$$

$$= \int_{\Omega} [N_1\delta\varepsilon_1^0 + N_2\delta\varepsilon_2^0 + N_6\varepsilon_6^0 + M_1\delta\kappa_1 + M_2\delta\kappa_2 + M_6\delta\kappa_6 + Q_1\delta\varepsilon_5^0 + Q_2\delta\varepsilon_4^0 - q\delta u_3]\alpha_1\alpha_2 d\xi_1 d\xi_2 \tag{6}$$

where q is the distributed transverse load, N_i and M_i are the stress and moment resultants, and Q_i is the shear force resultant:

$$(N_i, M_i) = \sum_{k=1}^{L} \int_{\zeta_{k-1}}^{\zeta_k} \sigma_i(1,\zeta)d\zeta \quad , \quad i = 1,2,6$$

$$Q_i = \sum_{k=1}^{L} K_i^2 \int_{\zeta_{k=1}}^{\zeta_k} \sigma_i d\zeta \quad , \quad i = 4,5, \tag{7}$$

where K_i (i = 1,2) are the shear correction factors (taken to be $K_1^2 = K_2^2 = 5/6$), and (ζ_{k-1},ζ_k) are the ζ-coordinates of the k-th layer, and L is the total number of layers in the laminated shell.

It is informative to note that the equations of equilibrium can be derived from Eq. (6) by integrating the displacement gradients in ε_i^0 by parts

and setting the coefficients of δu_i ($i = 1,2,3$) and $\delta \phi_i$ ($i=1,2$) to zero separately. We obtain [with $c_o = \frac{1}{2}\left(\frac{1}{R_2} - \frac{1}{R_1}\right)$ and $dx_i = \alpha_i d\xi_i$]

$$\frac{\partial N_1}{\partial x_1} + \frac{\partial}{\partial x_2}(N_6 - c_o M_6) + \frac{Q_1}{R_1} = 0$$

$$\frac{\partial}{\partial x_1}(N_6 + c_o M_6) + \frac{\partial N_2}{\partial x_2} + \frac{Q_2}{R_2} = 0$$

$$\frac{\partial Q_1}{\partial x_1} + \frac{\partial Q_2}{\partial x_2} - \left(\frac{N_1}{R_1} + \frac{N_2}{R_2} - q\right) + N(u_3) = 0$$

$$\frac{\partial M_1}{\partial x_1} + \frac{\partial M_6}{\partial x_2} - Q_1 = 0$$

$$\frac{\partial M_6}{\partial x_1} + \frac{\partial M_2}{\partial x_2} - Q_2 = 0 \tag{8}$$

where

$$N(u_3) = \frac{\partial}{\partial x_1}\left(N_1 \frac{\partial u_3}{\partial x_1} + N_6 \frac{\partial u_3}{\partial x_2}\right) + \frac{\partial}{\partial x_2}\left(N_6 \frac{\partial u_3}{\partial x_1} + N_2 \frac{\partial u_3}{\partial x_2}\right) \tag{9}$$

The resultants (N_i, M_i, Q_i) are related to (ε_i^o, κ_i) ($i,j = 1,2,6$) by

$$\begin{aligned} N_i &= A_{ij}\varepsilon_j^o + B_{ij}\kappa_j \\ M_i &= B_{ij}\varepsilon_j^o + D_{ij}\kappa_j \end{aligned} \tag{10}$$

$$\begin{aligned} Q_2 &= A_{44}\varepsilon_4^o + A_{45}\varepsilon_5^o \\ Q_1 &= A_{45}\varepsilon_4^o + A_{55}\varepsilon_5^o \end{aligned} \tag{11}$$

Here A_{ij}, B_{ij} and D_{ij} ($i,j = 1,2,6$) denote the extensional, flexural-extensional coupling, and flexural stiffnesses of the laminate:

$$(A_{ij}, B_{ij}, D_{ij}) = \sum_{k=1}^{L} \int_{\zeta_{k-1}}^{\zeta_k} Q_{ij}^{(k)} (1, \zeta, \zeta^2) d\zeta \quad (i,j = 1,2,6) \tag{12}$$

$$(A_{44},A_{45},A_{55}) = \sum_{k=1}^{L} \int_{\zeta_{k-1}}^{\zeta_k} (K_1^2 Q_{44}^{(k)}, K_1 K_2 Q_{45}^{(k)}, K_2^2 Q_{55}^{(k)}) d\zeta$$

The boundary conditions, derived from the virtual work statement, involve specifying either the essential boundary conditions (EBC) or the natural boundary conditions (NBC):

EBC		NBC
u_1	or	$N_1 n_1 + (N_6 - c_o M_6) n_2$
u_2	or	$N_2 n_2 + (N_6 + c_o M_6) n_2$
u_3	or	$(N_1 \frac{\partial u_3}{\partial x_1}) n_1 + (N_2 \frac{\partial u_3}{\partial x_2}) n_2 + (N_6 \frac{\partial u_3}{\partial x_2}) n_1 + (N_6 \frac{\partial u_3}{\partial x_1}) n_2 + Q_2 n_2 + Q_1 n_1$
ϕ_1	or	$M_1 n_1 + M_6 n_2$
ϕ_2	or	$M_2 n_2 + M_6 n_1$

(13)

where (n_1,n_2) denote the direction cosines of the unit normal on the boundary of the midsurface of the shell.

The exact form of the spatial variation of the solution of Eqs. (8)-(13), for the small-displacement theory, can be obtained under the following conditions (see Reddy [27]):

(i) Symmetric or antisymmetric cross-ply laminates: i.e., laminates with

$$A_{16} = A_{26} = B_{16} = B_{26} = D_{16} = D_{26} = A_{45} = 0. \tag{14}$$

(ii) Freely supported boundary conditions:

$$N_1(0,x_2) = N_1(a,x_2) = M_1(0,x_2) = M_1(a,x_2) = 0$$
$$u_3(0,x_2) = u_3(a,x_2) = u_2(0,x_2) = u_2(a,x_2) = 0$$

$$N_2(x_1,0) = N_2(x_1,b) = M_2(x_1,0) = M_2(x_1,b) = 0$$
$$u_3(x_1,0) = u_3(x_1,b) = u_1(x_1,0) = u_1(x_1,b) = 0$$
$$\phi_2(0,x_2) = \phi_2(a,x_2) = \phi_1(x_1,0) = \phi_1(x_1,b) = 0 \qquad (15)$$

where a and b are the dimensions of the shell middle surface along the x_1 and x_2 axes, respectively. The time variation of the load does not influence the spatial form of the solution.

Note that the exact solution can be obtained only for cross-ply laminated shells with simply supported boundary conditions. For general lamination schemes, exact solutions are not available to date.

FINITE-ELEMENT MODEL

A typical finite element is a doubly-curved shell element in the x_1x_2-surface. Over the typical shell element $\Omega^{(e)}$, the displacements $(u_1,u_2,u_3,\phi_1,\phi_2)$ are interpolated by expressions of the form,

$$u_i = \sum_{j=1}^{N} u_i^j \psi_j(x_1,x_2) \quad , \quad i = 1,2,3$$

$$\phi_i = \sum_{j=1}^{N} \phi_i^j \psi_j(x_1,x_2) \quad , \quad i = 1,2 \qquad (16)$$

where ψ_j are the interpolation functions, and u_i^j and ϕ_i^j are the nodal values of u_i and ϕ_i, respectively. For a linear isoparametric element (N = 4) this interpolation results in a stiffness matrix of order 20 by 20. For a nine-node quadratic element the element stiffness matrix is of order 45 by 45.

Substitution of Eq. (21) into the virtual work principle, Eq. (9) yields an element equation of the form

$$[K(\Delta)]\{\Delta\} = \{F\} \tag{17}$$

where $\{\Delta\} = \{\{u_1\}, \{u_2\}, \{u_3\}, \{\phi_1\}, \{\phi_2\}\}^T$, $[K]$ the element stiffness matrix, and $\{F\}$ is the force vector. In the interest of brevity, the coefficients of the stiffness matrices are included in Appendix I.

The element equations (17) can be assembled, boundary conditions can be imposed, and the resulting equations can be solved at each load step. Note that the stiffness matrix $[K]$ is a function of the unknown solution vector $\{\Delta\}$; therefore, an iterative solution procedure is required for each load step. In the present study, we used the direct iteration technique, which can be expressed as

$$[K(\{\Delta\}^r)]\{\Delta\}^{r+1} = \{F\} \tag{18}$$

where $\{\Delta\}^r$ denotes the solution vector obtained in the r-th iteration (at any given load step). At the beginning of the first load step, we assume that $\{\Delta\}^0 = \{0\}$ and obtain the linear solution at the end of the first iteration. The solution obtained at the end of the r-th iteration is used to compute the stiffness matrix for the (r+1)-th iteration. At the end of each iteration (for any load step), the solutions obtained in two consecutive iterations are compared to see if they are close enough to terminate the iteration and to move on to the next load step. The following convergence criterion is used in the present study:

$$\left[\sum_{i=1}^{N} |\Delta_i^r - \Delta_i^{r+1}|^2 \Big/ \sum_{i=1}^{N} |\Delta_i^r|^2 \right]^{1/2} < 0.01 \tag{19}$$

where N is the total number of unknown generalized displacements in the finite element mesh.

To accelerate the convergence, a weighted average of the solution from last two iterations are used to compute the stiffness matrix:

$$[K(\gamma\{\Delta\}^{r-1} + (1 - \gamma)\{\Delta\}^{r})]\{\Delta\}^{r+1} = \{F\} \qquad (20)$$

where γ is the acceleration parameter, $0 \leq \gamma \leq 1$. In the present study a value of 0.25 - 0.35 was used.

NUMERICAL RESULTS

Here we present numerical results for some sample problems. To illustrate the accuracy of the present element, first few examples are taken from the literature on isotropic and orthotropic shells. Then results (i.., deflections and strsses) for several laminated shell problems are presented. The results for laminated shells should serve as references for future investigations.

All of the results reported here were obtained using the double-precision arithmatic on an IBM 3081 processor. Most of the sample problems were analyzed using a 2 x 2 uniform mesh of the nine-node (quadratic) isoparametric rectangular element.

1. Bending of a simply supported plate strip (or, equivalently, a beam) under uniformly distributed load.

The problem is mathematically one-dimensional and an analytical solution of the problem, based on the classical theory, can be found in Timoshenko and Womowsky-Krieger [28]. The plate length along the y-coordinate is assumed to be large compared to the width, and it is simply supported on edges parallel

to the y-axis. The following simply supported boundary conditions are assumed:

$$w = \phi_2 = 0 \text{ along edges } x = \pm 127\text{mm} \qquad (21)$$

All inplane displacement degrees of freedom are restrained. A 5 x 1 mesh of four-node rectangular elements in the half plate is used to analyze the problem. The data and results are presented in Fig. 2. The present result is in good agreement with the analytical solution.

2. Clamped square plate under uniform load.

Due to the biaxial symmetry, only one quadrant of the plate is modelled with the 2 x 2 mesh of nine-node elements (4 x 4 mesh of linear elements give almost the same result). Pertinent data and results are presented in Fig. 3 for side to thickness ratios a/h = 10 and 500. The result for a/h = 500 is in agreement with the results of Way [29]. The difference is attributed to the fact that the present model includes the inplane displacement degrees of freedom and transverse shear deformation.

Figure 4 contains transverse deflection versus load for clamped orthotropic, cross-ply, and angle-ply plates. The lamina properties are

$$E_1 = 25 \times 10^4 \text{ N/mm}^2,\ E_2 = 2 \times 10^4 \text{ N/mm}^2,\ G_{12} = G_{13} = 10^4 \text{ N/mm}^2$$

$$G_{23} = 0.4 \times 10^4 \text{ N/mm}^2,\ \nu_{12} = 0.25.$$

For the same total thickness the clamped orthotropic square plate is stiffer than both two-layer angle-ply and cross-ply plates.

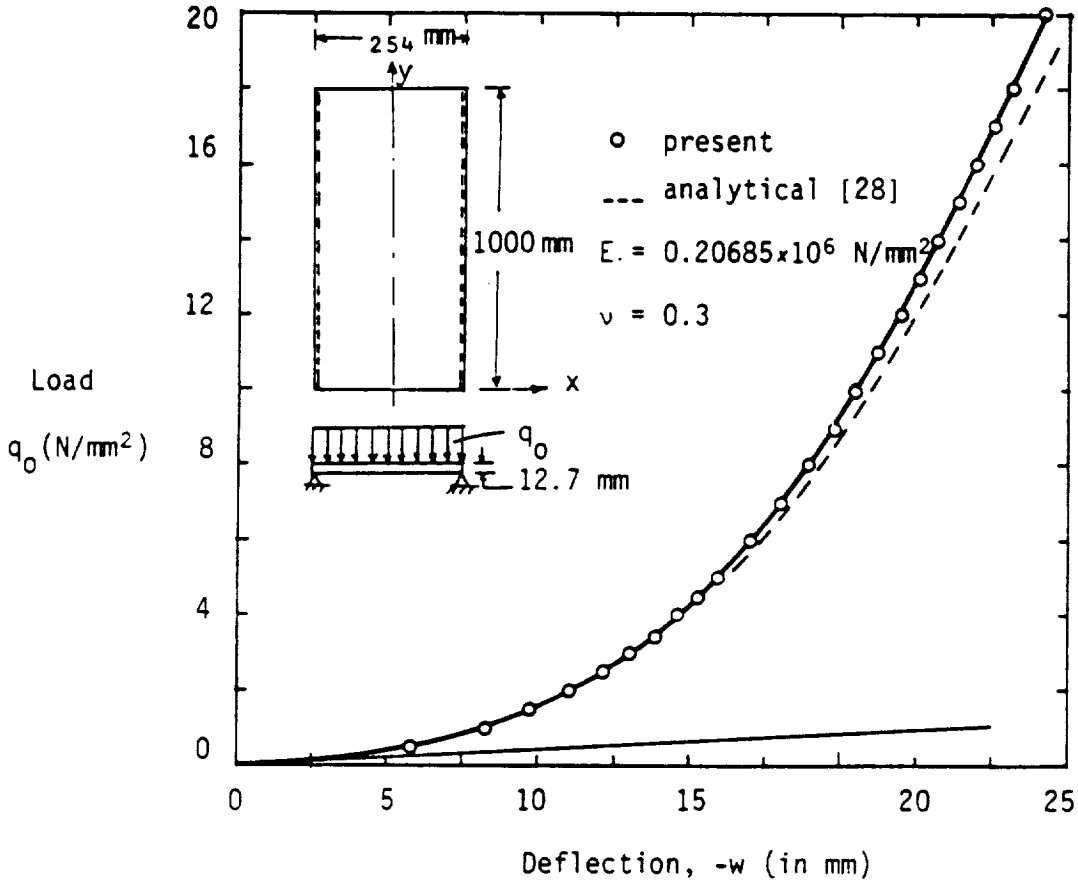

Figure 2. Bending of an isotropic simply supported plate strip under uniform load.

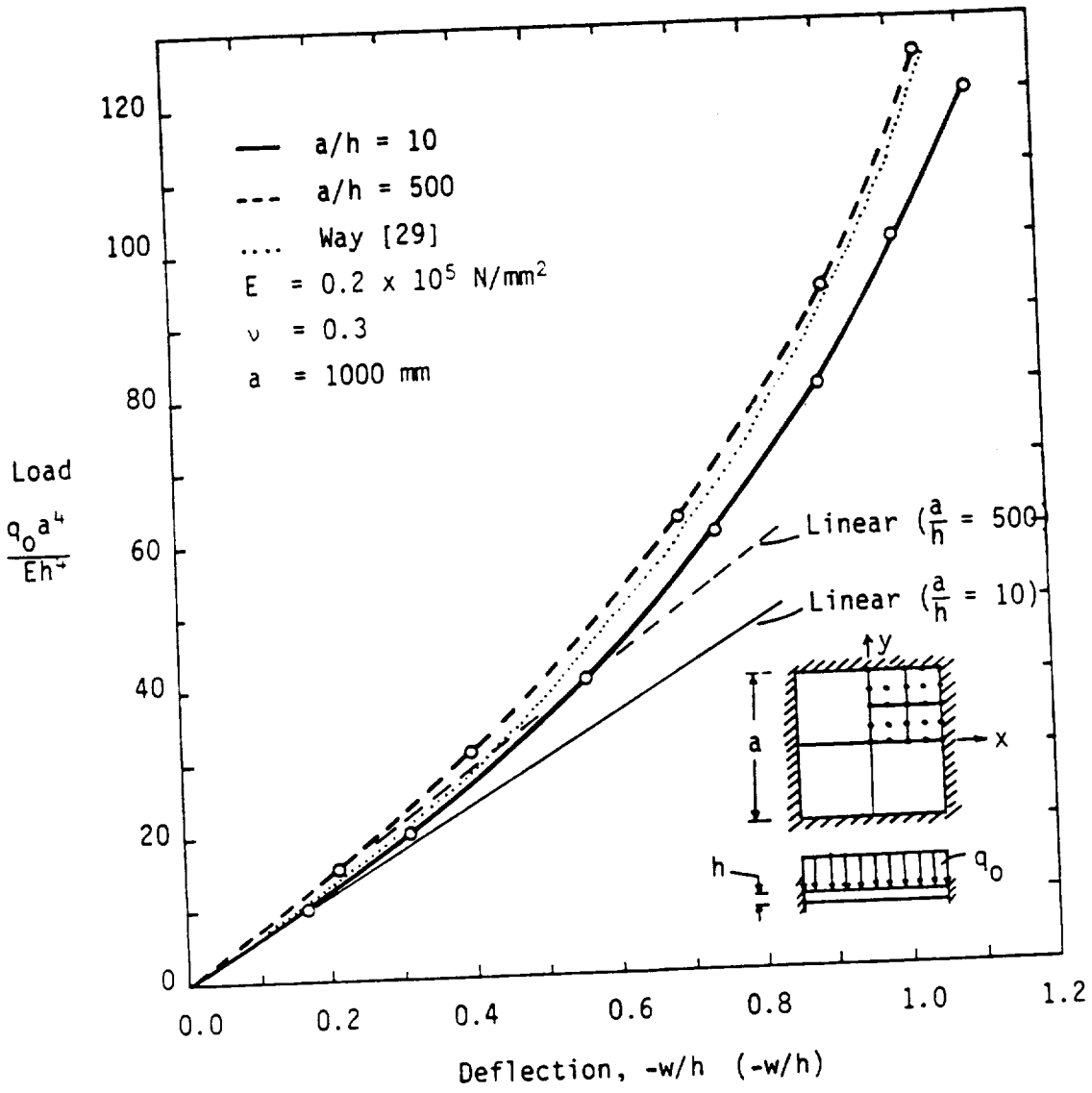

Figure 3. Bending of clamped isotropic square plate under uniform load.

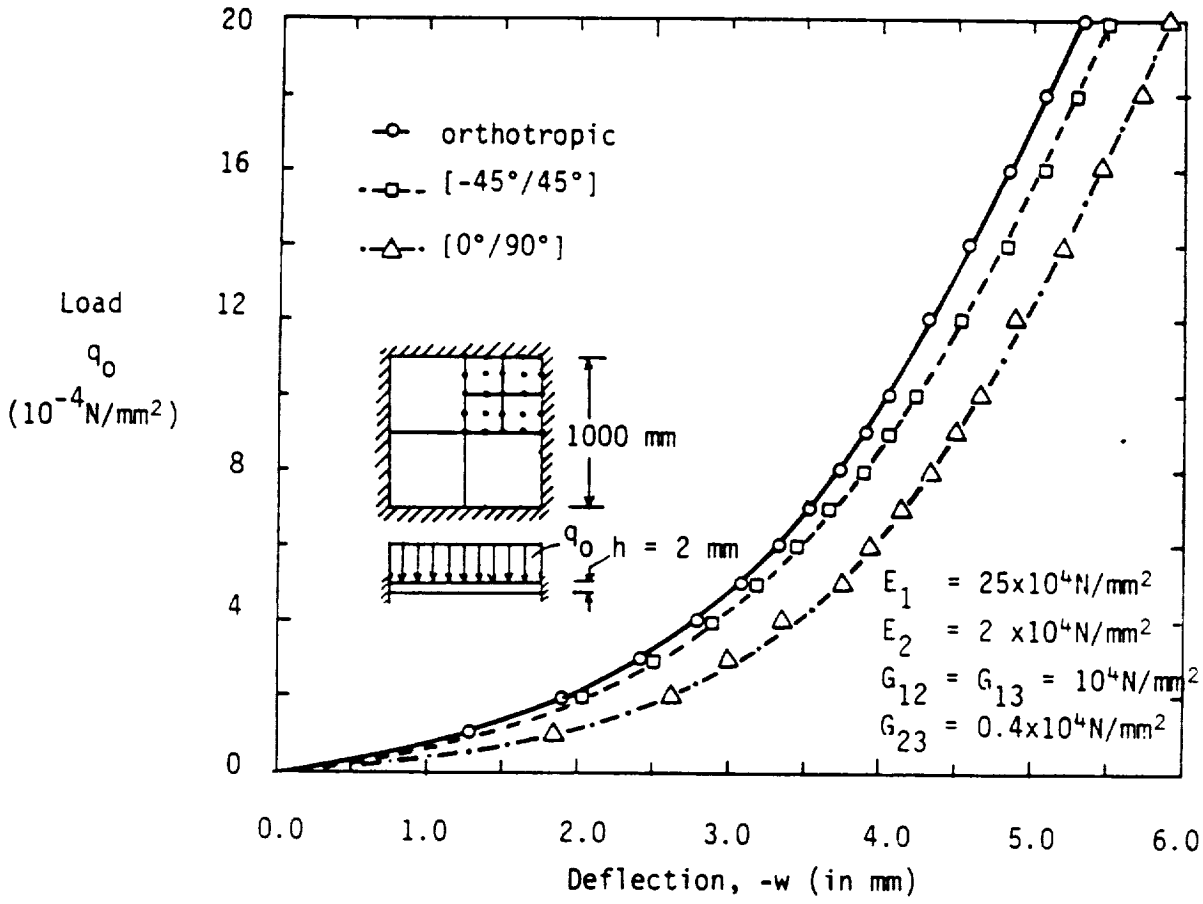

Figure 4. Bending of clamped orthotropic and laminated square plates under uniform load.

3. Simply supported, isotropic spherical shell under point load.

The pertinent data of the shell is shown in Fig. 5. A uniform mesh of 2 by 2 quadratic elements is used in a quadrant. The effect of three types of simply supported conditions on the center deflection and center normal stress is investigated:

$$\begin{aligned}
&\text{SS-1:}\quad u = w = \phi_1 = 0 \quad \text{at } y = b; \quad v = w = \phi_2 = 0 \quad \text{at } x = a \\
&\text{SS-2:}\quad u = v = w = \phi_1 = 0 \quad \text{at } y = b; \quad u = v = w = \phi_2 = 0 \quad \text{at } x = a \\
&\text{SS-3:}\quad v = w = \phi_1 = 0 \quad \text{at } y = b; \quad u = w = \phi_2 = 0 \quad \text{at } x = a
\end{aligned} \tag{22}$$

Table 1 contains the results for the three boundary conditions. It is clear from the results that all three boundary conditions give virtually the same results for a/h = 160, and differ significantly (especially SS-1 differs from both SS-2 and SS-3) for a/h = 16. Thus, the effect is more in thick shells than in thin shells. The stress σ_x shown in Fig. 5 is evaluated at point x = y = 1.691" in the top layer

4. Simply supported isotropic cylindrical shell under point load.

The geometry and finite-element mesh of the shell are shown in Fig. 6. Once again, the effect of various simply supported boundary conditions (22) on the deflections and stresses for the problem is investigated using a uniform mesh of 2 x 2 quadratic elements. The results are presented in Table 2. For the geometry and loading used here (R = 2540, a = 254, h = 12.7), the boundary conditions have very significant effect on the solution. Boundary conditions SS-2 and SS-3 give almost the same results whereas SS-1 gives about 2-1/2 times the deflection given by SS-2 or SS-3 boundary conditions.

Table 1. Effect of various simply supported boundary conditions on the center deflections and normal stress in spherical shells under point load ($E = 10^7$ psi, $\nu = 0.3$).

Load P/h^2	Solution	SS-1		SS-2		SS-3	
		a/h=160	a/h=16	a/h=160	a/h=16	a/h=160	a/h=16
4,000	$-w^*$	0.0155	-	0.0152	-	0.0152	-
	$-\sigma_x$*	893	-	984	-	894	-
8,000	$-w^x$	0.0329	0.0349	0.0324	0.0255	0.0324	0.0258
	$-\sigma_x$	1,880	6,535	1,882	6,015	1,882	6,031
12,000	$-w^x$	0.0529	-	0.0522	-	0.0521	-
	$-\sigma_x$	2,980	-	2,985	-	2,986	-
16,000	$-w^x$	0.0760	0.0793	0.0752	0.0520	0.0751	0.0525
	$-\sigma_x$	4,220	13,230	4.228	12,200	4,229	12,240
20,000	$-w^x$	0.1038	-	0.1028	-	0.1027	-
	$-\sigma_x$	5,657	-	5,671	-	5,672	-
24,000	$-w^x$	0.1364	0.1083	0.1354	0.0792	0.1353	0.0800
	$-\sigma_x$	7,268	20,110	7,289	18,500	7,291	18,550
28,000	$-w^x$	0.1761	-	0.1752	-	0.1751	-
	$-\sigma_x$	9,128	-	9,160	-	9,162	-
32,000	$-w^x$	0.2234	0.1472	0.2227	0.1072	0.2227	0.1083
	$-\sigma_x$	11,180	27,170	11,220	24,930	11,230	25,000

* $w(0,0)$, $\sigma_x(A,A)$; $A = 1.691$

Table 2. Effect of various types of simply supported boundary conditions on the deflections and stresses of anisotropic cylindrical shell under point load.

Load,P (N)	SS-1		SS-2		SS-3	
	-w(mm)	$-\sigma_y$ (N/mm^2)	-w	$-\sigma_y$	-w	$-\sigma_y$
250	2.5804(2)	2.868	0.6544(4)	1.706	0.6698(4)	1.706
500	5.1626(2)	5.713	1.3533(4)	3.478	1.3843(4)	3.477
750	7.7343(2)	8.506	2.1057(4)	5.327	2.1522(4)	5.321
1,000	10.278(2)	11.210	2.9234(4)	7.265	2.9855(4)	7.242
1,250	12.733(2)	13.80	3.8241(4)	9.312	3.9017(4)	9.288
1,500	15.204(2)	16.25	4.8349(4)	11.50	4.9279(4)	11.46
1,750	17.560(2)	18.560	6.0331(5)	13.91	6.1423(5)	13.85
2,000	19.843(2)	20.730	7.5316(6)	16.66	7.6610(6)	16.57

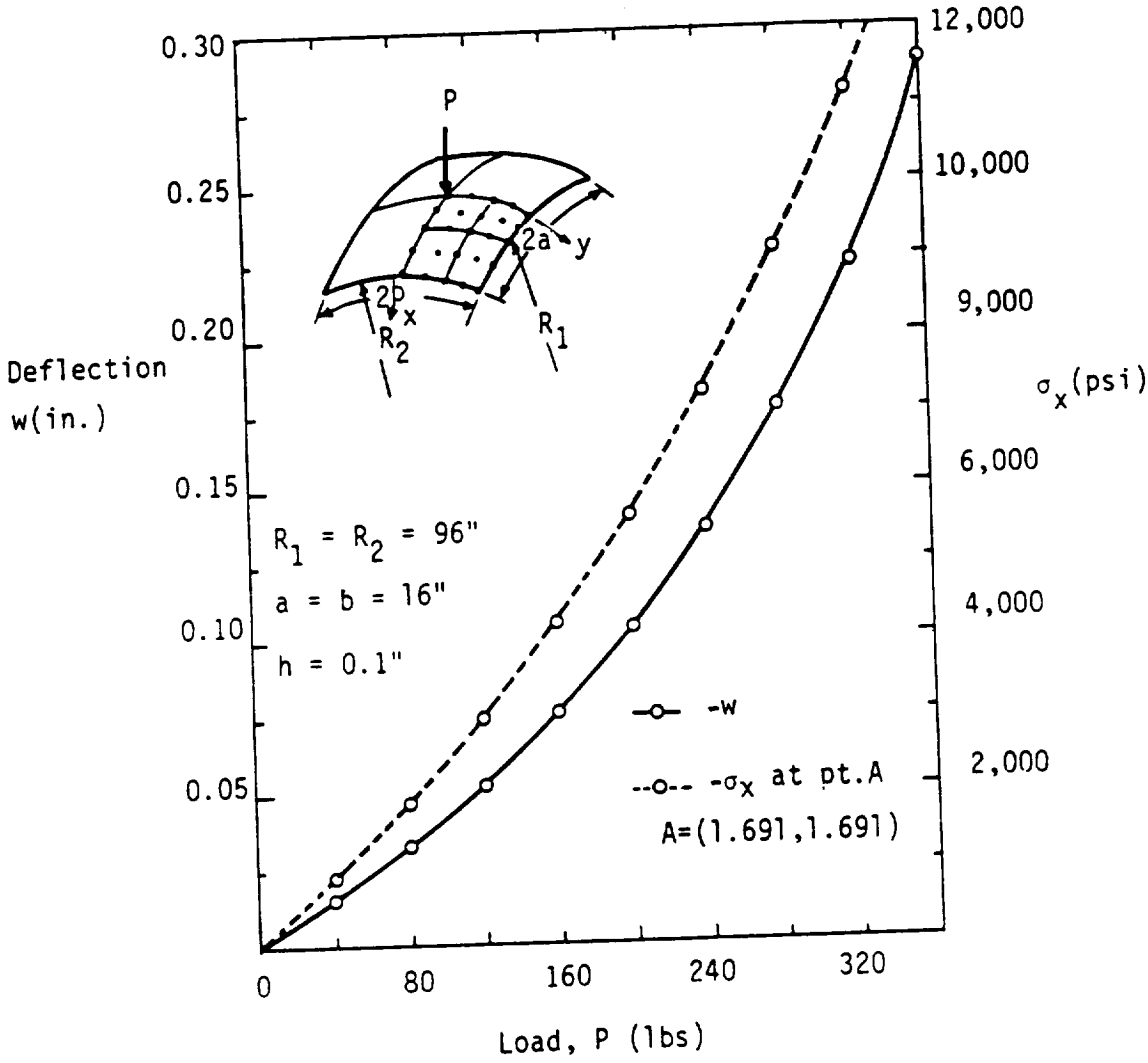

Figure 5. Bending of a simply supported (SS-3), isotropic, spherical shell under point load.

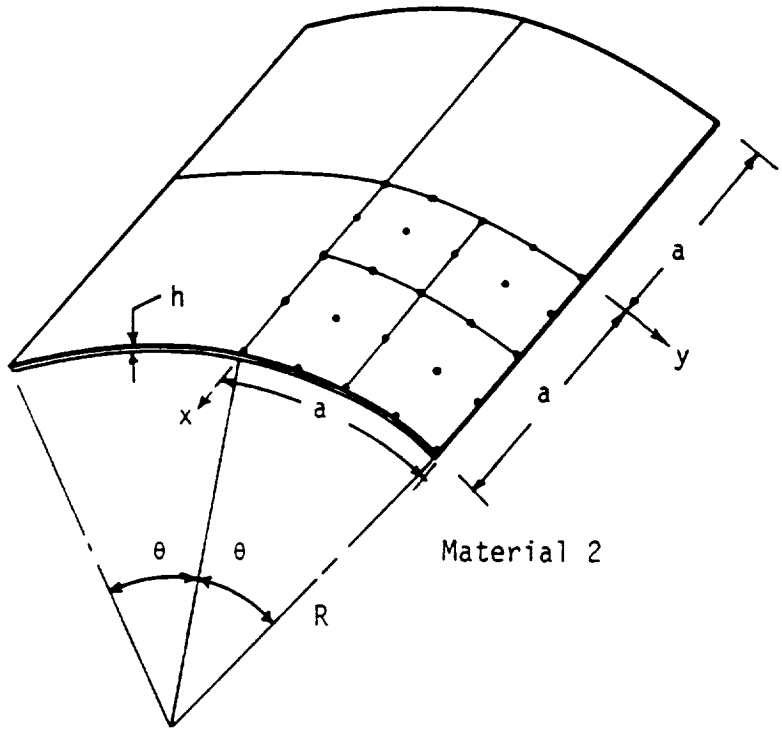

Figure 6. Geometry of a cylindrical shell.

5. Clamped isotropic cylindrical shell under uniform loading.

Figure 7 contains the pertinent data and results for a clamped cylindrical shell (isotropic) subjected to uniform load. The results are compared with those obtained by Dhatt [30]. The agreement is very good.

6. Clamped orthotropic cylindrical shell subjected to internal pressure.

Figure 8 contains the geometry and plots of center deflection and center stress versus the internal pressure for the problem. The orthotropic material properties used in the present study are:

$$E_1 = 7.5 \times 10^6 \text{ psi}, \; E_2 = 2 \times 10^6 \text{ psi}, \; G_{12} = G_{13} = G_{23} = 1.25 \times 10^6 \text{ psi}$$

$$\nu_{12} = 0.25 \tag{23}$$

The present result, obtained using the 2 x 2 mesh of quadratic elements, is in excellent agreement with that obtained by Chang and Sawamiphakdi [31].

7. Nine-layer [0°/90°/0°.../0°] cross-ply spherical shell subjected to uniformly distributed load.

The following geometrical data is used in the analysis (with SS-3 boundary conditions):

$$R_1 = R_2 = R = 1{,}000 \text{ in.}, \; a = b = 100 \text{ in.}, \; h = 1 \text{ in.} \tag{24}$$

Individual layers are assumed to be of equal thickness ($h_i = h/9$), with the zero-degree layers being the inner and outer layers. The following two sets of orthotropic-material constants, typical high modulus graphite epoxy material (the ratios are more pertinent here), for individual layers are used:

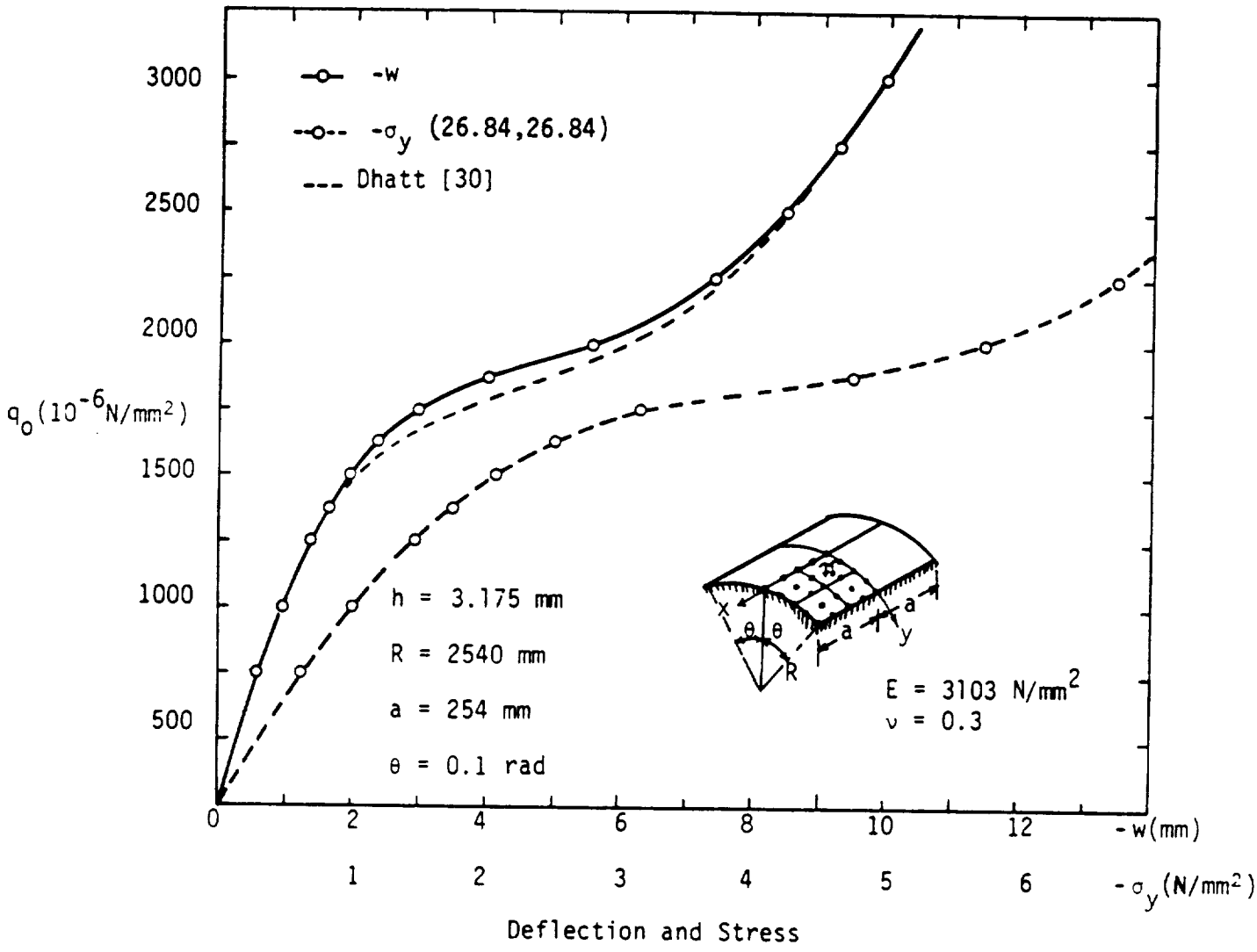

Figure 7. Bending of a clamped, isotropic, cylindrical shell under uniform load.

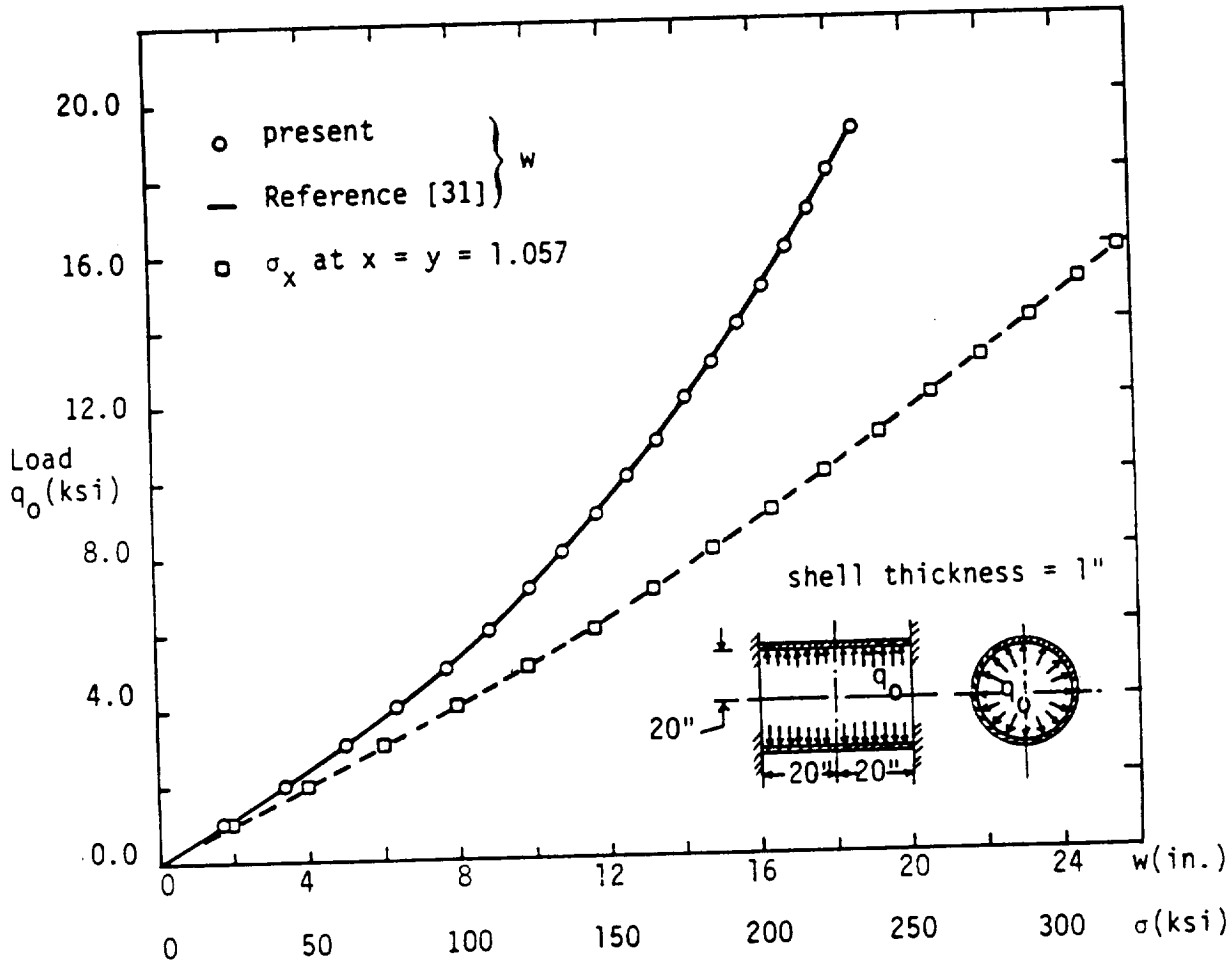

Figure 8. Bending of a clamped orthotropic cylindrical shell subjected to internal pressure.

Mat.-1: $E_1 = 25 \times 10^6$ psi, $E_2 = 10^6$ psi, $G_{12} = G_{13} = 0.5 \times 10^6$ psi

$$G_{23} = 0.2 \times 10^6 \text{ psi}, \quad \nu_{12} = 0.25 \tag{25}$$

Mat.-2: $E_1 = 40 \times 10^6$ psi, $E_2 = 10^6$ psi, $G_{12} = G_{13} = 0.6 \times 10^6$ psi

$$G_{23} = 0.5 \times 10^6 \text{ psi}, \quad \nu_{12} = 0.25 \tag{26}$$

Figure 9 contains plots of center deflecton (w/h) versus the load parameter ($\bar{P} = q_0 R^2/E_2 h^2$) for the two materials. Shell constructed of Material 1 deflects more, for a given load, than the shell laminated of Material 2 (because Material 2 is stiffer), and consequently experiences greater degree of nonlinearity. Note that the difference between the nonlinear deflections of the two shells increase nonlinearly, indicating that the shell made of Material 2 can take much more (ultimate) load than apparent from the ratio of moduli of the two materials, $E_1^{(2)}/E_1^{(1)}$.

8. Effect of various simply-supported boundary conditions on the deflections of two-layer cross-ply spherical shells under uniform load.

As pointed out in Problems 3 and 4, the transverse deflection is sensitive to the boundary conditions on the inplane displacements of simply supported shells. To further illustrate this effect for laminated shells, a set of four types of boundary conditions are used, and the results are presented in Table 3. Here SS-4 has the following meaning:

SS-4

$$\begin{aligned} w = \phi_1 &= 0 \text{ on } x = a \\ w = \phi_2 &= 0 \text{ on } y = b \end{aligned} \tag{27}$$

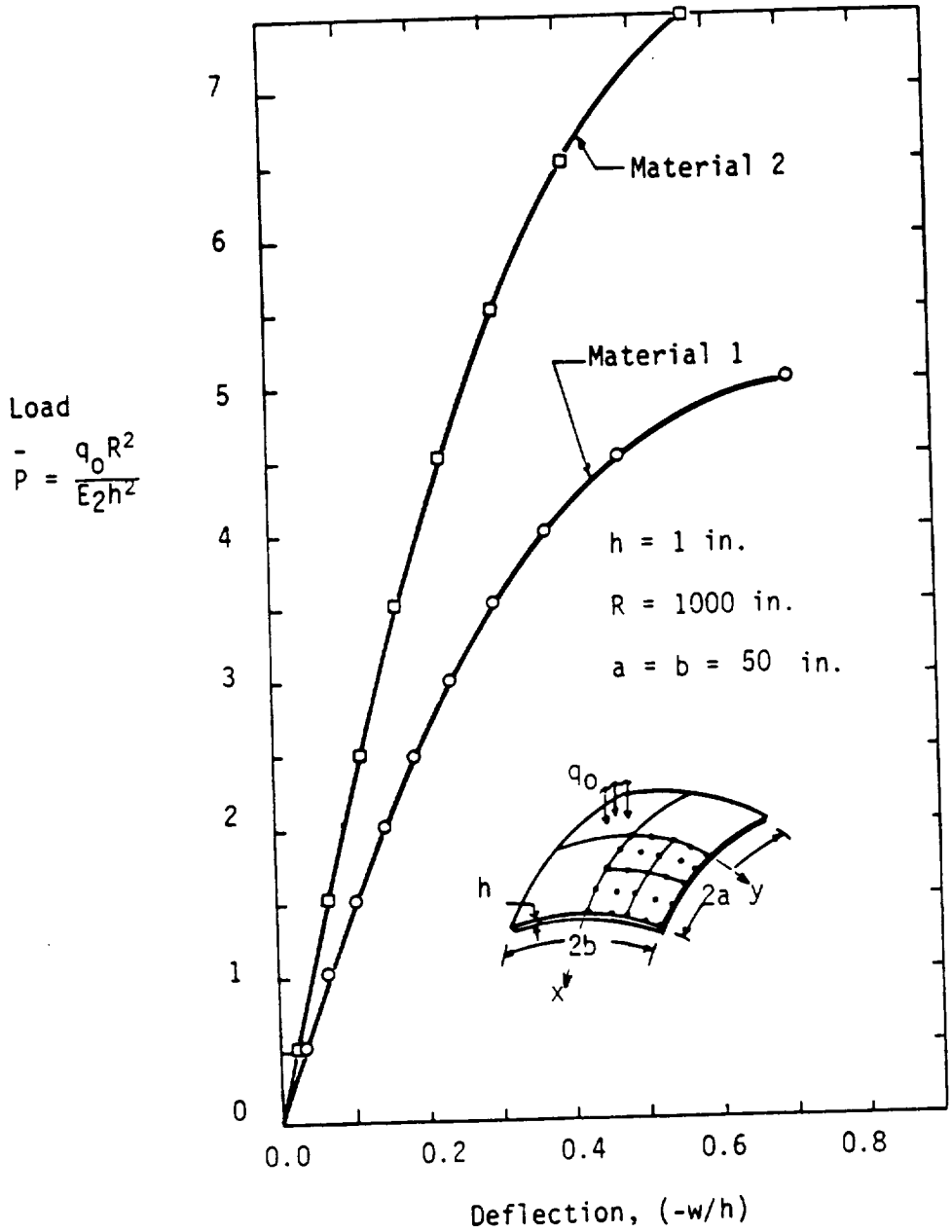

Figure 9. Bending of nine-layer cross-ply [0°/90°/0°/...] spherical shell subjected to uniformly distributed load.

Table 3. Effect of various simply-supported boundary conditions on the transverse deflections of cross-ply [0°/90°] spherical shells under uniform load (Material 1; shell dimensions are the same as those in Fig.

q_o (psi)	-w (in.)			
	SS-1	SS-2	SS-3	SS-4
0.50	0.3344	0.04246	0.04257	0.4592
0.75	0.5757	0.06599	0.06617	0.8255
1.00	0.9485	0.09144	0.09171	1.3845
1.25	1.6529	0.11926	0.11966	1.9589
1.50	2.2826	0.15008	0.15063	2.3597
1.75	2.6421	0.18478	0.18556	2.5951
2.00	2.8499	0.22473	0.22584	2.8074
2.25	3.0764	0.27425	0.27593	3.0284
2.50	3.2432	0.33534	0.33795	3.1948
2.75	3.4214	0.42970	0.43487	3.3719

Once again we note that SS-2 and SS-3 give almost the same deflections. Boundary conditions SS-1 and SS-4 give deflections an order of magnitude higher than those given by SS-2 and SS-3. Thus, boundary conditions SS-2 and SS-3 make the shell quite stiffer.

9. Two-layer cross-ply [0°/90°] and angle-ply [-45°/45°], simply-supported (SS-3) spherical shells.

Figure 10 contains the pertinent data and results (with different scales) for the cross-ply and angle-ply shells (of Material 2). It is interesting to note that the type of nonlinearity exhibited by the two shells is quite different; the cross-ply shell gets softer whereas the angle-ply shell gets stiffer with an increase in the applied load. While both shells have bending-stretching coupling due to the lamination scheme ($B_{22} = -B_{11}$ nonzero for the cross-ply shell and B_{16} and B_{26} are nonzero for the angle-ply shell), the angle-ply experiences shear coupling that stiffens the spherical shell relatively more than the normal coupling (note that, in general, shells get softer under externally applied inward load).

Figure 11 contains plots of center deflection, normal stress ($-\sigma_y$) and shear stress (σ_{yz}) at x = y = 5.283" versus load for two-layer cross-ply (0°/90°) spherical shell (Material 1) under point load at the center of the shell. The nonlinearity exhibited by the stresses (especially σ_{yz}) is less compared to that exhibited by the transverse deflection.

10. Two-layer clamped cylindrical shells under uniform loads.

Figures 12 and 13 contain results (i.e., w, σ_y, σ_{xz} versus load) for cross-ply [0°/90°] and angle-ply [-45°/45°] clamped cylindrical shells under uniform load. The load-deflection curve for the cros-ply shell resembles that

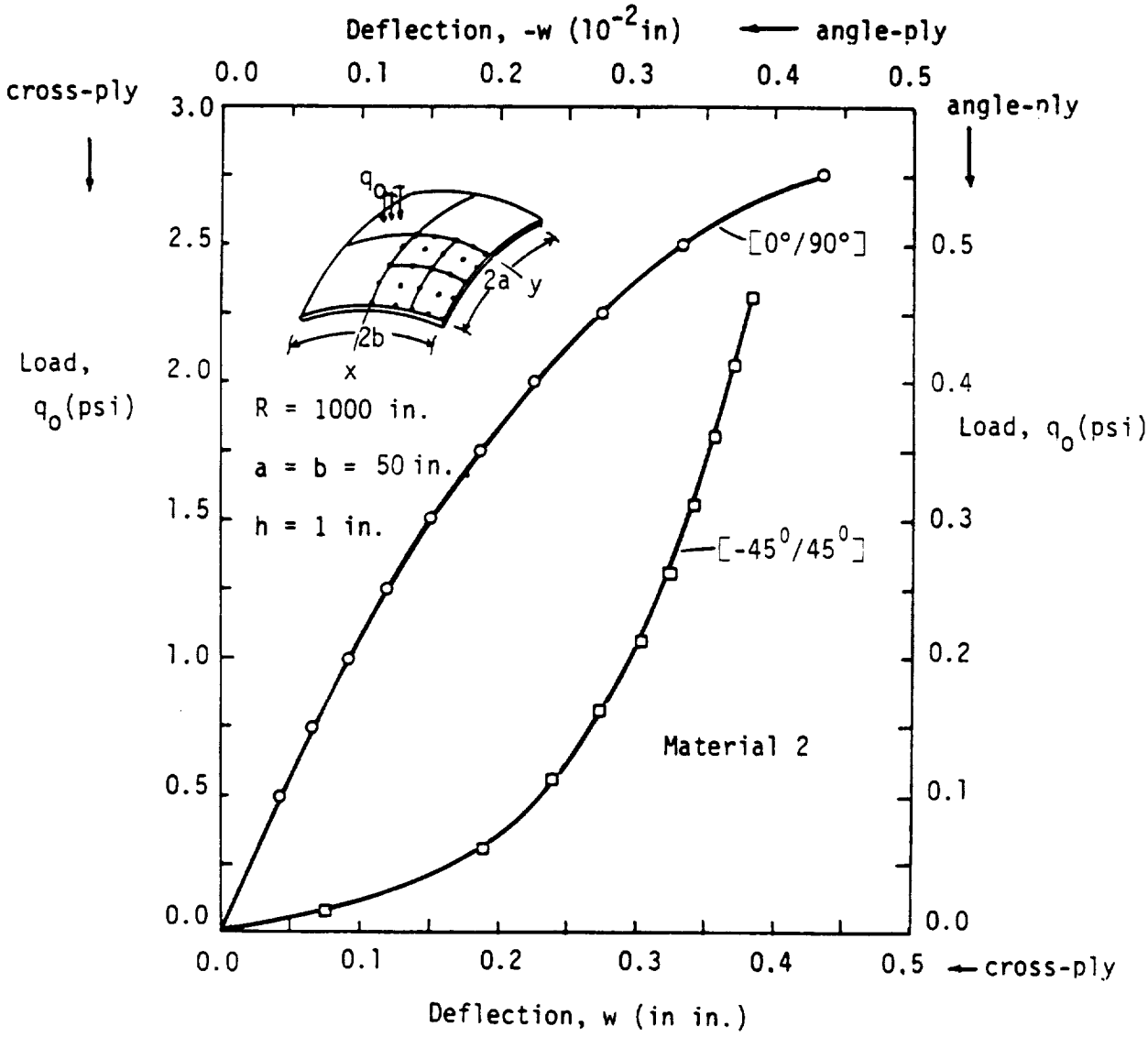

Figure 10. Bending of two-layer cross-ply and angle-ply, simply supported (SS-3) spherical shells under uniform load.

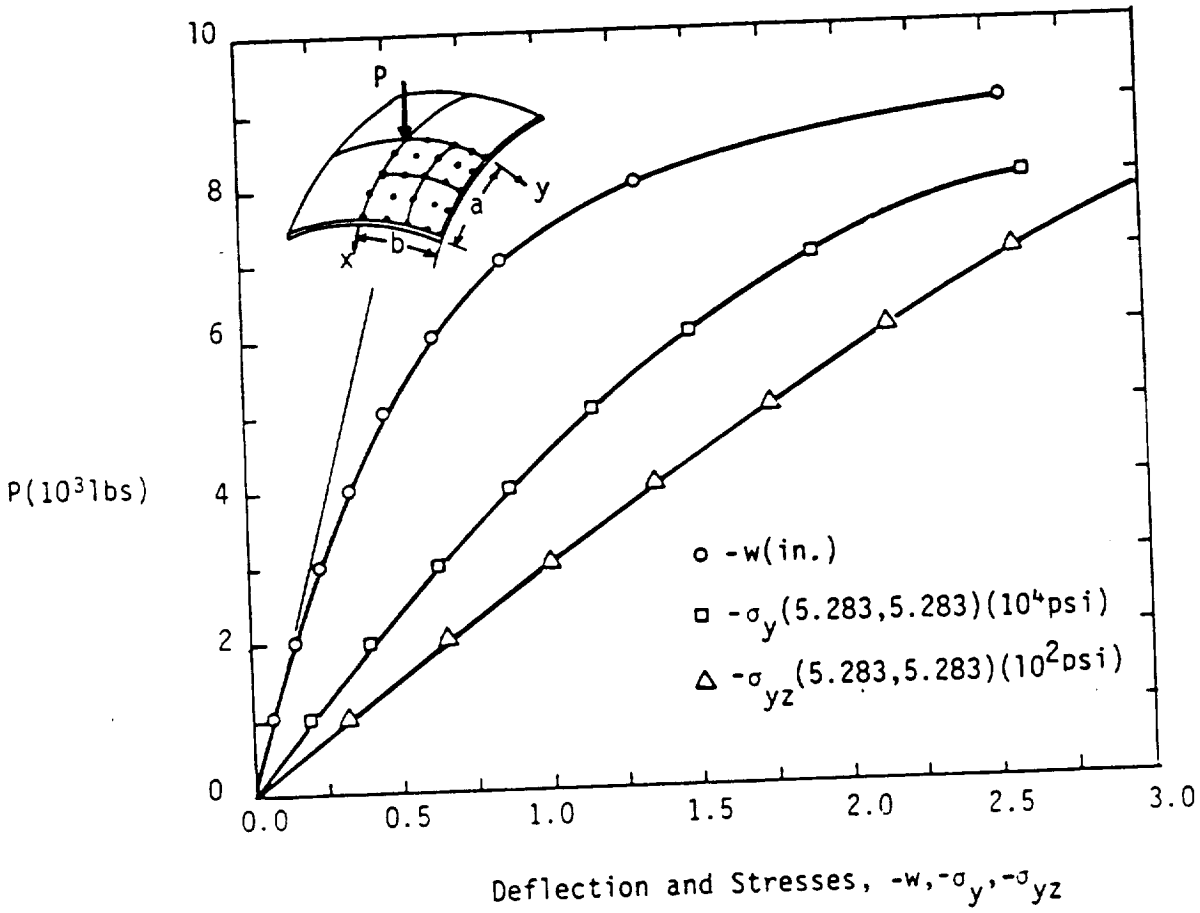

Figure 11. Bending of a cross-ply [0°/90°] spherical shell (SS-3, Material 1), under point load. (see Fig. 10 for the shell dimensions)

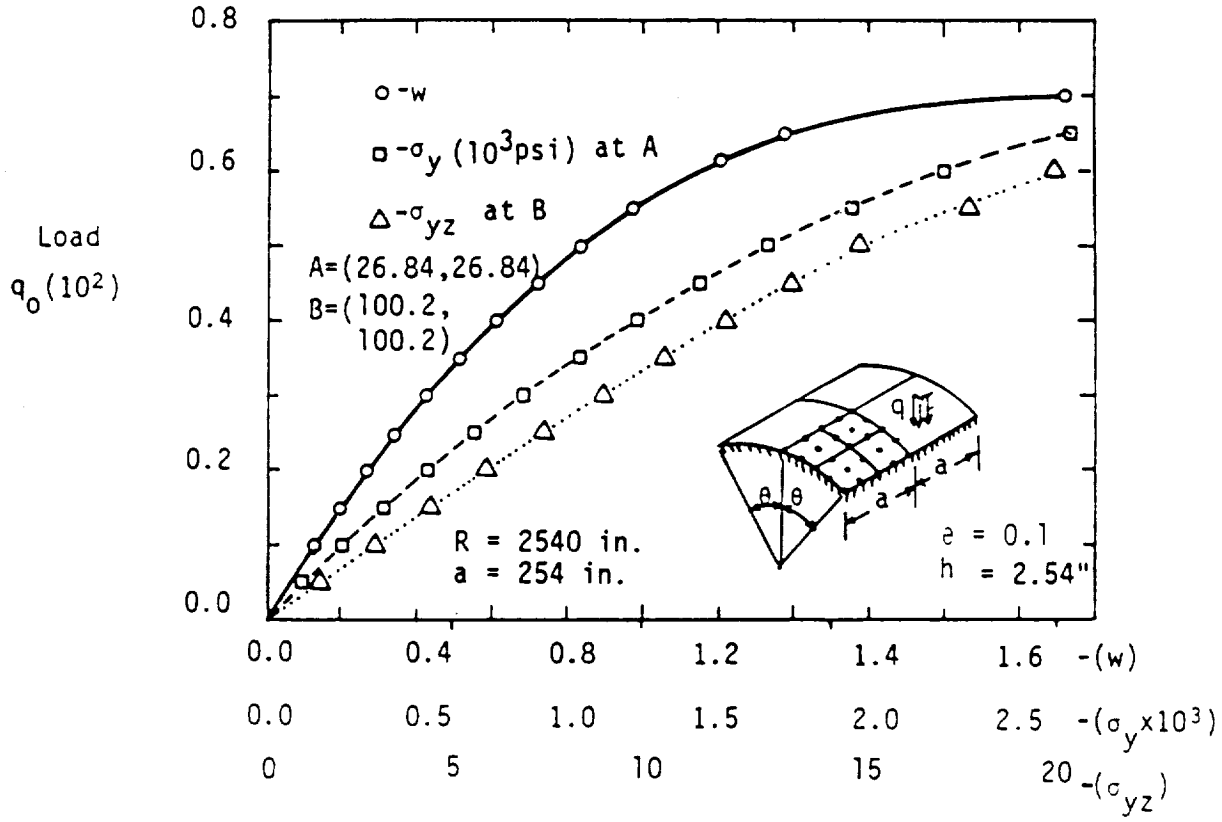

Figure 12. Bending of a clamped angle-ply [-45°/45°] cylindrical shell under uniform load. (Material 1)

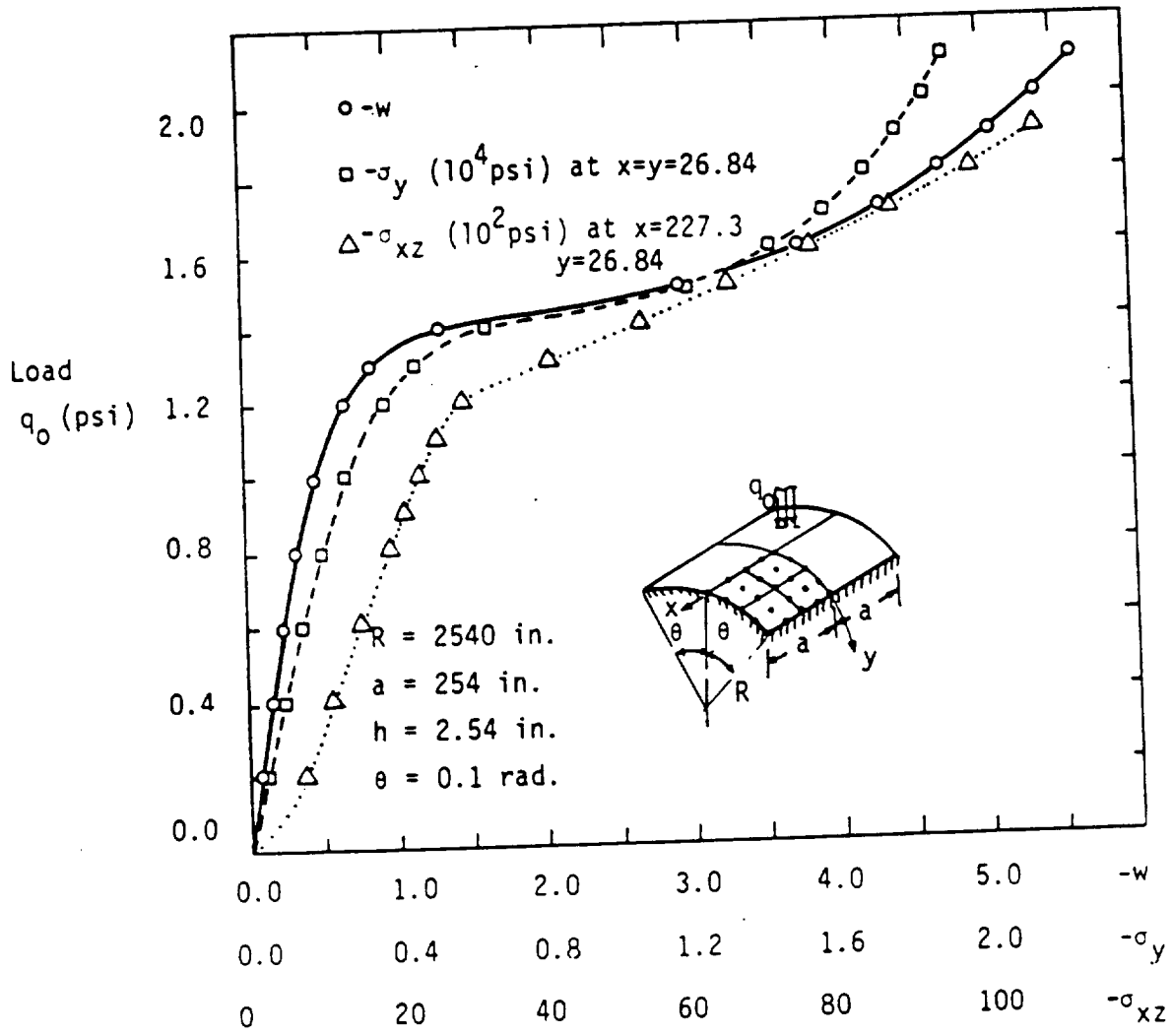

Figure 13. Bending of a clamped cross-ply [0°/90°] cylindrical shell under uniform load (Material 1)

of the isotropic shell in Fig. 7, but exhibits greater degree of nonlinearity (being stiffer). The angle-ply shell exhibits different type of nonlinearity (softening type) for all loads.

11. Quasi-isotropic, clamped, cylindrical shell under uniform load.

Two types of quasi-isotropic clamped cylindrical shells are analyzed:

$$\begin{aligned} &\text{Type 1: } [0°/45°/90°/-45°]_{sym.} \\ &\text{Type 2: } [0°/\pm 45°/90]_{sym.} \end{aligned} \tag{28}$$

Material 1 properties are assumed for each lamina (8 layers). The geometric data and results are presented in Fig. 14. Compared to the results presented in Figs. 12 and 13, the quasi-isotropic shells have the 'near-inflection' point at higher loads; the load-deflection curve has essentially the same form as that of the cross-ply shell (see Fig. 12).

CONCLUSIONS

A shear-flexible finite element based on the shear deformation version of the Sanders' theory and the von Karman strains is developed, and its application to isotropic, orthotropic, and laminated (cross-ply and angle-ply) shells is illustrated via numerous sample problems. Many of the results, especially those of laminated shells, are not available in the literature and therefore should serve as references for future investigations. From the numerical computations it is observed that boundary conditions on the inplane displacements have significant effect on the shell deflections and stresses. Also, it is noted that the form of nonlinearities exhibited by different lamination schemes.

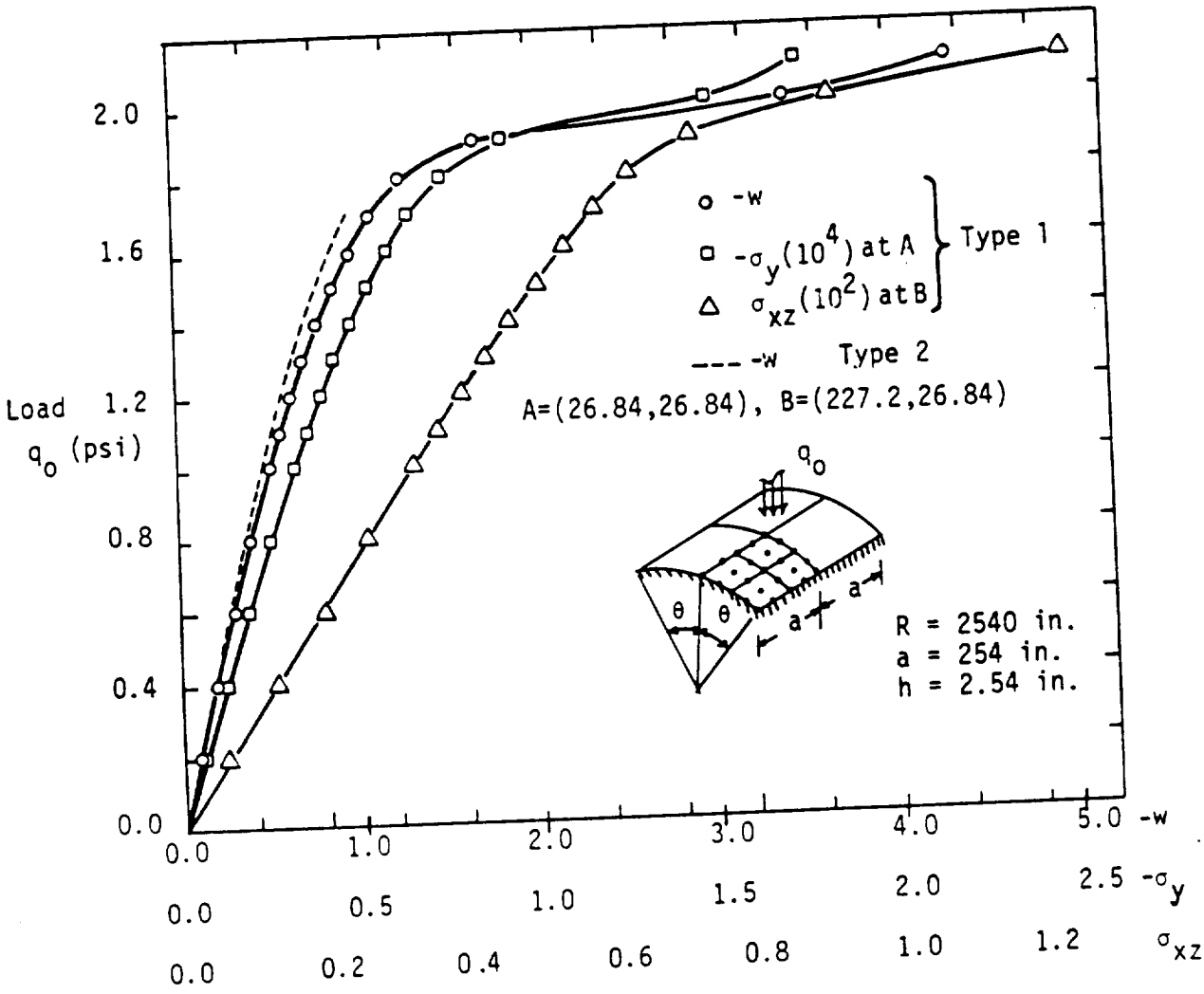

Figure 14. Bending of clamped quasi-isotropic cylindrical shells under uniform load.

REFERENCES

1. P. M. Naghdi, "A Survey of Recent Progress in the theory of Elastic Shells," Appl. Mech. Reviews, Vol. 9, No. 9, pp. 365-368, 1956.

2. C. W. Bert, "Analysis of Shells,"Analysis and Performance of Composites, L. J. Broutman (ed.), Wiley, New York, pp. 207-258, 1980.

3. A. E. H. Love, "On the Small Free Vibrations and Deformations of the Elastic Shells," Phil. Trans. Roy, Soc. (London), Ser. A, Vol. 17, pp. 491-546, 1888.

4. E. Reissner, "A New Derivation of the Equations for the Deformation of Elastic Shells," Am. Jour. Math., Vol. 63, No. 1, pp. 177-184, 1941.

5. E. Reissner, "On Some Problems in Shell Theory," Structural Mechanics (Proceedings of the First Symposium on Naval Structural Mechanics), J. N. Goodier and N. J. Hoff (eds.), Pergamon Press, New York, pp. 74-114, 1960.

6. E. Reissner, "A Note on Generating Generalized Two-Dimensional Plate and Shell Theories," J. Appl. Math. Physics (ZAMP), Vol. 28, pp. 633-642, 1977.

7. J. L. Sanders, "An Improved First-Approximation Theory for Thin Shells," NASA Technical Report R-24, 1959.

8. S. A. Ambartsumyan, "Calculation of Laminated Anisotropic Shells," Izvestiia Akademiia Nauk Armenskoi SSR, Ser. Fiz. Mat. Est. Tekh. Nauk., Vol. 6, No. 3, p. 15, 1953.

9. S. A. Ambartsumyan, Theory of Anisotropic Shells, Moscow, 1961; English translation, NASA TT F-118, May 1964.

10. S. B. Dong, K. S. Pister, and R. L. Taylor, "On the Theory of Laminated Anisotropic Shells and Plates," Journal of Aerospace Sicneces, Vol. 29, p. 969-975, 1962.

11. L. H. Donnell, "Stability of Thin Walled Tubes in Torsion," NACA Report 479, 1933.

12. G. E. O. Widera, and S. W. Chung, "A Theory for Non-Homogeneous Anisotropic Cylindrical Shells," Journal of Applied Mechanics (ZAMP), Vol. 21, pp. 378-399, 1970.

13. J. A. Zukas, and J. R. Vinson, "Laminated Transversely Isotropic Cylindrical Shells," Journal of Applied Mechanics, pp. 400-407, 1971.

14. S. B. Dong, and F. K. W. Tso, "On a Laminated Orthotropic Shell Theory Including Transverse Shear Deformation," Journal of Applied Mechanics, Vol. 39, pp. 1091-1097, 1972.

15. J. M. Whitney, and C. T. Sun, "A Refined Theory for Lamianted Anisotropic, Cylindrical Shells," Journal of Applied Mechanics, Vol. 41, pp. 471-476, 1974.

16. G. E. O. Widera, and D. L. Logan, "Refined Theories for Nonhomogeneous Anisotropic Cylindrical Shells: Part I-Derivation," Journal of the Engineering Mechanics Division, Vol. 106, No. EM6, pp. 1053-1074, 1980.

17. D. L. Logan, and G. E. O. Widera, "Refined Theories for Nonhomogeneous Anisotropic Cylindrical Shells: Part II-Application," Journal of the Engineering Mechanics Division, Vol. 106, No. EM6, pp. 1075-1090, 1980.

18. L. A. Schmit, and G. R. Monforton, "Finite Element Analysis of Sandwich Plate and Laminate Shells with Laminated Faces," American Institute of Aeronautics and Astronautics Journal, Vol. 8, pp.1454-1461, 1970.

19. S. C. Panda, and R. Natarajan, "Finite Element Analysis of Laminated Shells of Revolution," Computers and Structures, Vol. 6, pp. 61-64, 1976.

20. K. N. Shivakumar, and A. V. Krishna Murty, "a High Precision Ring Element for Vibrations of Laminated Shells," Journal of Sound and Vibration, Vol. 58, No. 3, pp. 311-318, 1978.

21. K. P. Rao, "A Rectangular Laminated Anisotropic Shallow Thin Shell Finite Element," Computer Methods in Applied Mechanics and Engineering,Vol. 15, 1978, pp. 13-33.

22. P. Siede, and P. H. H. Chang, "Finite Element Analysis of Laminated Plates and Shells," NASA CR-157106, 1978 (132 pages).

23. Y. S. Hsu, J. N. Reddy, and C. W. Bert, "Thermoelasticity of Circular Cylindrical Shells Laminated of Bimodulus Composite Materials," Journal of Thermal Stresses, Vol. 4, No. 2, pp. 115-177, 1981.

24. J. N. Reddy, "Bending of Laminated Anisotropic Shells by a Shear Deformable Finite Element," Fibre Science and Technology, Vol. 17, pp. 9-24, 1982.

25. A. Venkatesh and K. P. Rao, 'A Doubly Curved Quadrilateral Finite Element for the Analysis of Laminated Anisotropic Thin Shells of Revolution," Computers and Structures, Vol. 12, pp. 825-832, 1980.

26. A. Venkatesh and K. P. Rao, "Analysis of Laminated Shells with Laminated Stiffners Using Rectangular Shell Finite Elements," Computer Methods in Appl. Mech. Engng., Vol. 38, pp. 255-272, 1983.

27. J. N. Reddy, "Exact Solutions of Moderately Thick Laminated Shells," J. Engineering Mechanics, ASCE, to appear.

28. S. Timoshenko and S. Woinowsky-Krieger, Theory of Plates and Shells, 2nd ed., McGraw-Hill, New York, 1959.

29. S. Way, "Uniformly Loaded, Clamped, Rectangular Plates with Large Deformation," Proc. 5th Inter. Congr. of Appl. Mech., Cambridge, MA, 1938.

30. G. S. Dhatt, "Instability of Thin Shells by the Finite Element Method," IASS Symposium for Folded Plates and Prismatic Structures, Vienna, 1970.

31. T. Y. Chang and K. Sawamiphakdi, "Large Deformation Analysis of Laminated Shels by Finite Element Method," Computers and Structures, Vol. 13, pp. 331-340, 1981.

APPENDIX I

Stiffness Coefficients:

Let $f_1 = \frac{1}{2}\frac{\partial u_3}{\partial x_1}$, $f_2 = \frac{1}{2}\frac{\partial u_3}{\partial x_2}$

$$[K^{11}] = A_{11}[S^{11}] + A_{16}([S^{12}] + [S^{21}]) + A_{66}[S^{22}]$$

$$- c_o(B_{16}([S^{12}] + [S^{21}]) + 2B_{66}[S^{22}] - c_o D_{66}[S^{22}]) + \frac{A_{55}}{R_1^2}[S^{00}]$$

$$[K^{12}] = A_{12}[S^{12}] + A_{16}[S^{11}] + A_{26}[S^{22}] + A_{66}[S^{21}]$$

$$- c_o(B_{26}[S^{22}] - B_{16}[S^{11}] + c_o D_{66}[S^{21}]) + \frac{A_{45}}{R_1 R_2}[S^{00}]$$

$$[K^{13}] = f_1(A_{11}[S^{11}] + A_{16}[S^{12}] + [S^{21}]) + A_{66}[S^{22}])$$

$$+ f_2(A_{12}[S^{12}] + A_{16}[S^{11}] + A_{26}[S^{22}] + A_{66}[S^{21}])$$

$$+ \frac{1}{R_1}(A_{11}[S^{10}] + A_{16}[S^{20}]) + \frac{1}{R_2}(A_{12}[S^{10}] + A_{26}[S^{20}])$$

$$- c_o(\frac{B_{16}}{R_1}[S^{20}] + \frac{B_{26}}{R_2}[S^{20}]) - \frac{1}{R_1}(A_{45}[S^{02}] + A_{55}[S^{01}])$$

$$- c_o[f_1(B_{16}[S^{21}] + B_{66}[S^{22}]) + f_2(B_{26}[S^{22}] + B_{66}[S^{21}])]$$

$$[K^{14}] = B_{11}[S^{11}] + B_{16}([S^{12}] + [S^{21}]) + B_{66}[S^{22}]$$

$$- c_o(D_{16}[S^{21}] + D_{66}[S^{22}]) - \frac{1}{R_1}A_{55}[S^{00}]$$

$$[K^{15}] = B_{12}[S^{12}] + B_{16}[S^{11}] + B_{26}[S^{22}] + B_{66}[S^{21}]$$

$$- c_o(D_{26}[S^{22}] + D_{66}[S^{21}]) - \frac{1}{R_1} A_{45}[S^{00}]$$

$$[K^{21}] = [K^{12}]^T$$

$$[K^{22}] = A_{22}[S^{22}] + A_{26}([S^{12}] + [S^{21}]) + A_{66}[S^{11}] + 2c_o B_{66}[S^{11}]$$

$$+ c_o(B_{26}([S^{12}] + [S^{21}]) + c_o D_{66}[S^{11}]) - \frac{A_{44}}{R_2^2}[S^{00}]$$

$$[K^{23}] = f_1(A_{12}[S^{21}] + A_{26}[S^{22}] + A_{16}[S^{11}] + A_{66}[S^{12}])$$

$$+ f_2(A_{22}[S^{22}] + A_{26}([S^{21}] + [S^{12}]) + A_{66}[S^{11}])$$

$$+ \frac{1}{R_1}(A_{12}[S^{20}] + A_{16}[S^{10}]) + \frac{1}{R_2}(A_{22}[S^{20}] + A_{26}[S^{10}])$$

$$+ c_o\left(\frac{B_{16}}{R_1} + \frac{B_{26}}{R_2}\right)[S^{10}] - \frac{1}{R_2}(A_{44}[S^{02}] + A_{45}[S^{01}])$$

$$+ c_o[f_1(B_{16}[S^{11}] + B_{66}[S^{12}]) + f_2(B_{26}[S^{12}] + B_{66}[S^{11}])]$$

$$[K^{24}] = B_{12}[S^{21}] + B_{26}[S^{22}] + B_{16}[S^{11}] + B_{66}[S^{12}]$$

$$+ c_o(D_{16}[S^{11}] + D_{66}[S^{12}]) - \frac{1}{R_2} A_{45}[S^{00}]$$

$$[K^{25}] = B_{22}[S^{22}] + B_{26}([S^{21}] + [S^{12}]) + B_{66}[S^{11}]$$

$$+ c_o(D_{26}[S^{12}] + D_{66}[S^{11}]) - \frac{1}{R_2} A_{44}[S^{00}]$$

$[K^{31}]_{NL} = [2K^{13}]^T_{NL}$, NL = Nonlinear portion of the matrix

$[K^{32}]_{NL} = [2K^{23}]^T_{NL}$

$$[K^{33}] = A_{45}[S^{12}] + A_{55}[S^{11}] + A_{44}[S^{22}] + A_{45}[S^{21}]$$

$$+ 2[S^{11}](A_{11}f_1^2 + 2A_{16}f_1f_2 + A_{66}f_2^2)$$

$$+ 2([S^{12}] + [S^{21}])[f_1^2A_{16} + (A_{12} + A_{66})f_1f_2 + f_2^2A_{26}]$$

$$+ 2[S^{22}](A_{66}f_1^2 + 2A_{26}f_1f_2 + A_{22}f_2^2)$$

$$+ [S^{00}][\frac{1}{R_1}(\frac{A_{11}}{R_1} + \frac{A_{12}}{R_2}) + \frac{1}{R_2}(\frac{A_{12}}{R_1} + \frac{A_{22}}{R_2})]$$

$$+ ([S^{01}] + 2[S^{10}])[f_1(\frac{A_{11}}{R_1} + \frac{A_{12}}{R_2}) + f_2(\frac{A_{16}}{R_1} + \frac{A_{26}}{R_2})]$$

$$+ ([S^{02}] + 2[S^{20}])[f_1(\frac{A_{16}}{R_1} + \frac{A_{26}}{R_2}) + f_2(\frac{A_{12}}{R_1} + \frac{A_{22}}{R_2})]$$

$$[K^{34}] = A_{55}[S^{10}] + A_{45}[S^{20}]$$

$$+ 2f_1(B_{11}[S^{11}] + B_{16}([S^{12}] + [S^{21}]) + B_{66}[S^{22}])$$

$$+ 2f_2(B_{12}[S^{21}] + B_{66}[S^{12}] + B_{26}[S^{22}] + B_{16}[S^{11}])$$

$$+ (\frac{B_{11}}{R_1} + \frac{B_{12}}{R_2})[S^{01}] + (\frac{B_{16}}{R_1} + \frac{B_{26}}{R_2})[S^{02}]$$

$$[K^{35}] = A_{45}[S^{10}] + A_{44}[S^{20}]$$

$$+ 2f_1(B_{12}[S^{12}] + B_{66}[S^{21}] + B_{16}[S^{11}] + B_{26}[S^{22}])$$

$$+ 2f_2(B_{22}[S^{22}] + B_{26}[S^{12}] + B_{26}[S^{21}] + B_{66}[S^{11}])$$

$$+ \left(\frac{B_{16}}{R_1} + \frac{B_{26}}{R_2}\right)[S^{01}] + \left(\frac{B_{12}}{R_1} + \frac{B_{22}}{R_2}\right)[S^{02}]$$

$$[K^{41}] = [K^{14}]^T,\ [K^{42}] = [K^{24}]^T,\ [K^{43}]_{NL} = \frac{1}{2}[K^{34}]^T_{NL}$$

$$[K^{44}] = D_{11}[S^{11}] + D_{16}([S^{12}] + [S^{21}]) + D_{66}[S^{22}] + A_{55}[S^{00}]$$

$$[K^{45}] = D_{12}[S^{12}] + D_{16}[S^{11}] + D_{26}[S^{22}] + D_{66}[S^{21}] + A_{45}[S^{00}]$$

$$[K^{51}] = [K^{15}]^T,\ [K^{52}] = [K^{25}]^T,\ [K^{53}]_{NL} = \frac{1}{2}[K^{35}]^T_{NL}$$

$$[K^{54}] = [K^{45}]^T$$

$$[K^{55}] = D_{22}[S^{22}] + D_{26}([S^{12}] + [S^{21}]) + D_{66}[S^{11}] + A_{44}[S^{00}]$$

$$[K^{\alpha\beta}]_{Linear} = [K^{\beta\alpha}]^T_{Linear}$$

where

$$S^{\alpha\beta}_{ij} = \int_{\Omega^e} \frac{\partial\psi_i}{\partial x_\alpha}\frac{\partial\psi_j}{\partial x_\beta}\,dx_1dx_2\ ,\ S^{00}_{ij} = \int_{\Omega^e} \psi_i\psi_j\,dx_1dx_2$$

It should be noted that although f_1 and f_2 are shown factored outside the matrices, in the evaluation of the coefficients by the Gauss quadrature f_1 and f_2 are considered as parts of the integrals. For example $f_1 A_{11}[S^{11}]$ is evaluated by

$$\int_{\Omega^e} f_1 A_{11} \psi_i \psi_j dx_1 dx_2 \doteq \frac{1}{2} \sum_{I=1}^{N} \sum_{J=1}^{N} A_{11}\left[\left(\frac{\partial u_3}{\partial x_1}\right)\psi_i \psi_j\right]_{x_1=Z_I, x_2=Z_J} W_I W_J \det J_o$$

where N is the number of Gauss points, W_I and W_J are the Gauss weights, Z_I and Z_J are the Gauss points, and J_o is the Jacobian of the transformation.

PART 2

ANALYSIS OF LAMINATED COMPOSITE SHELLS USING A DEGENERATED 3-D ELEMENT

W. C. Chao* and J. N. Reddy
Department of Engineering Science and Mechanics

(This paper is to appear in Int. Journal of Numerical Methods in Engng.)

SUMMARY

A special three-dimensional element based on the total Lagrangian description of the motion of a layered anisotropic composite medium is developed, validated, and employed to analyze laminated anisotropic composite shells. The element contains the following features: geometric nonlinearity, dynamic (transient) behavior, and arbitrary lamination scheme and lamina properties. Numerical results of nonlinear bending, natural vibration, and transient response are presented to illustrate the capabilities of the element.

INTRODUCTION

Composite materials and reinforced plastics are increasingly used in automobiles, space vehicles, and pressure vessels. With the increased use of fiber-reinforced composites as structural elements, studies involving the thermomechanical behavior of shell components made of composites are receiving considerable attention. Functional requirements and economic considerations of design have forced designers to use accurate but economical methods of determining stresses, natural frequencies, buckling loads etc.

---

* Graduate Research Assistant; presently at the University of Dayton Research Institute

Majority of the research papers in the open literature on shells is concerned with bending, vibration, and buckling of isotropic shells. As composites materials are making their way into many engineering structures, analyses of shells made of such materials becomes important. The application of advanced fiber composites in jet engine fan or compressor blades and high performance aircraft require studies involving transient response of composite shell structures to assess the capability of these materials under dynamic loads.

Finite-element analysis of shell structures in the past have used one of the three types of elements: 1. a 2-D element based on a two-dimensional shell theory; 2. a 3-D element based on three-dimensional elasticity theory of shells; and 3. a 3-D degenerated element derived from the 3-D elasticity theory of shells. The 2-D shell theory is derived form the three dimensional continuum field equations via simplifying assumptions. The simplifications require the introduction of the static and kinematic resultants, which are used to describe the equations of motion. The unavailability of a convenient general nonlinear 2-D shell theory makes the 2-D shell element restrictive in its use. The degree of geometric nonlinearity included in the 2-D shell element is that of the von Karman plate theory. In contrast to the 2-D shell theory, no specific shell theory is employed in the 3-D degenerated element; instead, the geometry and the displacement fields are directly discretized and interpolated as in the analysis of continuum problems.

Finite-element analyses of the large-displacement theory of solids are based on the principle of virtual work or the associated principle of stationary potential energy. Horrigmoe and Bergan [1] presented

classical variational principles for nonlienar problems by considering incremental deformations of a continum. A survey of various principles in incremental form is presented by Wunderlich [2]. Stricklin et al. [3] presented a survey of various formulations and solution procedures for nonlinear static and dynamic structural analysis. The formulations include the pseudo force method, the total Lagrangian method, the updated Lagrangian method, and the convected coordinate method.

The only large-deflection analyses of laminated composite shells that can be found in the literature are the static analysis of Noor and Hartley [4] and Chang and Sawamiphakdi [5]. Noor and Hartley employed the shallow shell theory with transverse shear strains and geometric nonlinearities to develop triangular and quadrilateral finite elements. Chang and Sawamiphakdi presented a formulation of the 3-D degenerated element for geometrically nonlinear bending analysis of laminated composite shells. The formulation is based on the updated Lagrangian description and it does not include any numerical results for laminated shells.

From the review of the literature it is clear that first, there does not exist any finite-element analysis of geometrically nonlinear transient response of laminated anisotropic shells, and second, the 3-D degenerated element is not exploited for geometrically nonlinear analysis of laminated anisotropic shells. In view of these observations, the present study was undertaken to develop a finite-element analysis capability for the static and dynamic analysis of geometrically nonlinear theory of laminated anisotropic shells. A 3-D degenerated element with total Lagrangian description is developed and used to analyze various shell problems.

INCREMENTAL, TOTAL-LAGRANGIAN FORMULATION OF A CONTINUOUS MEDIUM

The primary objective of this section is to review the formulation of equations governing geometrically nonlinear motion of a continuous medium. In the interest of brevity only necessary equations are presented. For additional details the reader is referred to References [6-10].

We describe the motion of a continuous body in a cartesian coordinate system. The simultaneous position of all material points (i.e., the configuration) of the body at time t is denoted by C_t, and C_o and $C_{t+\Delta t}$ denote the configurations at reference time t = 0 and time t + Δt, respectively (see Fig. 1). In the updated Lagrangian description all kinetic and kinematic variables are referred to the current configuration at each time and load step. In the total Lagrangian description all dependent variables are referred to the reference configuration. The updated Lagrangian is more suitable for motions that involve very large distortions of the body (e.g., high-velocity impact). The total Lagrangian is more convenient for motions that involve only moderately large deformations. In the present study the total Lagrangian formulation is adopted.

Here we present a derivation of the equilibrium equations at different time steps using the total Lagrangian approach. The coordinates of a typical point in C_t is denoted by ${}^t\underset{\sim}{x} = ({}^tx_1, {}^tx_2, {}^tx_3)$. The displacement of a particle at time t is given by

$$ {}^t\underset{\sim}{u} = {}^t\underset{\sim}{x} - {}^o\underset{\sim}{x} \text{ or } {}^tu_i = {}^tx_i - {}^ox_i \tag{1} $$

The increment of displacement during time t to t + Δt is defined by

$$ u_i = {}^{t+\Delta t}u_i - {}^tu_i \tag{2} $$

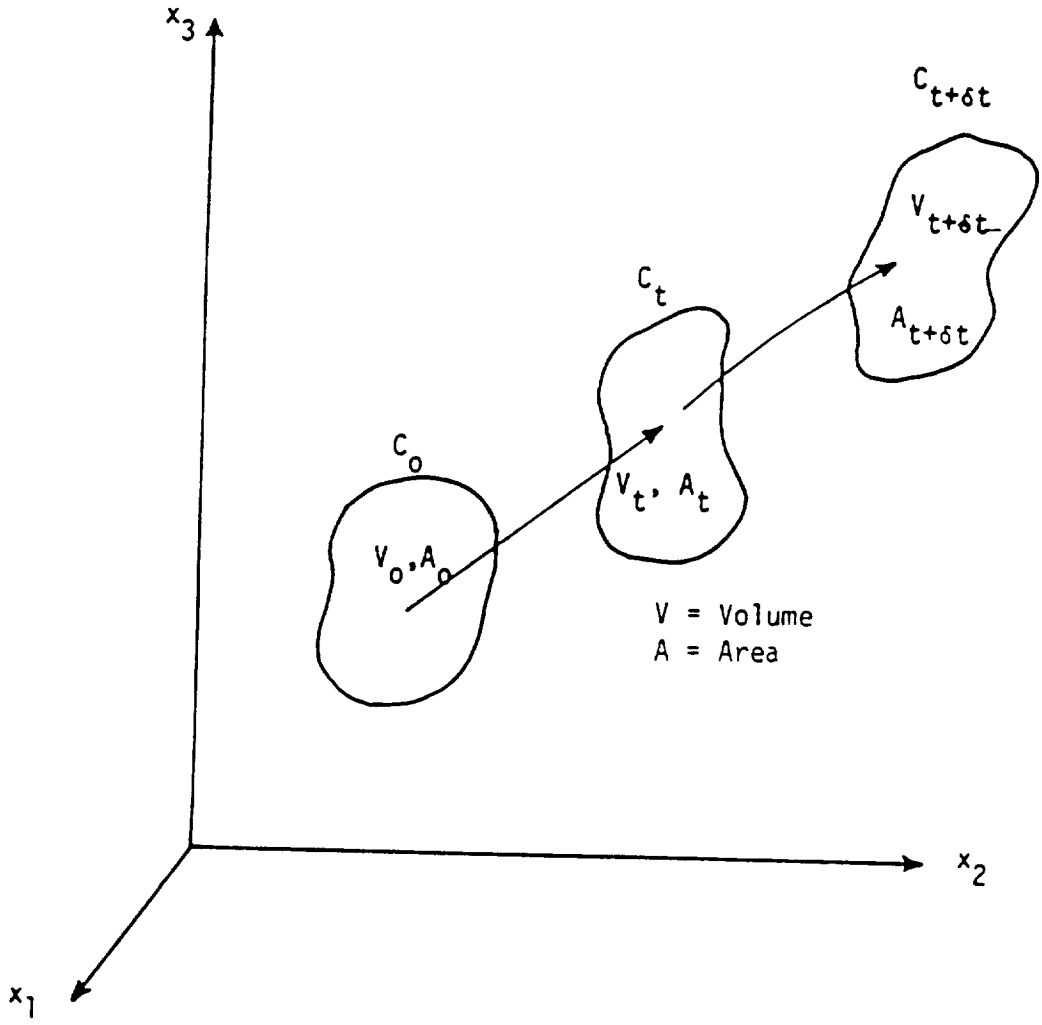

Figure 1 Motion of a continuous body in Cartesian coordinates

The principle of virtual displacements can be employed to write the equilibrium equations at any fixed time t. The principle, applied to the large-displacements case, can be expressed mathematically as

$$\int_{V_o} \rho_o \, {}^{t+\Delta t}\ddot{u}_i \, \delta u_i \, dV_o + \int_{V_o} {}^{t+\Delta t}S_{ij} \, \delta({}^{t+\Delta t}\varepsilon_{ij}) dV_o$$

$$= \int_{A_o} {}^{t+\Delta t}T_i \, \delta u_i \, dA_o + \int_{V_o} \rho_o \, {}^{t+\Delta t}F_i \, \delta u_i \, dV_o \qquad (3)$$

where summation on repeated indices is implied; V_o, A_o, and ρ_o denote, respectively, a volume element, area element, and density in the initial configuration, S_{ij} are the components of second Piola-Kirchhoff stress tensor, ε_{ij} the components of Green-Lagrangian strain tensor, T_i the components of boundary stresses, and F_i are the components of the body force vector; the superposed dots on u_i denotes differentiation with respect to time, and δ denotes the variational symbol. In writing Eq. (3) it is assumed that ε_{ij} is related to the displacement components by the kinematic relations

$${}^{t+\Delta t}\varepsilon_{ij} = \frac{1}{2} ({}^{t+\Delta t}u_{i,j} + {}^{t+\Delta t}u_{j,i} + {}^{t+\Delta t}u_{m,i} \, {}^{t+\Delta t}u_{m,j}) \qquad (4)$$

where $u_{i,j} = \partial u_i / \partial x_j$. The strain components ${}^{t+\Delta t}\varepsilon_{ij}$ can be expressed in terms of current strain and incremental strain components as

$${}^{t+\Delta t}\varepsilon_{ij} = \frac{1}{2} ({}^{t}u_{i,j} + {}^{t}u_{j,i} + {}^{t}u_{m,i} \, {}^{t}u_{m,j})$$

$$+ \frac{1}{2} (u_{i,j} + u_{j,i} + {}^{t}u_{m,i} \, u_{m,j} + u_{m,i} \, {}^{t}u_{m,j}) + \frac{1}{2} u_{m,i} \, u_{m,j}$$

$$\equiv {}^{t}\varepsilon_{ij} + (e_{ij} + \eta_{ij}) \qquad (5)$$

where e_{ij} and η_{ij} denote the linear and nonlinear incremental strains. The stress components ${}^{t+\Delta t}S_{ij}$ can be decomposed into two parts:

$$ {}^{t+\Delta t}S_{ij} = {}^{t}S_{ij} + S_{ij} \tag{6} $$

where S_{ij} is the incremental stress tensor. The incremental stress components S_{ij} are related to the incremental Green-Lagrange strain components, $\varepsilon_{ij} = e_{ij} + \eta_{ij}$, by the generalized Hooke's law:

$$ S_{ij} = C_{ijk\ell}\varepsilon_{k\ell}, \tag{7} $$

where $C_{ijk\ell}$ are the components of the elasticity tensor. Using Eq. (4)-(7), Eq. (3) can be expressed in the alternate form

$$ \int_{V_o} \rho_o \, {}^{t+\Delta t}\ddot{u}_i \delta u_i \, dV_o + \int_{V_o} C_{ijk\ell}(e_{k\ell}\delta\eta_{ij} + \eta_{k\ell}\delta e_{ij})dV_o $$

$$ + \int_{V_o} {}^{t}S_{ij} \, \delta e_{ij} \, dV_o = \delta W - \int_{V_o} {}^{t}S_{ij} \, \delta\eta_{ij} \, dV_o \tag{8} $$

where δW is the virtual work due to external loads.

FINITE-ELEMENT MODEL

Geometry of the Element

Consider the solid three-dimensional element shown in Fig. 2. The coordinates of a typical point in the element can be written as

$$ x_i = \sum_{j=1}^{n} \psi_j(\xi_1,\xi_2) \, \frac{1+\zeta}{2} \, (x_i^j)_{top} + \sum_{j=1}^{n} \psi_j(\xi_1,\xi_2) \, \frac{1-\zeta}{2} \, (x_i^j)_{bottom} \tag{9} $$

where n is the number of nodes, $\psi_i(\xi_1,\xi_2)$ are the finite-element interpolation (or shape) functions, which take in the element, the value of unity at node i and zero at all other nodes, ξ_1 and ξ_2 are the normalized curvilinear coordinates in the middle plane of the shell, and ζ is a linear coordinate in the thickness direction and x_1^i, x_2^i, and x_3^i

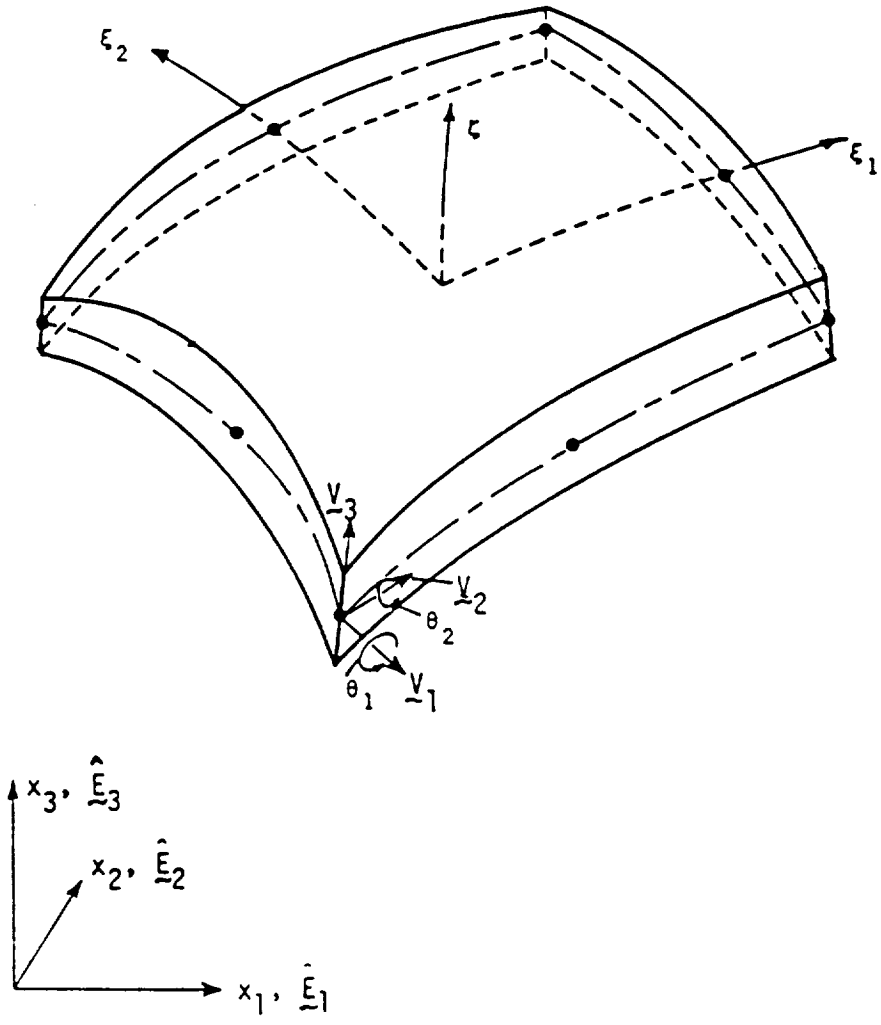

Figure 2 Geometry of the degenerated three-dimensional element

are the global coordinates at node i. Here ξ_1,ξ_2, and ζ are assumed to vary between -1 and +1. Now let (see Fig. 2)

$$v_{3k}^i = (x_k^i)_{top} - (x_k^i)_{bottom} \tag{10}$$

$$\hat{e}_{\sim 3}^i \equiv \underset{\sim}{v}_3^i / |\underset{\sim}{v}_3^i|$$

where v_{3k}^i is the k-th component of the vector $\underset{\sim}{v}_3^i$. Then Eq. (9) becomes

$$x_i = \sum_{j=1}^{n} [\psi_j (x_i^j)_{mid} + \psi_j \frac{\zeta}{2} h_j \hat{e}_{3i}^j] \tag{11}$$

where h_j is the thickness of the element at node j. For small deformation, the displacement of every point in the element can be written as

$$u_i = \sum_{j=1}^{n} \psi_j [u_i^j + \zeta \frac{h}{2} (\hat{e}_{1i}^j \theta_2^j - \hat{e}_{2i}^j \theta_1^j)] \tag{12}$$

where θ_1^i and θ_2^i are the rotations about (local) unit vectors $\hat{e}_{\sim 1}^i$ and $\hat{e}_{\sim 2}^i$, respectively, u_1, u_2, and u_3 are the displacement components corresponding to the global coordinates x_1, x_2, x_3 directions respectively, and u_1^i, u_2^i and u_3^i are the values of the displacements (referred to $\underset{\sim}{x}$) at node i. In writing Eq. (12), we assumed that a line that is straight and normal to the middle surface before deformation is still straight but not necessarily 'normal' to the middle surface after deformation. The strain energy corresponding to stress perpendicular to the middle surface is ignored to improve numerical conditioning when the three dimensional element is employed. This constraint corresponds only

to a part of the usual assumptions of a two-dimensional shell theory. The relaxation of the requirement that straight lines perpendicular to the middle surface remain normal to the deformed middle surface permits the shell to experience shear deformation - an important feature in thick shell situations.

Displacement Field in the Element

In the present study the current coordinates ${}^{t}x_i$ are interpolated by the expression

$$ {}^{t}x_i = \sum_{j=1}^{n} \psi_j ({}^{t}x_i^j + \frac{1}{2} \zeta h_j \, {}^{t}\hat{e}_{3i}^j) \tag{13} $$

and the displacement by

$$ {}^{t}u_i = \sum_{j=1}^{n} \psi_j \, [{}^{t}u_i^j + \frac{1}{2} \zeta h_j \, ({}^{t}e_{3i}^j - {}^{o}e_{3i}^j)] \tag{14} $$

$$ u_i = \sum_{j=1}^{n} \psi_j [u_i^j + \frac{1}{2} \zeta h_j \, ({}^{t+\Delta t}\hat{e}_{3i}^j - {}^{t}\hat{e}_{3i}^j)] \tag{15} $$

Here ${}^{t}u_i^j$ and u_i^j denote, respectively, the displacement and incremental displacement components in the x_i-direction at the j-th node. The unit vectors $\hat{e}_1^i$ and $\hat{e}_2^i$ can be obtained from the relations

$$ \hat{e}_1^i = (\hat{E}_2 \times {}^{t}\hat{e}_3^i) / |\hat{E}_2 \times {}^{t}\hat{e}_3^i| $$

$$ \hat{e}_2^i = {}^{t}\hat{e}_3^i \times {}^{t}\hat{e}_1^i \tag{16} $$

where $\hat{E}_2$ is the unit vector along the (global) x_2-axis. If we assume that the angles θ_1^i and θ_2^i are very small, then we can write

$$\hat{e}_3^i = - {}^t\hat{e}_2^i \theta_1^i + {}^t\hat{e}_1^i \theta_2^i \tag{17}$$

Substituting Eq. (17) into Eq. (15), we obtain

$$u_i = \sum_{j=1}^{n} \psi_j [u_i^j + \frac{1}{2} \zeta h_j (- {}^t\hat{e}_{2i}^j \theta_1^j + {}^t\hat{e}_{1i}^j \theta_2^j)] \tag{18a}$$

or

$$\{u\} = [T]\{\Delta\} \tag{18b}$$

where $\{u\}$ is the column of three displacements at a point, $\{\Delta\}$ is the column of 5n (five per node) displacements: u_i^j, θ_1^j, θ_2^j, $j = 1,2,\ldots,n$; $i = 1,2,3$, and $[T]$ is the transformation matrix defined by Eq. (18a). Thus for each time step one can find the normal vectors from Eq. (16) and (17), and the incremental displacements at each point from Eq. (18) once the five generalized displacements at each node are known.

Element Stiffness Matrix

The strain-displacement equations (4) can be expressed in the operator form

$$\{e\} = [A]\{u_o\} \tag{19}$$

where $\{e\} = \{e_{11}\ e_{22}\ e_{33}\ 2e_{12}\ 2e_{13}\ 2e_{23}\}^T$, $[A]$ is a function of ${}^t u_{oi,j}$, and $\{u_o\}$ is the vector of the components of the displacement gradient

$$\{u_o\} = \{u_{1,1}\ u_{1,2}\ u_{1,3}\ u_{2,1}\ u_{2,2}\ u_{2,3}\ u_{3,1}\ u_{3,2}\ u_{3,3}\}^T \tag{20}$$

The vectors $\{u_o\}$ and $\{e\}$ are related to the displacement increments by

$$\{u_o\} = [N]\{u\} = [N][T]\{\Delta\} \tag{21}$$

$$\{e\} = [A][N][T]\{\Delta\} \equiv [B]\{\Delta\} \tag{22}$$

where $[N]$ is the operator of differentials.

Substitution of Eq. (22) into Eq. (8) yields

$$\int_{V_o} \rho_o [T]^t\{\ddot{\Delta}\} dV_o + ({}^t[K_L] + {}^t[K_{NL}])\{\Delta\} = {}^{t+\Delta t}\{R\} - {}^{t+\Delta t}\{F\} \qquad (23)$$

where ${}^t[K_L]$, ${}^t[K_{NL}]$, $\{R\}$, and $\{F\}$ are the linear and nonlinear stiffness matrices, force vector, and unbalanced force vectors:

$${}^t[K_L] = \int_{V_o} {}^t[B]^T[C]\ {}^t[B] dV_o \quad , \quad {}^t[K_{NL}] = \int_{V_o} {}^t[B]^T[S]\ {}^t[B] dV_o$$

$$\{F\} = \int_{V_o} {}^t[B]^T\{\hat{S}\} dV_o \qquad (24)$$

Here [S] and $\{\hat{S}\}$ denote the matrix and vector, respectively, of the second Piola-Kirchhoff stress.

Since we are dealing with laminated composite structures, the important thing is how to perform the integration through the thickness. One way is to pick Gaussian points through the thickness direction. This increases the computational time as the number of layers is increased, because the integration should be performed separately for each layer. An alternative way is to perform explicit integration through the thickness and reduce the problem to a two dimensional one. The Jacobian matrix, in general, is a function of ξ_1, ξ_2, and ζ. The terms in ζ to the first power may be neglected, provided the thickness to curvature ratios are small. This approximation implies that derivative of x_i with respect to ξ_1, ξ_2, and ζ are substantially the same at either end of a mid-surface-normal line. Thus the Jacobian [J] becomes independent of ζ and explicit integration can be employed. If ζ terms are retained in [J],

Gaussian points through the thickness should be added. In the present study, it is assumed that the Jacobian is independent of ζ.

Time Integration

The Newmark integration scheme is used to convert the ordinary differential equations in time, Eq. (23), to algebraic equations. In the Newmark scheme, displacements and accelerations are approximated by

$$^{t+\Delta t}\{\Delta\} = {}^{t}\{\Delta\} + \Delta t\,{}^{t}\{\dot{\Delta}\} + [(\tfrac{1}{2} - \beta)\,{}^{t}\{\ddot{\Delta}\} + \beta\,{}^{t+\Delta t}\{\ddot{\Delta}\}](\Delta t)^2$$

$$^{t+\Delta t}\{\dot{\Delta}\} = {}^{t}\{\dot{\Delta}\} + [(1 - \gamma)\,{}^{t}\{\ddot{\Delta}\} + \gamma\,{}^{t+\Delta t}\{\ddot{\Delta}\}]\Delta t \qquad (25)$$

where $\{\Delta\}$ is the generalized displacement vector of any point and β and γ are the dimensionless parameters of the approximation. For the constant average acceleration case, we have $\beta = \frac{1}{3}$ and $\gamma = \frac{1}{2}$, and for the linear acceleration method $\beta = \frac{1}{6}$ and $\gamma = \frac{1}{2}$ (see [11]).

Substituting Eq. (25) into Eq. (23), and some algebraic manipulation leads to

$$(a_0\,{}^{t}[M] + {}^{t}[K])\{\Delta^{(k)}\} = {}^{t+\Delta t}\{R\} - {}^{t+\Delta t}\{F^{(k-1)}\} + a_3\{P_4\}$$

$$+ a_2[{}^{t}\{P_1\} - \frac{1}{\Delta t}({}^{t}\{P_2\} - {}^{t}\{P_3\})] \qquad (26)$$

where

$$a_0 = \frac{1}{\beta(\Delta t)^2}\ , \quad a_2 = \frac{1}{\beta\Delta t}\ , \quad a_3 = \frac{1}{2\beta} - 1\ , \quad \text{and}$$

$$[M] = \int_{V_o} \rho_o\, {}^{t}[T]^T\, {}^{t}[T]\, dV_o$$

$$\{P_1\} = \int_{V_o} \rho_o \, {}^{t}\{\dot{\Delta}\} \, [T] dV_o$$

$$\{P_2\} = \int_{V_o} \rho_o \, {}^{t+\delta t}\{\Delta\}^{(k-1)} [T] dV_o$$

$$\{P_3\} = \int_{V_o} \rho_o \, {}^{t}\{\Delta\} [T] dV_o$$

$$\{P_4\} = \int_{V_o} \rho_o \, {}^{t}\{\ddot{\Delta}\} \, [T] dV_o \qquad (27)$$

This completes the finite-element formulation of the 3-D degenerated element.

DISCUSSION OF THE NUMERICAL RESULTS

The results to be discussed are grouped into three major categories: (1) static bending, (2) natural vibration, and (3) transient response. All results, except for the vibrations, are presented in a graphical form. All of the results presented here were obtained on an IBM 370/3081 computer with double precision arithmatic.

Static Analysis

Here we present a discussion of four example problems, all involving shell structures.

1. Cylindrical Shell Subjected to Radial Pressure Consider a circular cylindrical panel of the type shown in Fig. 3. The shell is clamped along all four edges and subjected to uniform radial inward pressure. The loading is nonconservative, that is, the direction of the applied load is normal to the cylindrical surface at any time during the deformation. The geometric and material properties are

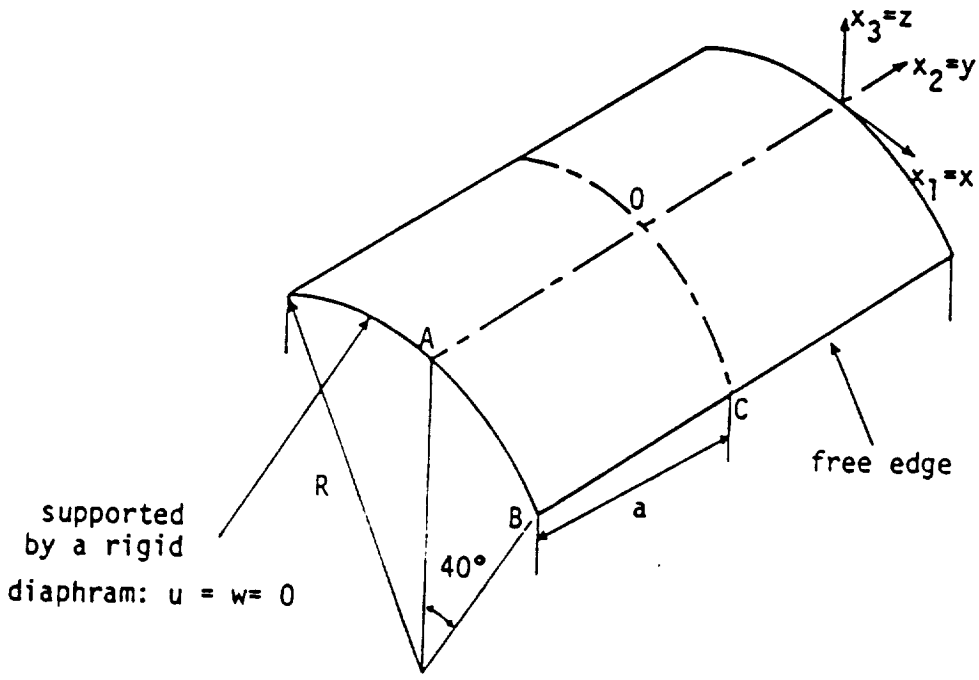

Figure 3 Geometry of the cylindrical shell used in Problem 1 of the static analysis.

$$R = 2540 \text{ mm}, \; a = b = 254 \text{ mm}, \; h = 3.175 \text{ mm},$$

$$\theta = 0.1 \text{ rad}, \; E = 3.10275 \text{ kN/mm}^2, \; \nu = 0.3$$

Due to the symmetry of the geometry and deformation, only one quarter of the panel is analyzed. A load step of 0.5 KN/m^2 was used in order to get a close representation of the deformation path. Fig. 4 contains the plot of central deflection versus the pressure. The solution agrees very closely with that obtained by Dhatt [13].

2. Orthotropic Cylinder Subjected to Internal Pressure Consider a clamped orthotropic ($E_2 = 20 \times 10^6$ psi, $E_1/E_2 = 3.75$, $G_{12}/E_2 = 0.625$, $\nu = 0.25$) cylinder of radius R = 20" and length 20", and subjected to internal pressure, $p_o = 6.41/\pi$ psi. A mesh of 2x2 nine-node elements is used to analyze the problem. The linear center deflections obtained by the 2-D and 3-D elements are 0.0003764 in., and 0.0003739 in., respectively. These values compare favorably with 0.000366 in. of Rao [14] and 0.000367 in. of Timoshenko's analytical solution [15]. The latter two solutions are based on the classical shell theory.

In the large-deflection analysis the present results are compared with those of Reference 5. A value of 2.5 ksi is used for the load step. Figure 5 contains a comparison of the present deflection with that of Reference 5, which used a 3-D degenerated element based on the updated Lagrangian approach. The agreement is very good.

3. Nine-Layer Cross-Ply (0°/90°/0°/...) Spherical Shell Subjected to Uniform Loading Consider a spherical shell laminated of nine layers of graphite-epoxy material ($E_1/E_2 = 40$, $G_{12}/E_2 = 0.6$, $G_{13} = G_{12} = G_{23}$, $\nu_{12} = .25$), subjected to uniformly distributed loading, and simply supported on all its edges (i.e., transverse deflection and tangential

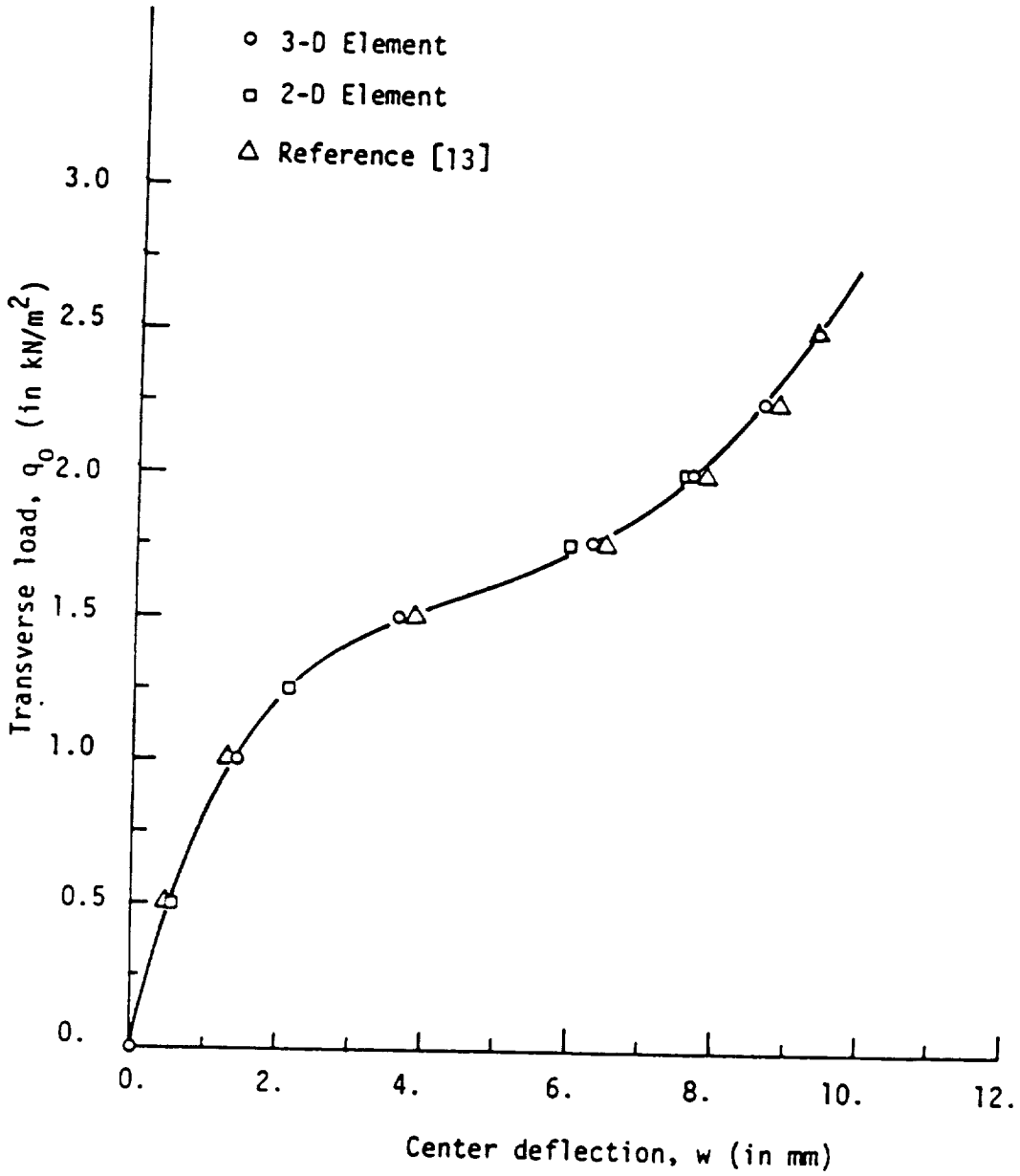

Figure 4 Load-deflection curve for the clamped cylindrical shell

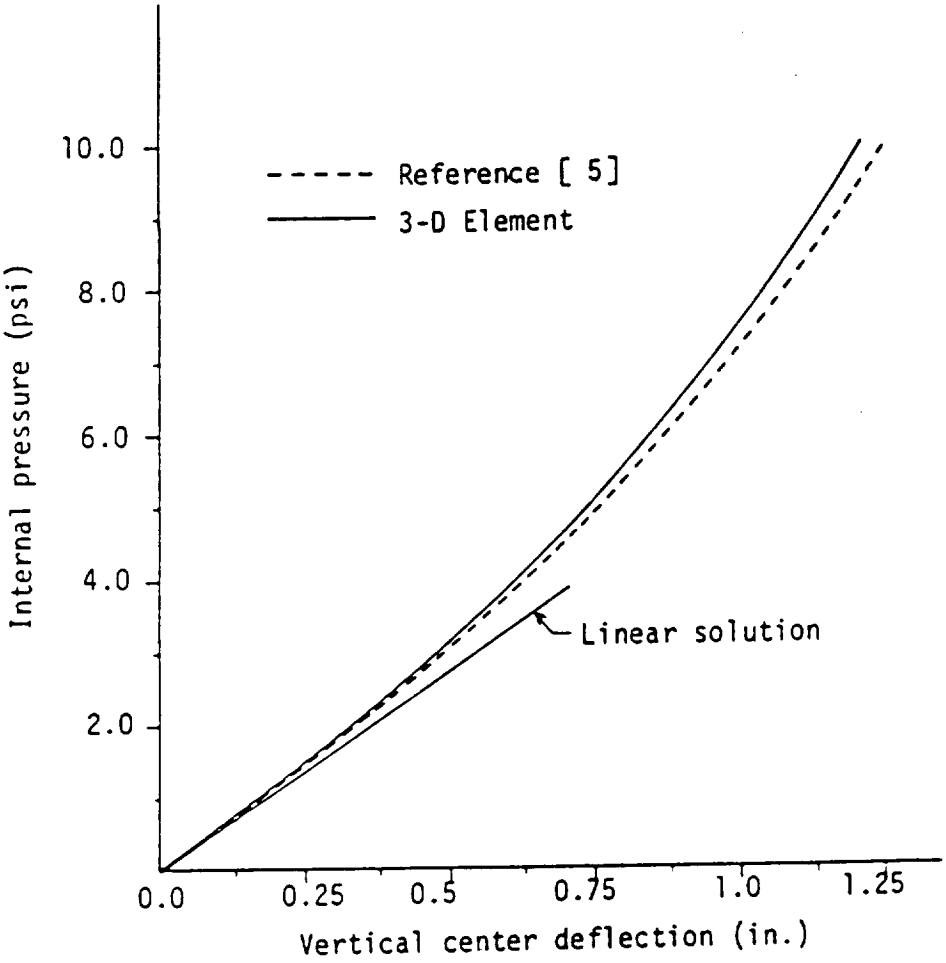

Figure 5 Center transverse deflection versus internal pressure

rotations are zero). A comparison of the load-deflection curves obtained by the present elements with those obtained by Noor [4] is presented (for the parameters h/a = 0.01 and R/a = 10) in Fig. 6. The results agree very well with each other, the present 2-D results being closer to Noor's solution. This is expected because Noor's element is based on a shell theory.

4. Two-Layer Cross-Ply and Angle-Ply (45°/-45°) Shells Under Uniform Loading The geometry of the cylindrical shell used here is the same as that shown in Fig. 3. The shell is assumed to be simply supported on all edges. The material properties of individual lamina are the same as those used in Problem 3. A mesh of 2x2 nine-node elements in a quarter shell is used to model the problem. The results of the analysis are presented in the form of load-deflection curves in Fig. 7. From the results, one can conclude that the angle-ply shell is more stiffer than the cross-ply shell.

The geometry and boundary conditions used for the spherical shells are the same as those used in Problem 3. The geometric parameters used are: R/a = 10, a/h = 100. The load-deflection curves for the cross-ply and angle-ply shells are shown in Fig. 8. From the plot it is apparent that, for the load range considered, the angle-ply shell, being stiffer, does not exhibit much geometric nonlinearity. The load-deflection curve of the cross-ply shell exhibits varying degree of nonlinearity with the load. For load values between 100 and 150, the shell becomes relatively more flexible.

Natural Vibration of Cantilevered Twisted Plates

Here we discuss the results obtained for natural frequencies of various twisted plates. This analysis was motivated by their relevance

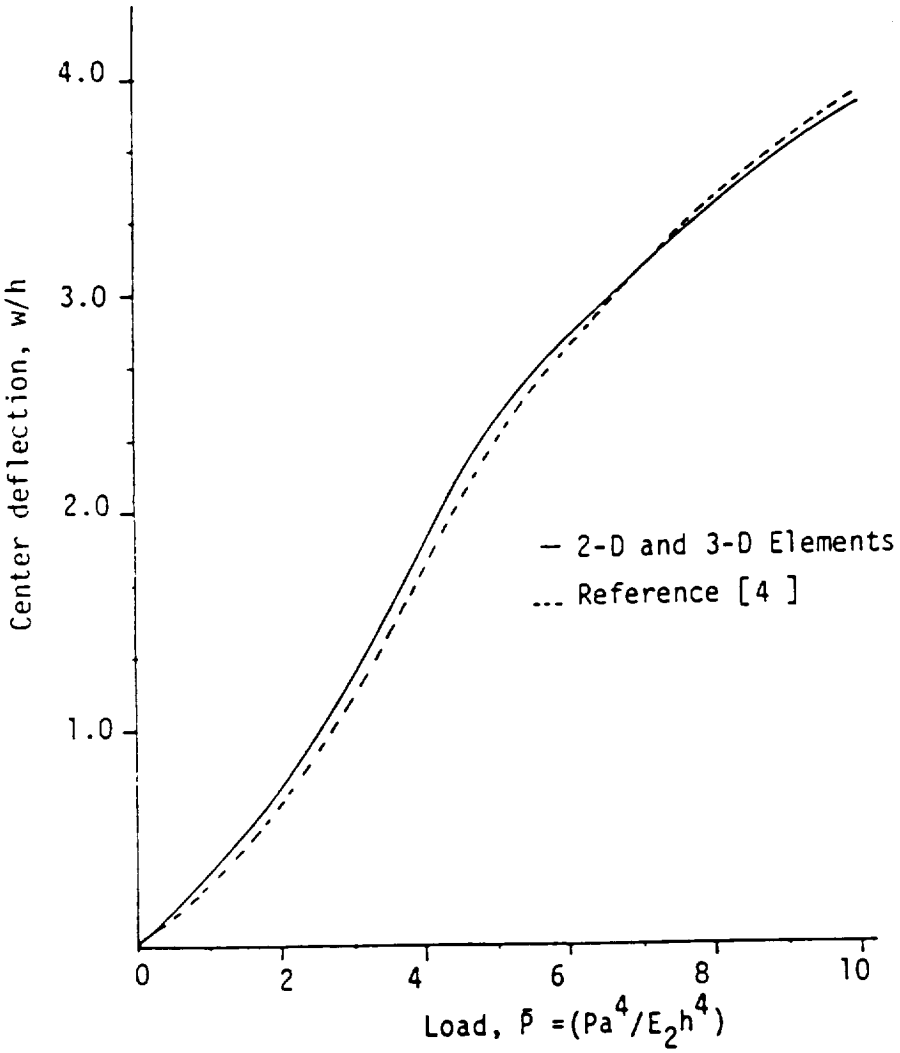

Figure 6 Deflection versus load parameter for a nine-layere cross-ply (0°/90°/0°/...) spherical shell

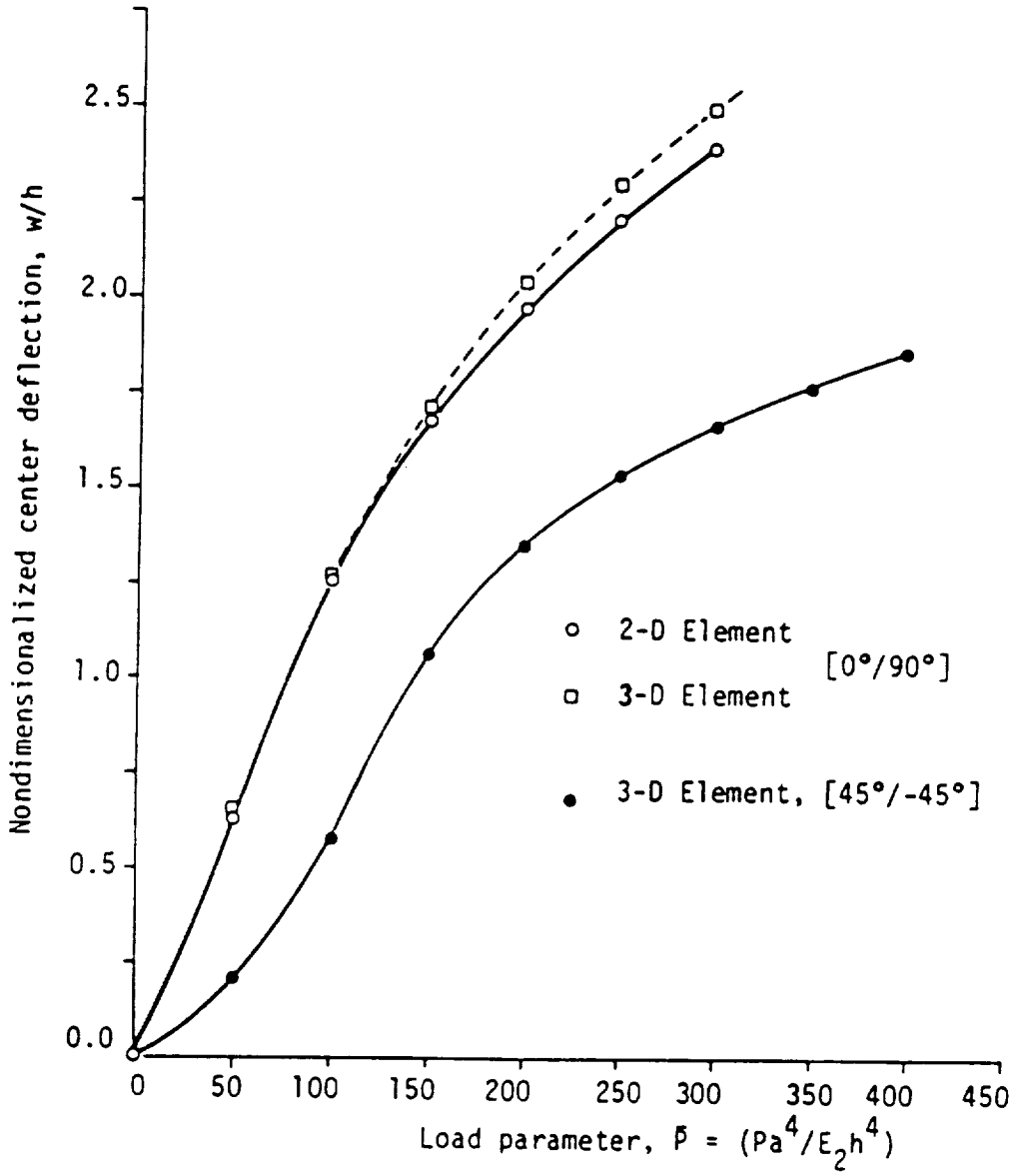

Figure 7 Deflection versus the load parameter for two-layer composite cylindrical shell

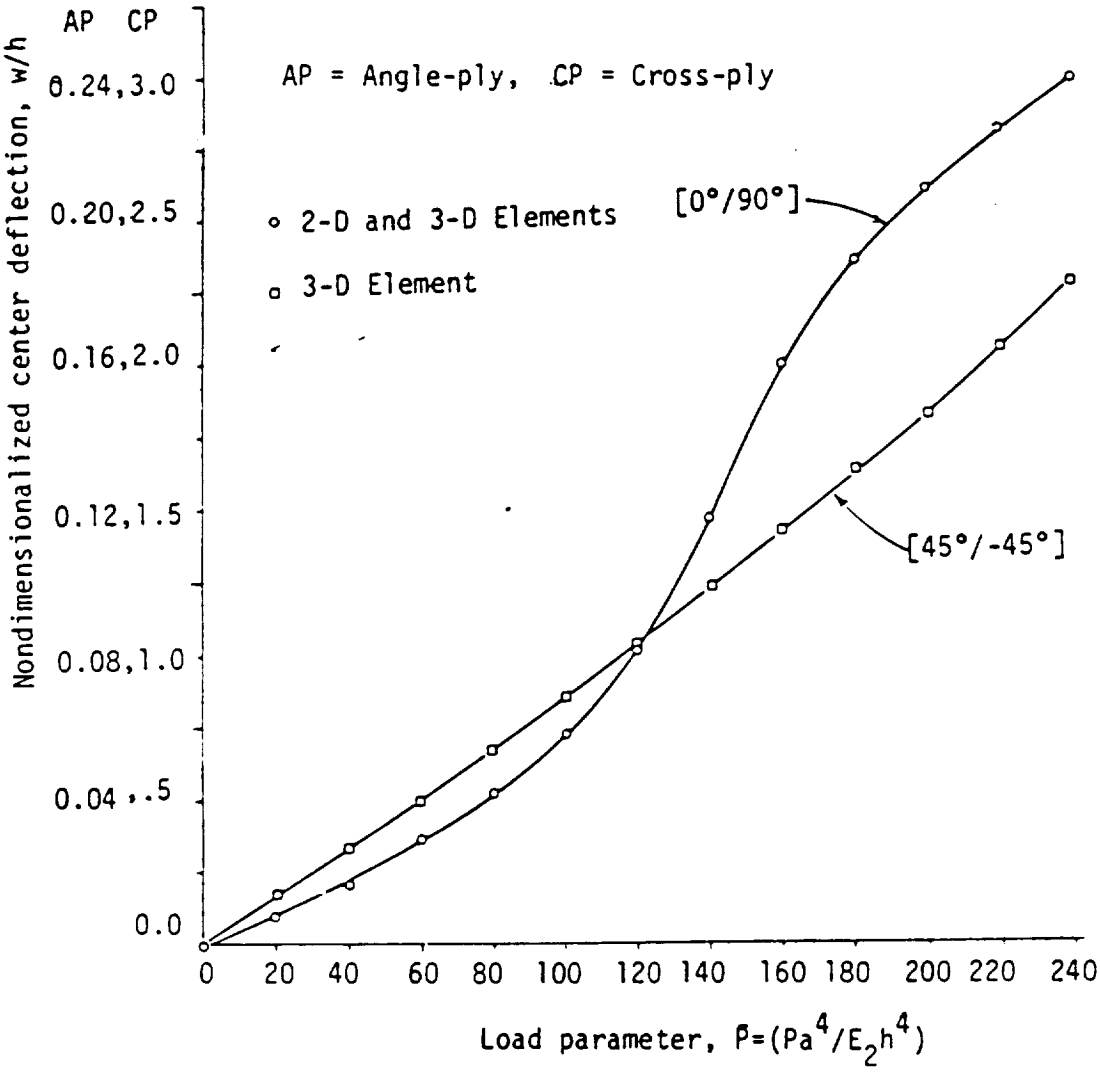

Figure 8 Nondimensionalized deflection versus the load for laminated shells

to natural vibrations of turbine blades. Consider an isotropic cylindrical panel with a twist angle θ at the free end. Table 1 contains the natural frequencies of a square plate for various values of the twist angle θ and ratios of side to thickness. A 2x2 mesh and 4x4 mesh of 9-node elements are employed to study the convergence trend. The results of the refined mesh are included in the parentheses. The results obtained by using the 4x4 mesh are lower than those predicted by the 2x2 mesh, showing the convergence. The results agree with many others published in a recent NASA report. Table 2 contains natural frequencies of twisted plates for the aspect ratio of 3.

Transient Analysis

1. Spherical Cap Under Axisymmetric Pressure Loading Consider a spherical cap, clamped on the boundary and subjected to axisymmetric pressure loading, p_o. The geometric and material properties are

$R = 22.27$ in., $h = 0.41$ in., $E = 10.5 \times 10^6$ psi, $\nu = 0.3$,

$\rho = 0.095$ lb/in^3, $\theta = 26.67°$, $p_o = 100$ psi, $\Delta t = 10^{-5}$ sec.

This problem has been analyzed by Stricklin, et al. [16] using an axisymmetric shell element. In the present study the spherical cap is discretized into five nine-node 2-D and 3-D elements. Figure 9 contains the plot of center deflection versus time. The present solutions obtained using the 3-D and 2-D elements are in excellent agreement in most places with that of Stricklin et al [16]. The difference between the solutions is mostly in the regions of local minimum and maximum.

2. Two-Layer Cross-Ply Plate Under Uniform Load A cylindrical shell with a = b = 5", R = 10", h = 0.1" is simply-supported on the four edges, is analyzed. The shell is laminated by 2 layers (0°/90°) and exerted by a uniform step load $\hat{P} = \frac{a^4 p}{E_2 h^4} = 50$. Figure 10 contains a plot

Table 1 Natural Frequencies of Twisted Square Plates

$$\overline{\omega} = \omega a^2 \sqrt{\rho h / D}\ , \quad D = \frac{Eh^3}{12(1-\nu^2)}\ , \quad \nu = 0.3$$

$\frac{a}{h}$	Twist Angle	Mode 1	2	3	4	5	6
20	0°	* 3.4556 † (3.4583)	8.4110 (8.3353)	22.0999 (21.0238)	28.2089 (26.7465)	31.9740 (30.1454)	55.1625 (52.0784)
	15°	3.4359	10.2920	21.5199	27.2054	32.7430	44.5375
	30°	3.3790 (3.3694)	13.7014 (14.2222)	19.9840 (18.9795)	25.0943 (26.8104)	34.3341 (34.4591)	45.8987 (45.7547)
	45°	3.2908	18.1009	15.9097	23.5680	35.5332	45.7013
	60°	6.1800	17.8319	15.5635	24.1842	36.1466	44.9152
5	0°	* 3.33916 **(3.3390)	7.3948 (7.3559)	10.8083 (10.883)	18.4930 (17.757)	23.7907 (22.769)	26.0552 (24.125)
	15°	3.31713 (3.3170)	7.4816 (7.4504	10.8053 (10.774)	18.4043 (17.771)	23.6767 (22.694)	24.9474 (24.083)
	30°	3.2538 (3.2538)	7.7593 (7.7089)	10.5248 (10.478)	18.4091 (17.795)	23.3734 (22.471)	24.6116 (23.943)
	45°	3.1570 (3.1569)	8.1435 (8.0728)	10.1270 (10.062)	18.3843 (17.79)	22.9126 (22.117)	24.0566 (23.651)
	60°	3.0370 (3.0366)	8.5855 (8.4814)	9.67198 (8.5911)	18.3089 (17.730)	22.3670 (21.684)	23.3533 (23.160)

* 2x2, 9-node mesh
**3x3, 9-node mesh
† 4x4, 9-node mesh

Table 2 Natural Frequencies of Twisted Rectangular Plates
(b/a = 3, 3x3 mesh of nine-node elements)

$$\bar{\omega} = \omega b^2 \sqrt{\rho h / D} \quad , \quad D = \frac{E h^3}{12(1-\nu)^2} \quad , \quad \nu = 0.3$$

$\frac{a}{h}$	Twist Angle	Mode 1	2	3	4	5	6	7
20	0°	3.4150	20.8772	21.6190	65.9706	66.2590		127.256
	15°	3.4009	20.8798	22.1118	21.6032	68.0938	69.3258	130.284
	30°	3.3598	19.4048	25.3743	60.2183	73.5180	77.4493	138.176
	45°	3.2956	17.5289	29.8404	58.2600	80.9488	88.5246	148.8975
	60°	3.2136	15.7431	34.8827	55.8921	89.2028	100.7760	155.070
5	0°	3.3908	15.551	19.124	21.065	59.924	61.949	
	15°	3.3161	15.192	19.231	21.572	60.088	60.830	
	30°	3.3336	14.379	19.549	22.811	60.576	58.472	
	45°	3.2674	13.449	20.060	24.404	61.360	55.874	
	60°	3.1833	12.548	20.741	26.139	62.416	53.381	

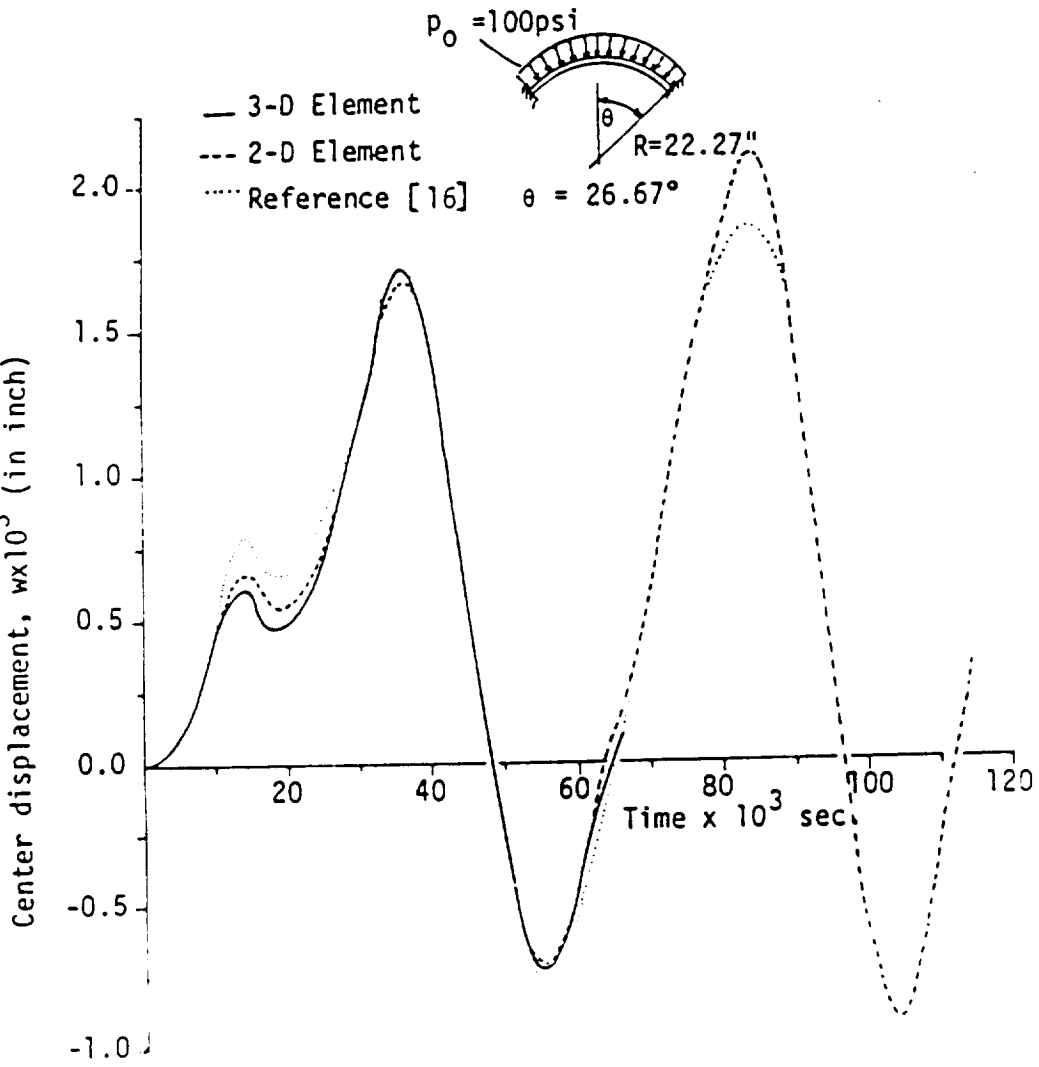

Figure 9 Center transverse displacement versus time for a spherical cap under axisymmetric dynamic loading (load = 100 psi.)

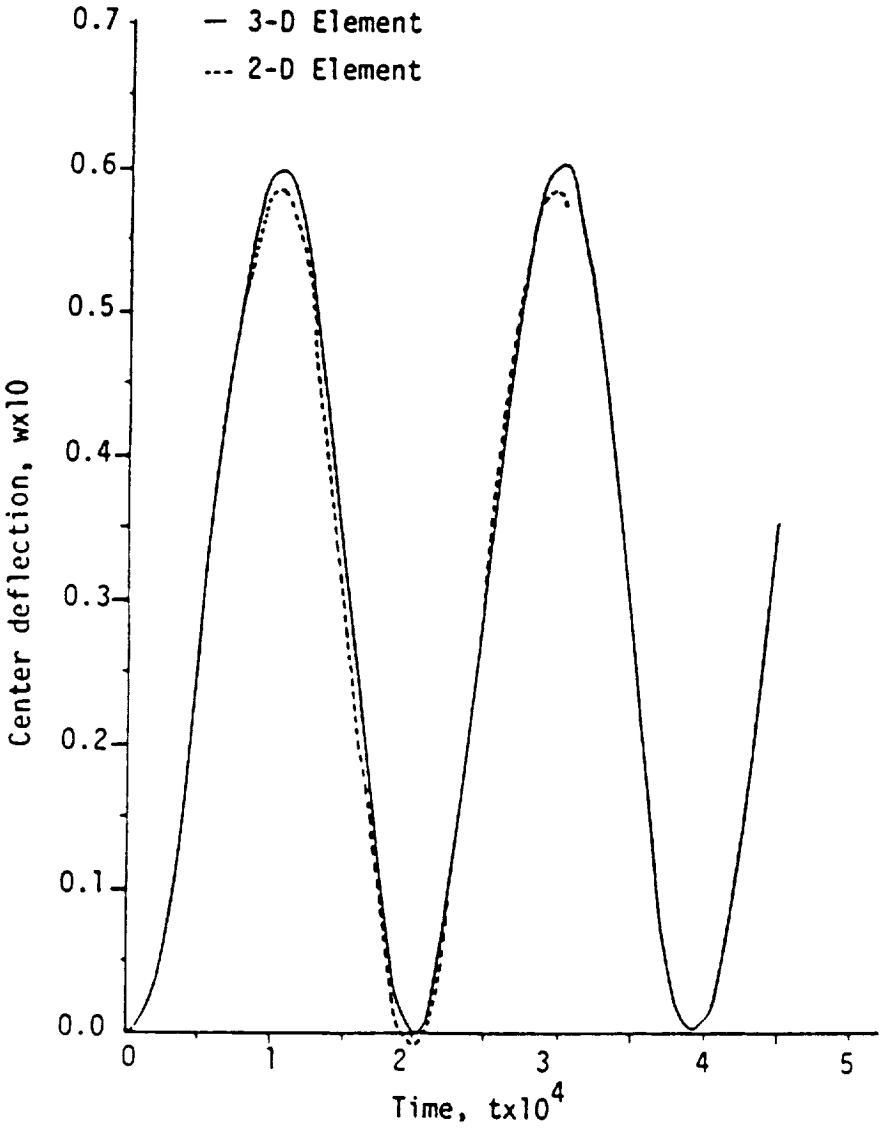

Figure 10 Center deflection versus time for two-layer cross-ply cylindrical shell subjected to uniform step load

of the center deflection versus time for 2-D and 3-D elements. The time step used is $\Delta t = 0.1 \times 10^{-4}$ sec. The solutions obtained using the two elements are in good agreement.

3. Two-Layer Angle-Ply (45°/-45°) Spherical Shell Under Uniform Loading Consider a spherical shell with a = b = 10", R = 20" and h = 0.1", simply supported at four edges and is exerted by a uniform step load. The shell consists of two layers, (45°/-45°). Figure 11 contains the plot of center deflection versus time for $\hat{P} = 50$ and $\hat{P} = 500$ with time step 0.2×10^{-5} sec. For the small load the curve is relatively smooth compared to that of the larger load. This is due to the fact that the geometric nonlinearity exhibited at $\hat{P} = 50$ is smaller compared to that at $\hat{P} = 500$.

CONCLUSIONS

The present 3-D degenerated element has computational simplicity over a fully three-dimensional element, such as those developed in [17], and the element accounts for full geometric nonlinearities in contrast to 2-D elements based on shell theories. As demonstrated via numerical examples, the deflections obtained by the 2-D shell element deviate from those obtained by the 3-D element for deep shells. Further, the 3-D element can be used to model general shells that are not necessarily doubly-curved. For example, the vibration of twisted plates cannot be studied using the 2-D shell element discussed in [12]. Of course, the 3-D degenerated element is computationally more demanding than the 2-D shell theory element for a given problem. In summary, the present 3-D element is an efficient element for the analysis of laminated composite plates and shells undergoing large displacements and transient motion.

The 3-D element presented herein can be modified to include thermal stress analysis capability and material nonlinearities. While the

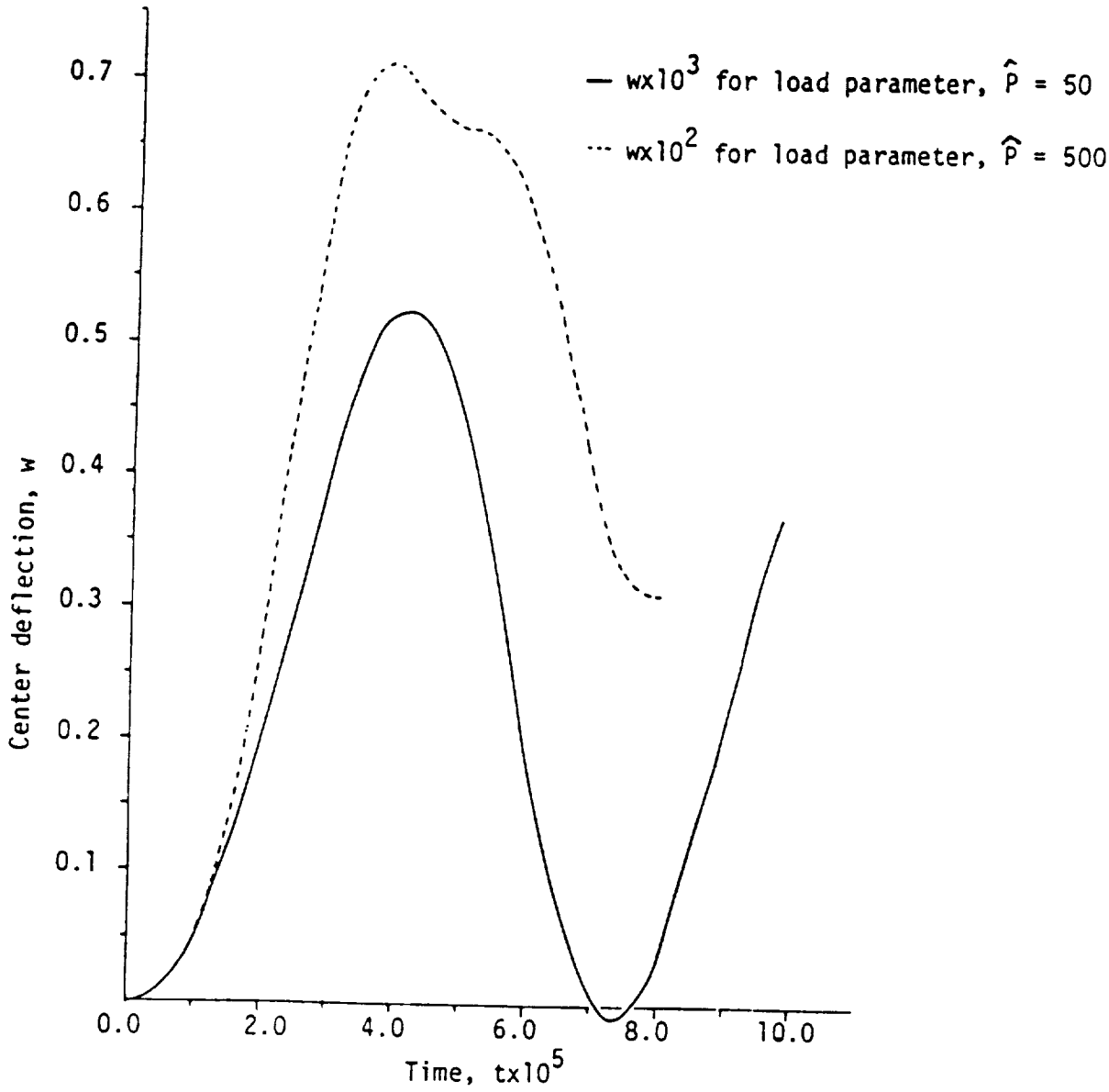

Figure 11 Center deflection versus time for two-layer angle-ply [45°/-45°] spherical shell under uniformly distributed step loading.

inclusion of thermal stresses is a simple exercise, the inclusion of nonlinear material effects is a difficult task (see [18-20]). An acceptable material model should be a generalization of Ramberg-Osgood relation to an anisotropic medium. Another area that requires further study is the inclusion of damping effects, which are more significant than the shear deformation effects.

REFERENCES

1. G. Horrigmoe and P. G. Bergan, "Incremental Variational Principles and Finite Element Models for Nonlinear Problems," Computer Methods in Applied Mechanics and Engineering, 7, 201-217 (1976).

2. W. Wunderlich, "Incremental Formulations for Geometrically Nonlinear Problems," Formulations and Algorithm in Finite Element Analysis, by Bathe, Oden and Wunderlich ed., 193-239.

3. A. Stricklin, W. E. Haisler and W. A. Von Risemann, "Evaluation of Solution Procedures for Material and/or Geometrically Nonlinear Structural Analysis," AIAA Journal, 11, 292-299 (1973).

4. A. K. Noor and S. J. Hartley, "Nonlinear Shell Analysis Via Mixed Isoparametric Elements," Computers and Structures, 7, 615-626 (1977).

5. T. Y. Chang and K. Sawamiphakdi, "Large Deformation Analysis of Laminated Shells by Finite Element Method," Computers and Structures, 13, 331-340 (1981).

6. B. Krakeland, "Nonlinear Analysis of Shells Using Degenerate Isoparametric Elements," Finite Elements in Nonlinear Mechanics, International Conference on Finite Elements in Nonlinear Solid and Structural Mechanics, At Geilo, Norway, 265-284 (1977).

7. K. J. Bathe, E. Ramm and E. L. Wilson, "Finite Element Formulations for Large Deformation Dynamic Analysis," International Journal for Numerical Methods in Engineering, 9, 353-386 (1975).

8. G. A. Dupur's, H. D. Hibbit, S. F. McNamara and P. V. Marcal, "Nonlinear Material and Geometric Behavior of Shell Structures," Computers and Structures, 1, 223-239 (1971).

9. G. Horrigmoe and P. G. Bergan, "Nonlinear Analysis of Free-Form Shells by Flat Finite Elements," Computer Methods in Applied Mechanics and Engineering, 16, 11-35 (1978).

10. W. C. Chao and J. N. Reddy, "Geometrically nonlinear analysis of layered composite plates and shells," NASA CR 168182, Department of Engineering Science and Mechanics, Virginia Polytechnic Institute, Blacksburg, VA 24061, February 1983.

11. J. N. Reddy, An Introduction to the Finite Element Method, McGraw-Hill, New York (1984).

12. J. N. Reddy, "Bending of Laminated Anisotropic Shells by a Shear Deformable Finite Element," Fibre Science and Technology, 17, 9-24, (1982).

13. G. S. Dhatt, "Instability of Thin Shells by the Finite Element Method," IASS Symposium for Folded Plates and Prismatic Structures, Vienna, 1970.

14. K. P. Rao, "A Rectangular Anisotropic Shallow Thin Shell Finite Element," Computer Methods in Applied Mechanics and Engineering, 15, 13-83 (1978).

15. S. Timoshenko, and S. Woinowsky-Krieger, Theory of Plates and Shells, McGraw-Hill, New York, 1959.

16. J. A. Stricklin, J. E. Martinez, J. R. Tillerson, J. H. Hong, and W. E. Haisler, "Nonlinear Dynamic Analysis of Shells of Revolution by Matrix Displacement Method," AIAA, 9, (4), 629-636 (1971).

17. J. N. Reddy and T. Kuppusamy, "Analysis of Layered Composite Plates by Three-Dimensional Elasticity Theory," Research Report No. VPI-E-82.31, Virginia Polytechnic Institute and State University, Blacksburg, VA, 1982.

18. D. R. J. Owen and J. A. Figueiras, "Elasto-plastic Analysis of Anisotropic Plates and Shells by the Semiloof Element," Int. J. Numer. Meth. Engng., 19 (4), 521-540 (1983).

19. D. R. J. Owen and J. A. Figueiras, "Anisotropic elast-plastic finite element analysis of thick and thin plates and shells," Int. J. Numer. Meth. Engng., 19(4), 541-566 (1983).

20. T. Kuppusamy, A Nanda, and J. N. Reddy, "Three-dimensional analysis of composite plates with material nonlinearity," Report No. VPI-E-83.34, Virginia Polytechnic Institute and State University, Blacksburg, VA, 1983.

PART 3

NONLINEAR MATERIAL MODELS FOR COMPOSITE PLATES AND SHELLS

K. Chandrashekhara and J. N. Reddy
Department of Engineering Science and Mechanics

SUMMARY

Nonlinear material models for laminated structures are described and their incorporation in the finite-element formulation of laminated plates and shells is presented. Numerical results for several sample problems of plates and shells are presented and validated by comparison with those available in the literature.

INTRODUCTION

Composite materials are known to exhibit significant non-linearities in stress-strain behaviour even at low strains. Most of the currently used matrix materials in composites have high strain capabilities and the investigation of the bending of composite shells undergoing large deformation, yielding is apt to occur and its effect must be accounted for in the analysis. The nonlinearity is not isotropic but varies with direction, as do the elastic properties. Models for such elastic-plastic behavior of orthotropic and anisotropic materials are not well developed.

The total stress-strain laws are mathematically more convenient than incremental laws but are physically not sound. The criterion approximately describing the yielding of isotropic material is that of von-Mises. The simplest yield criterion for anisotropic material is therefore one which reduces to von-Mises law when the anisotropy is vanishingly small. Hill's yield criteria assumes relatively simple ease of orthotropic anisotropy, that is, there are three mutually orthogonal

planes of symmetry at every point and the intersection of these planes are considered as the principal axes of anisotropy. Fiber reinforced composite structures almost invariably possess this kind of symmetry.

In the present study a nonlinear material model is developed for composite plates and shells, and numerical results for bending are presented using the finite element method as exact solutions are not tractable for elastic-plastic problems involving complex geometries.

MATERIAL MODEL

In the present model, Hill's anisotropic yield criteria for elsatic-perfectly plastic material is used. Hill's [1] yield function is,

$$f(\sigma_{ij}) = F(\sigma_2 - \sigma_3)^2 + G(\sigma_3 - \sigma_1)^2 + H(\sigma_1 - \sigma_2)^2 + 2L\sigma_{23}^2 + 2M\sigma_{13}^2 + 2N\sigma_{12}^2 = 1 \qquad (1)$$

where F, G, H, L, M, N are parameters characteristic of the current state of anisotropy given by,

$$2F = \frac{1}{Y^2} + \frac{1}{Z^2} - \frac{1}{X^2} \quad ; \quad 2L = \frac{1}{R^2}$$

$$2G = \frac{1}{Z^2} + \frac{1}{X^2} - \frac{1}{Y^2} \quad ; \quad 2M = \frac{1}{S^2}$$

$$2H = \frac{1}{X^2} + \frac{1}{Y^2} - \frac{1}{Z^2} \quad ; \quad 2N = \frac{1}{T^2}$$

and X, Y, Z are the tensile yield stresses in the principal direction of anisotropy and R, S, T, are the yield stresses in shear with respect to the principal axes of anisotropy.

It should be noted that Hill's criteria is based on the assumption that the superposition of a hydrostatic stress does not influence yielding and there is no Bauschinger effect. Also, the yield criterion

has this form when the principal axes of anisotropy are the axes of references.

For a plane stress state in the 1-2 plane with transverse shear, equation (1) reduces to:

$$f = (G + H)\sigma_1^2 + (F + H)\sigma_2^2 - 2H\sigma_1\sigma_2 + 2L\sigma_{23}^2 + 2M\sigma_{13}^2 + 2N\sigma_{12}^2 = 1 \qquad (2)$$

For an isotropic material;

$$X = Y = Z = \sigma_o,$$

the yield stress in uniaxial tension and according to the von-Mises yield criteria [2]

$$R = S = T = \frac{\sigma_o}{\sqrt{3}}$$

Therefore, $F = G = H = \frac{1}{2\sigma_o^2}$ and $2L = 2M = 2N = \frac{3}{\sigma_o^2}$ and equation (2) becomes,

$$f = \sigma_1^2 + \sigma_2^2 - \sigma_1\sigma_2 + 3(\sigma_{23}^2 + \sigma_{13}^2 + \sigma_{12}^2) = \sigma_o^2$$

which is the familiar von-Mises yield criteria.

If the principal axes of anisotropy 1,2 do not coincide withthe reference axes x, y, but are rotated by an angle θ, then the stresses in equation (2) are obtained using the transformation as:

$$\sigma_1 = \sigma_x \cos^2\theta + \sigma_y \sin^2\theta + \sigma_{xy} \sin\theta \cos\theta$$

$$\sigma_2 = \sigma_x \sin^2\theta + \sigma_y \cos^2\theta - \sigma_{xy} \sin\theta \cos\theta$$

$$\sigma_{23} = -\sigma_{xz} \sin\theta + \sigma_{yz} \cos\theta$$

$$\sigma_{13} = \sigma_{xz} \cos\theta + \sigma_{yz} \sin\theta$$

$$\sigma_{12} = -2\sigma_x \sin\theta \cos\theta + 2\sigma_y \sin\theta \cos\theta + \sigma_{xy}(\cos^2\theta - \sin^2\theta)$$

Elastic-Plastic Constitutive Equations

In the incremental theory of plasticity, the total strain increment is the sum of the elastic and plastic components

$$d\varepsilon = d\varepsilon^e + d\varepsilon^p \tag{3}$$

The elastic strain increment is related to the stress increment by Hooke's law as,

$$d\varepsilon^e = [D^e]^{-1} d\sigma \tag{4}$$

where $[D^e]$ is the elastic modulus matrix which for orthotropic material takes the form,

$$[D^e] = \begin{bmatrix} \frac{E_1}{1-\nu_{12}\nu_{21}} & \frac{\nu_{12}E_2}{1-\nu_{12}\nu_{21}} & 0 & 0 & 0 \\ \frac{\nu_{12}E_2}{1-\nu_{12}\nu_{21}} & \frac{E_2}{1-\nu_{12}\nu_{21}} & 0 & 0 & 0 \\ 0 & 0 & G_{23} & 0 & 0 \\ 0 & 0 & 0 & G_{13} & 0 \\ 0 & 0 & 0 & 0 & G_{12} \end{bmatrix} \tag{5}$$

The normality rule for an associated plastic flow is,

$$d\varepsilon^p = d\lambda \frac{\partial f}{\partial \sigma}$$

where $d\lambda$ is the positive proportionality constant, evaluated using the condition that during the plastic deformation, the stresses remain on the yield surface so that,

$$df = \frac{\partial f}{\partial \sigma} d\sigma = 0$$

The stress-strain relation in the plastic range is given by [3],

$$d\sigma = [D^{ep}] d\varepsilon$$

where

$$[D^{ep}] = [D^e] - \frac{[D^e]\{\frac{\partial f}{\partial \sigma}\}\{\frac{\partial f}{\partial \sigma}\}^T[D^e]}{\{\frac{\partial f}{\partial \sigma}\}^T[D^e]\{\frac{\partial f}{\partial \sigma}\}} \tag{6}$$

Hence the modification called for in the elastic-plastic analysis would be solely the replacement of the elasticity matrix $[D^e]$ by the elastic-plastic matrix $[D^{ep}]$ for the yielded elements at the successive stages of calculation. It should be noted that the $[D^{ep}]$ matrix is populated and accordingly the transformation of the stress-strain relation from the material axes, ($\{\sigma\} = [D^{ep}]_{12}\{\varepsilon\}$), to the shell coordinate axes, ($\{\sigma\} = [D^{ep}]_{xy}\{\varepsilon\}$), will be modified as shown in Appendix I.

FINITE ELEMENT FORMULATION

Consider a laminated shell constructed of a finite number of uniform thickness orthotropic layers, oriented arbitrarily with respect to the shell coordinates (ξ_1,ξ_2,ζ). The orthogonal curvilinear coordinate system (ξ_1,ξ_2,ζ) is chosen such that ξ_1- and ξ_2- curves are lines of curvature on the midsurface $\zeta=0$, and ζ-curves are straight lines perpendicular to the surface $\zeta=0$.

For the small displacement Sanders shell theory which accounts for transverse shear deformation, the strain displacement relations are given by [5],

$$\varepsilon_i = \varepsilon_i^o + \zeta\kappa_i$$

where

$$\varepsilon_1^o = \frac{\partial u_1}{\partial x_1} + \frac{u_3}{R_1} \quad ; \quad \kappa_1 = \frac{\partial \phi_1}{\partial x_1}$$

$$\varepsilon_2^o = \frac{\partial u_2}{\partial x_1} + \frac{u_3}{R_2} \quad ; \quad \kappa_2 = \frac{\partial \phi_2}{\partial x_2}$$

$$\varepsilon_6^o = \frac{\partial u_1}{\partial x_2} + \frac{\partial u_2}{\partial x_1} \quad ; \quad \kappa_6 = \frac{\partial \phi_1}{\partial x_2} + \frac{\partial \phi_2}{\partial x_1} - c_o\left(\frac{\partial u_2}{\partial x_1} - \frac{\partial u_1}{\partial x_2}\right)$$

$$\varepsilon_4^o = \phi_2 + \frac{\partial u_3}{\partial x_2} - \frac{u_2}{R_2}$$

$$\varepsilon_5^o = \phi_1 + \frac{\partial u_3}{\partial x_1} - \frac{u_1}{R_1}$$

$$c_o = \frac{1}{2}\left(\frac{1}{R_1} - \frac{1}{R_2}\right) \quad , \quad dx_i = \alpha_i d\xi_i \quad (i = 1,2)$$

Here R_i $(i = 1,2)$ are the principal radii of curvature, u_i are the displacements of the reference surface along $\xi_i(\xi_3 = \zeta)$ axes, ϕ_1 and ϕ_2 are the rotations of the transverse normals about the ξ_2 and ξ_1-axes respectively.

The stress-strain relations, transformed to the shell coordinates, are of the form

$$\{\sigma\} = [Q]\{\varepsilon\}$$

where Q_{ij}^k are the material properties of k^{th}-layer (see Appendix I).

The principle of virtual work for the present problem is given by

$$0 = \sum_{i=1}^{L} \Big[\int_\Omega \sigma_1^{(k)}\delta\varepsilon_1 + \sigma_2^{(k)}\,\delta\varepsilon_2 + \sigma_6^{(k)}\,\delta\varepsilon_6 + \sigma_4^{(k)}\,\delta\varepsilon_4 + \sigma_5^{(k)}\,\delta\varepsilon_5 - q\delta u_3\Big\}\alpha_1\alpha_2 d\xi_1 d\xi_2\Big]d\zeta \tag{7a}$$

$$= \int_\Omega [N_1\delta\varepsilon_1^o + N_2\delta\varepsilon_2^o + N_6\delta\varepsilon_6^o + M_1\delta\kappa_1 + M_2\delta\kappa_2 + M_6\delta\kappa_6 + N_4\delta\varepsilon_4^o + N_5\delta\varepsilon_5^o - q\delta u_3\}\alpha_1\alpha_2 d\xi_1 d\xi_2 \tag{7b}$$

where q is the distributed transverse load, N_i and M_i are the stresses and moment resultants.

$$(N_i, M_i) = \sum_{k=1}^{L} \int_{\zeta_{k-1}}^{\zeta_k} \sigma_i(1,\zeta)d\zeta \quad (i = 1,2,6,4,5)$$

Here (ζ_{k-1},ζ_k) are the ζ-coordinates of the k^{th} layer, and L is the total number of layers in the laminated shell.

It should be noted that the equations of equilibrium can be derived from Eq. (7b) by integrating the displacement gradients in ε_i^o by parts and setting the coefficients of δu_i to zero separately. We obtain

$$\frac{\partial N_1}{\partial x_1} + \frac{\partial}{\partial x_2}(N_6 + c_o M_6) + \frac{N_5}{R_1} = 0$$

$$\frac{\partial}{\partial x_1}(N_6 - c_o M_6) + \frac{\partial N_2}{\partial x_2} + \frac{N_4}{R_2} = 0$$

$$\frac{\partial N_5}{\partial x_1} + \frac{\partial N_4}{\partial x_2} - \left(\frac{N_1}{R_1} + \frac{N_2}{R_2} - q\right) = 0$$

$$\frac{\partial M_1}{\partial x_1} + \frac{\partial M_6}{\partial x_2} - N_5 = 0$$

$$\frac{\partial M_6}{\partial x_1} + \frac{\partial M_2}{\partial x_2} - N_4 = 0$$

The resultants (N_i, M_i) are related to $(\varepsilon_i^o, \kappa_i)$ by,

$$\begin{aligned} N_i &= A_{ij}\varepsilon_j^o + B_{\ell p}\kappa_p \qquad i,j = 1,2,6,4,5 \\ M_\ell &= B_{\ell j}\varepsilon_j^o + D_{\ell p}\kappa_p \qquad \ell,p = 1,2,6 \text{ (with } \ell=i \text{ for } i = 1,2,6) \end{aligned} \tag{8}$$

Here A_{ij}, B_{ij} and D_{ij} denote the extensional, flexural-extensional coupling, and flexural stiffnesses of the laminate:

$$(A_{ij}, B_{ij}, D_{ij}) = \sum_{k=1}^{L} \int_{\zeta_{k-1}}^{\zeta_k} Q_{ij}^{(k)} (1, \zeta, \zeta^2) d\zeta \tag{9}$$

In the unabridged notation equation (8) takes the form:

$$\begin{Bmatrix} N_1 \\ N_2 \\ N_6 \\ N_4 \\ N_5 \\ M_1 \\ M_2 \\ M_6 \end{Bmatrix} = \begin{bmatrix} A_{11} & A_{12} & A_{16} & \underline{A}_{14} & \underline{A}_{15} & B_{11} & B_{12} & B_{16} \\ A_{12} & A_{22} & A_{26} & \underline{A}_{24} & \underline{A}_{25} & B_{12} & B_{22} & B_{26} \\ A_{16} & A_{26} & A_{66} & \underline{A}_{46} & \underline{A}_{56} & B_{16} & B_{26} & B_{66} \\ \underline{A}_{14} & \underline{A}_{24} & \underline{A}_{46} & A_{44} & A_{45} & \underline{B}_{14} & \underline{B}_{24} & \underline{B}_{46} \\ \underline{A}_{15} & \underline{A}_{25} & \underline{A}_{56} & A_{45} & A_{55} & \underline{B}_{15} & \underline{B}_{25} & \underline{B}_{56} \\ B_{11} & B_{12} & B_{16} & \underline{B}_{14} & \underline{B}_{15} & D_{11} & D_{12} & D_{16} \\ B_{12} & B_{22} & B_{26} & \underline{B}_{24} & \underline{B}_{25} & D_{11} & D_{22} & D_{26} \\ B_{16} & B_{26} & B_{66} & \underline{B}_{46} & \underline{B}_{56} & D_{16} & D_{26} & D_{66} \end{bmatrix} \begin{Bmatrix} \varepsilon_1^o \\ \varepsilon_2^o \\ \varepsilon_6^o \\ \varepsilon_4^o \\ \varepsilon_5^o \\ \kappa_1 \\ \kappa_2 \\ \kappa_6 \end{Bmatrix} \tag{10}$$

The underscored coefficients are due to material nonlinear stress-strain relationship. It should be noted that the coefficients A_{44}, A_{45} and A_{55} defined in equation (9) has to be corrected for the parabolic variation of the transverse shear stress, as

$$(A_{44},A_{45},A_{55}) = \sum_{k=1}^{L} \int_{\zeta_{k-1}}^{\zeta_k} (k_1^2 Q_{44}^{(k)},\ k_1 k_2 Q_{45}^{(k)},k_2^2 Q_{55}^{(k)})d\zeta \tag{11}$$

where k are the shear correction factor.

A typical finite element is a doubly-curved shell element whose projection is an isoparametric rectangular element. Over the typical shell $\Omega^{(e)}$, the displacements $(u_1,u_2,u_3,\phi_1,\phi_2)$ are interpolated by expressions of the form,

$$\begin{aligned} u_i &= \sum_{j=1}^{N} u_i^j \psi_j(x_1,x_2) \quad , \quad i = 1,2,3 \\ \phi_i &= \sum_{j=1}^{N} \phi_i^j \psi_j(x_1,x_2) \quad , \quad i = 1,2 \end{aligned} \tag{12}$$

where ψ_j are the interpolation functions, and u_i^j and ϕ_i^j are the nodal

values of u_i and ϕ_i, respectively. For a nine node quadratic element the element stiffness matrix is of order 45x45.

Substitution of equation (12) into the virtual work principle, Eq. (7b) yields an element equation of the form

$$[K]\{\Delta\} = \{F\} \tag{13}$$

where $\{\Delta\} = \{\{u_1\}, \{u_2\}, \{u_3\}, \{\phi_1\}, \{\phi_2\}\}^T$, $[K]$ is the element stiffness and $\{F\}$ is the force vector. In the interest of brevity, the coefficients of stiffness matrices are included in Appendix II.

It should be noted that the underscored coefficients in Eq. (10) are also redefined like the shear coefficients in Eq. (11) and reduced integration is performed for the terms arising in the element stiffness matrices due to the presence of these coefficients to avoid the so-called locking effect.

NUMERICAL RESULTS

The Parameters of Anisotropy

When considering the modeling of a material system, one must always survey the availability of material property data. In the present theory, to describe fully the state of anisotropy, the six independent yield stresses in Hill's criteria are needed to be known from uniaxial tests. For numerical results, two typical composite materials namely, boron/epoxy and graphite/epoxy are considered with the following material constants:

Boron/Epoxy

$$E_1 = 30.0 \times 10^6 \text{ psi} \quad , \quad E_2 = 3.2 \times 10^6 \text{ psi}$$

$$G_{12} = 1.05 \times 10^6 \text{ psi} \quad , \quad \nu_{12} = 0.21 \quad , \quad G_{23} = G_{13} = G_{12}$$

$$X = 195 \times 10^3 \text{psi} \quad ; \quad Y = Z = 12.5 \times 10^3 \text{ psi}$$

$$R = S = T = 18.0 \times 10^3 \text{ psi}$$

Graphite/Epoxy

$$E_1 = 18.88 \times 10^6 \text{ psi} \quad ; \quad E_2 = 1.376 \times 10^6 \text{ psi}$$

$$G_{12} = 0.688 \times 10^6 \text{ psi} \quad ; \quad \nu_{12} = 0.343 \quad ; \quad G_{23} = G_{13} = G_{12}$$

$$X = 222.7 \times 10^3 \text{ psi} \quad ; \quad Y = Z = 6.35 \times 10^3 \text{ psi}$$

$$R = S = T = 9.92 \times 10^3 \text{ psi}$$

Solution Procedure

The solution of the elastic plastic problem is reached by an incremental and iterative procedure. The direct iteration technique is followed in the present analysis.

For each load increment, the system of equations are established by assemblying the element matrices and the displacement $\{\Delta\}$ is obtained from Eq.(13). Consequently, the state of stress and the value of $f(\sigma_{ij})$ are calculated for each element. If $f < 0$, then the process is elastic and the material matrix is obtained from equation (5). If $f > 0$, then the total stresses are readjusted so as to make $f \approx 0$ and the elastic-plastic matrix is calculated from Eq. (6). Once the convergence is achieved, the next load increment is applied and the iteration procedure is repeated.

If the application of a small load increment causes very large deflection, the calculation is stopped and the limit load is considered to be found.

Sample Problems

The present elastic-perfectly plastic formulation is applied to a variety of bending problems using 2x2 mesh of a nine noded quadratic element. The shear correction factors $k_1^2 = k_2^2$ were taken to be 5/6.

All computations were made using an IBM 3081 processor with double precision arithmetic.

The results of the sample problems are presented and compared, if possible, with the existing solutions to evaluate the present formulation.

1. Cylindrical Shell Roof A cylindrical shell subjected to uniform vertical loading is considered. Due to symmetry, only a quadrant of the shell was analyzed. The geometry and modeling of the shell roof are shown in Fig. 1. The material behaviour is studied with the properties:

$$E_1 = E_2 = 2.1 \times 10^4 \text{ MN/m}^2 \quad ; \quad \nu = 0.0;$$

$$G_{12} = 1.05 \times 10^4 \text{ MN/m}^2 \quad ; \quad G_{23} = G_{13} = G_{12}$$

$$X = Y = Z = 4.1 \text{ Mn/m}^2 \quad ; \quad R = S = T = 2.367 \text{ MN/m}^2$$

The results obtained for the vertical displacement at the central point of the free edge A versus loading was shown in Fig. 1. The solution obtained compares well with those reported in Ref. [6]. The apparent discrepancy can possibly be due to a different boundary condition on the curved edges and the type of material model used.

2. Simply-Supported Square Plate A uniformly loaded simply supported square plate was studied in the second example. The geometry of the plate is shown in Fig. 2. The following material properties were considered:

$$E_1 = E_2 = 10 \times 10^6 \text{ psi} \quad ; \quad \nu = 0.3$$

$$G_{12} = 3.846 \times 10^6 \text{ psi} \quad ; \quad G_{23} = G_{13} = G_{12}$$

$$X = Y = Z = 144{,}000 \text{ psi} \quad ; \quad R = S = T = 83{,}138.4 \text{ psi}$$

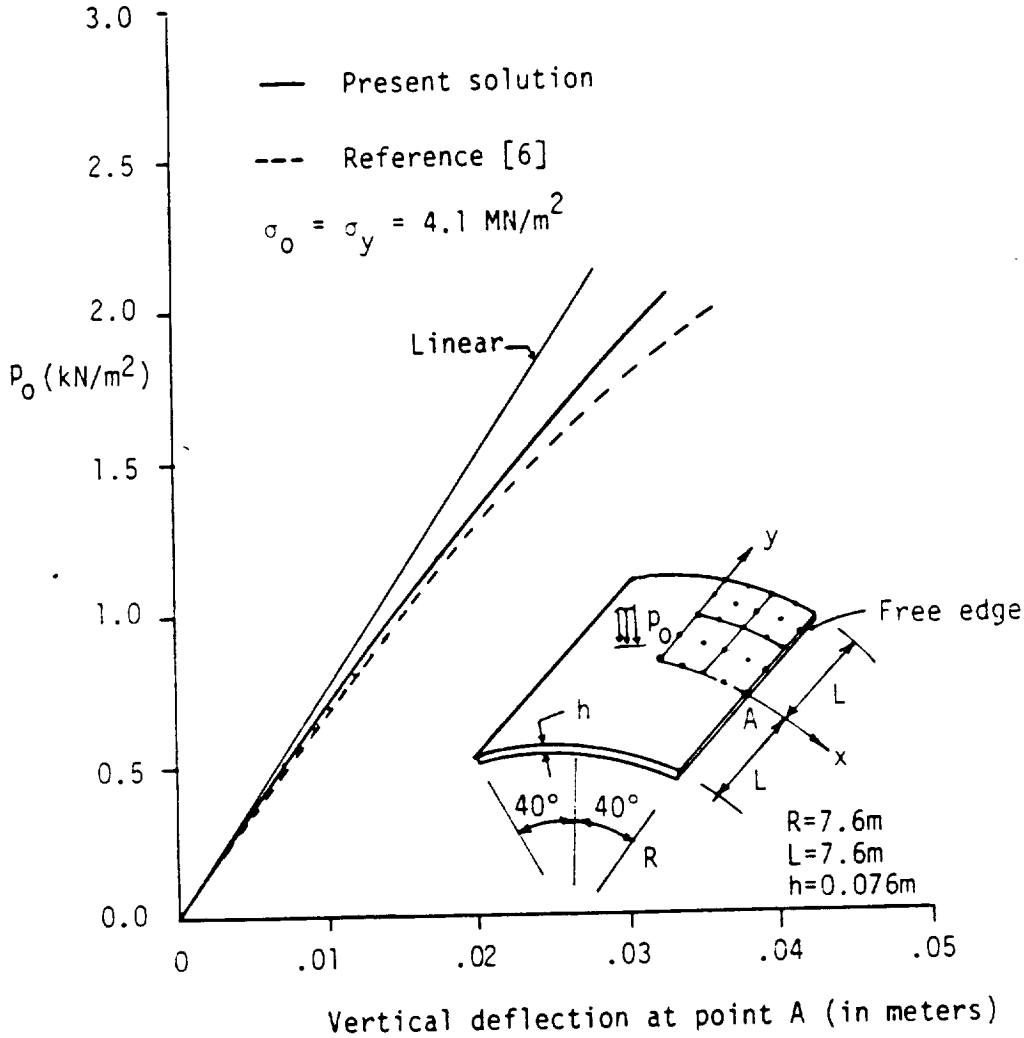

Figure 1. Load-deflection curves for a cylindrical panel under uniform transverse load

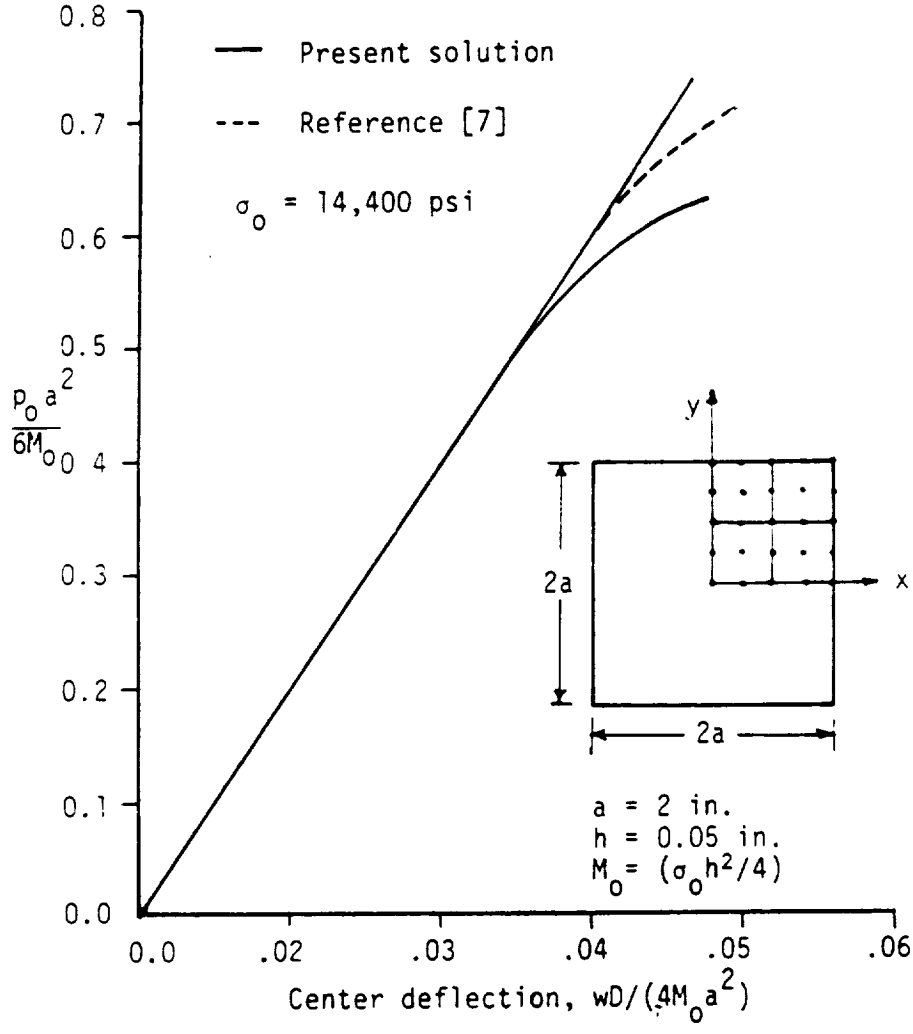

Figure 2. Load-deflection curves for a simply-supported square plate under uniform transverse load

A non-dimensionalized plot of the centre displacement of the plate versus the load are shown in Fig. 2. The results are compared with those presented in Ref. [7].

3. Two Layer Cross-Ply [0/90] and Angle-Ply [-45/45] Simply Supported Spherical Shells Figure 3 contains the results for the cross-ply shell made of two typical materials, namely, boron/epoxy and graphite/epoxy under uniform load. For a given load, the shell made of graphite/epoxy deflects more than the shell made of boron/epoxy which is stiffer, but experiences small degree of nonlinearity.

Figure 4 shows nonlinearity exhibited by the graphite/epoxy cross-ply and angle-ply shells under uniform load. Clearly, the angle-ply shows greater displacement and also nonlinearity than the cross-ply for the same load.

Figure 5 shows the material behaviour for the boron/epoxy cross-ply shell under concentrated load.

4. Clamped Cylindrical Cross-Ply (0/90) Shell Under Uniform Load The geometry of the shell is shown in Fig. 6. The shell is made of grpahite/epoxy and the plot of displacement versus load are shown in Fig. 6.

CONCLUSIONS

A finite element model based on Sander's shell theory, accounting for the transverse shear strains is used for the elastic-plastic analysis of lamianted composite shells. The parameters of anisotropy reflect the plastic material response by correcting the stress components in the Hill's yield function. Numerical results are presented for isotropic and laminated shell of cylindrical and spherical geometry to demonstrate the validity and efficiency of the present

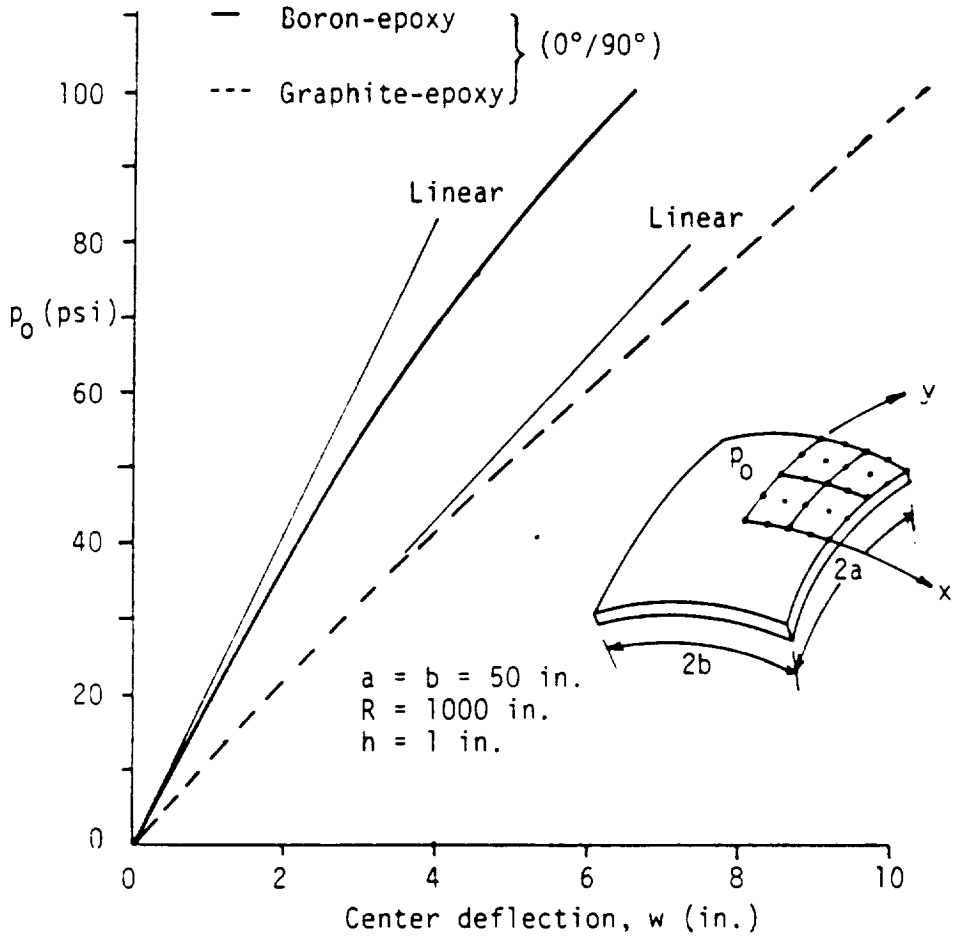

Figure 3. Load-deflection curves for a simply supported spherical shell under uniform transverse load

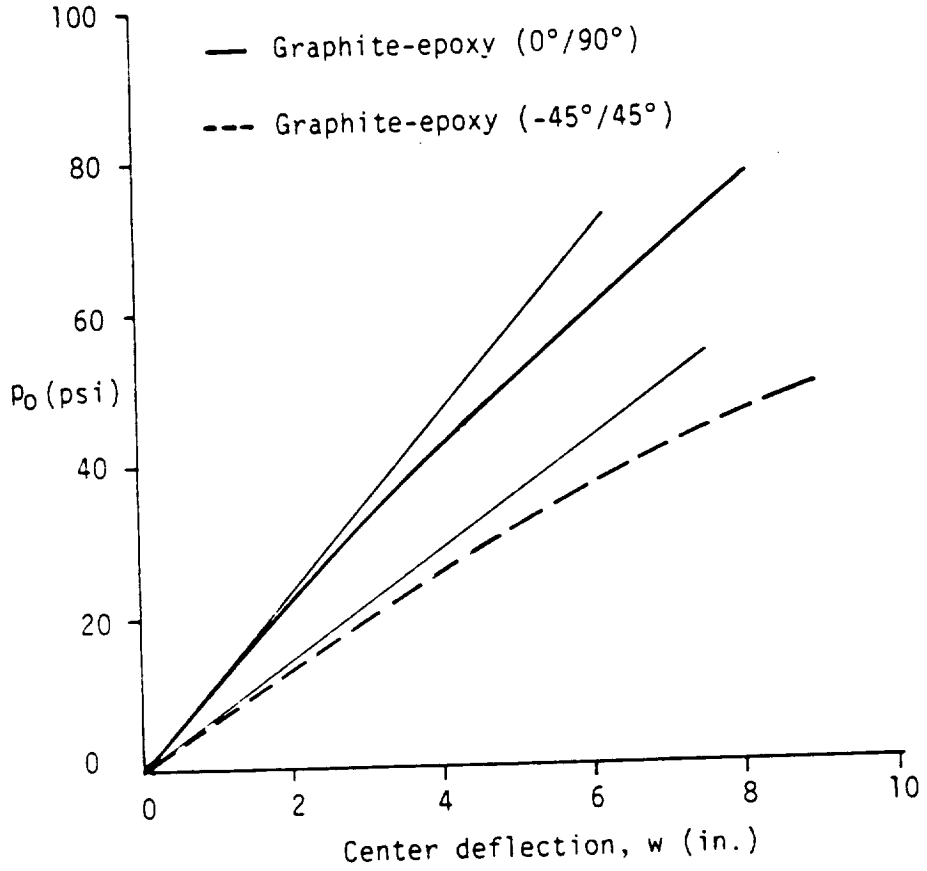

Figure 4. Load-deflection curves for a simply supported spherical shell (see Figure 3 for the geometry)

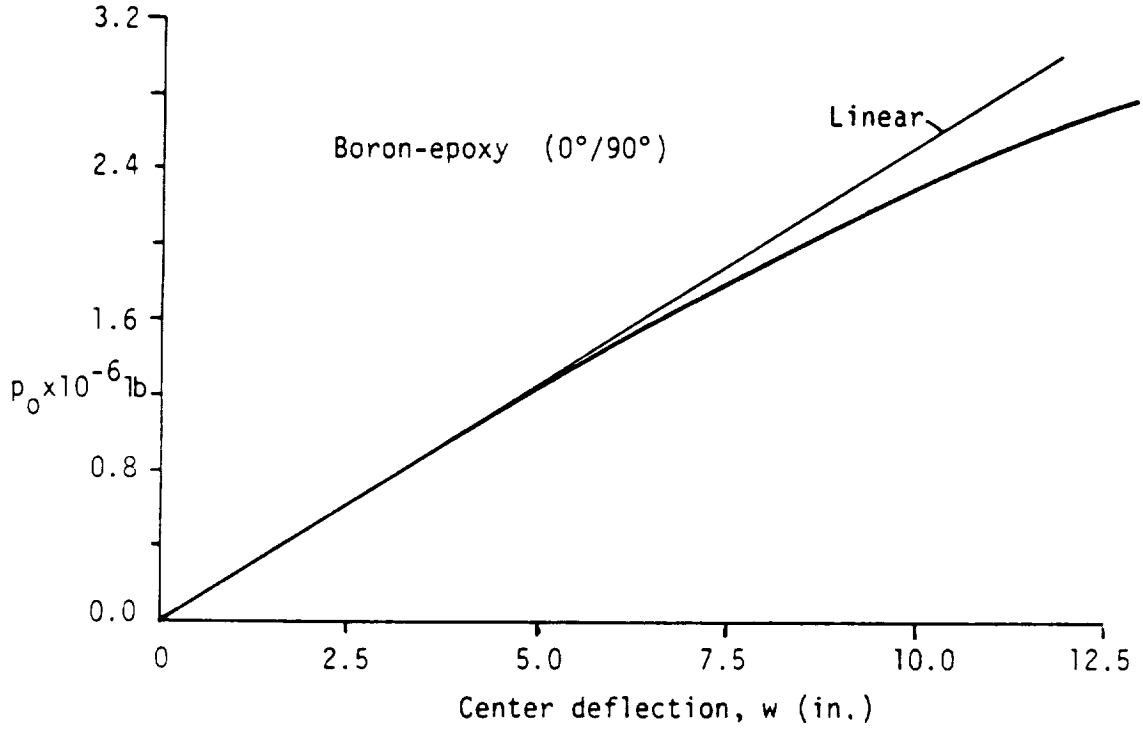

Figure 5. Load-deflection curves for a simply supported spherical shell under point load at the center (see Figure 3 for the geometry)

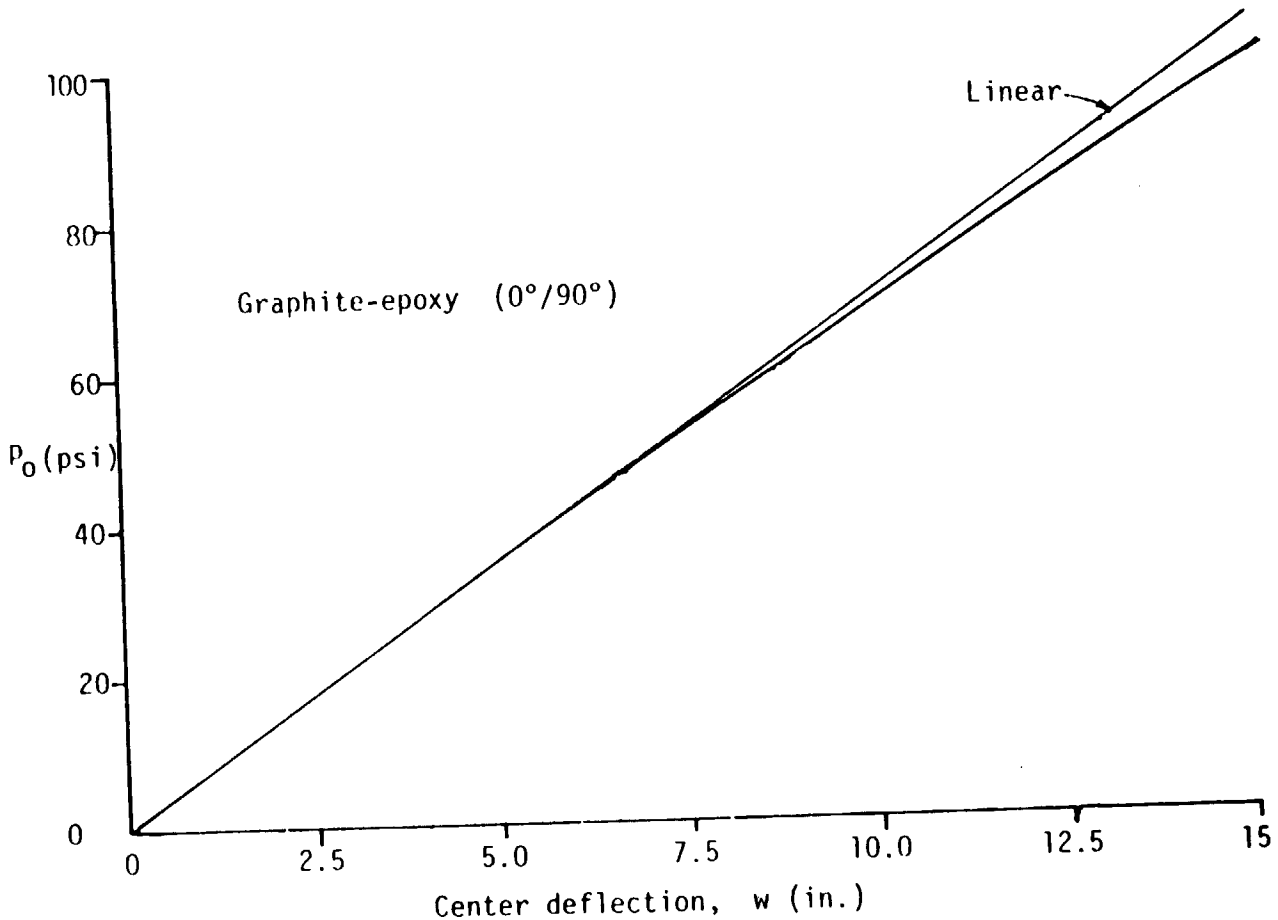

Figure 6. Load-deflection curve for a clamped cylindrical shell (see Figure 1 for the geometry with L = 50 in., R = 1000 in., and h = 1 in.) under uniform transverse load.

approach. For the isotropic case, the present results are in good agreement with those available in the literature.

REFERENCES

1. R. Hill, "A theory of yielding and plastic flow of anisotropic metals," Proc. Roy. Soc. Lond, Ser A193, 1948.

2. A. Mendelson, Plasticity: Theory and Application, The MacMillan Company, New York, 1968.

3. G. C. Nayak and O. C. Zienkiewicz, "Elastic-plastic stress analysis-a generalization for various constitutive relations, including strain softening," Int. J. Num. Meth. Engng. 5, 113-135 1972.

4. J. N . Reddy, Energy and Variational Methods in Applied Mechanics, John Wiley, New York, 1984.

5. J. N. Reddy, "Bending of laminated anisotropic shells by a shear deformable finite element," Fiber Science and Technology 17, pp. 9-24, 1982.

6. J. Backlund and H. Wennerstrom, "Finite element analysis of elastic-plastic shells," Int. J. Num. Meth. Engng. 8, pp. 415-424, 1974.

7. H. Armen, A. Pifko and H. S. Levine, "Finite element analysis of structures in the plastic range, NASA contractor report, CR-1649, 1971.

APPENDIX I

Transformation of the stress-strain matrix in Equation (6)

Let the elastic matrix in the material axes (1,2) be $[D^{ep}]_{12}$ and in the body axes be $[D^{ep}]_{xy}$

$$[D^{ep}]_{12} = [C] = \begin{bmatrix} C_{11} & C_{12} & C_{13} & C_{14} & C_{15} \\ & C_{22} & C_{23} & C_{24} & C_{25} \\ & & C_{33} & C_{34} & C_{35} \\ & \text{sym} & & C_{44} & C_{45} \\ & & & & C_{55} \end{bmatrix}$$

$$[D^{ep}]_{xy} = [Q] = \begin{bmatrix} Q_{11} & Q_{12} & Q_{13} & Q_{14} & Q_{15} \\ & Q_{22} & Q_{23} & Q_{24} & Q_{25} \\ & & Q_{33} & Q_{34} & Q_{35} \\ & \text{sym} & & Q_{44} & Q_{45} \\ & & & & Q_{55} \end{bmatrix}$$

then the transformation [4] is given as, (with $m = \cos\theta$, $n = \sin\theta$)

$$Q_{11} = m^4C_{11} + 2m^2n^2(C_{12} + 2C_{33}) - 4mn(m^2C_{13} + n^2C_{23}) + n^4C_{22}$$

$$Q_{12} = m^2n^2(C_{11} + C_{22} - 4C_{33}) + 2mn(m^2 - n^2)(C_{13} - C_{23}) + (m^4 + n^4)C_{12}$$

$$Q_{13} = m^2(m^2 - 3n^2)C_{13} + mn[m^2C_{11} - n^2C_{22} - (m^2 - n^2)(C_{12} + 2C_{66})] + n^2(m^2 - n^2)C_{26}$$

$$Q_{14} = m^3C_{14} - mn[(2C_{34} - C_{15})m - (C_{24} - 2C_{35})n] + C_{25}n^3$$

$$Q_{15} = m^3C_{15} - mn[(C_{14} + 2C_{35})m - (C_{25} + 2C_{34})n] - C_{24}n^3$$

$$Q_{22} = n^4C_{11} + 2m^2n^2(C_{12} + 2C_{33}) + 4mn(m^2C_{23} + n^2C_{13}) + m^4C_{22}$$

$$Q_{23} = \underline{m^2(m^2 - 3n^2)C_{23}} + mn[n^2C_{11} - m^2C_{22} + (m^2 - n^2)(C_{12} + 2C_{33})]$$
$$+ \underline{n^2(3m^2 - n^2)C_{13}}$$

$$Q_{24} = \underline{m^3C_{24} + mn[(C_{25} + 2C_{34})m + (C_{14} + 2C_{35})n] + C_{15}n^3}$$

$$Q_{25} = \underline{m^3C_{25} - mn[(C_{24} - 2C_{35})m - (C_{15} - 2C_{34})n] - C_{14}n^3}$$

$$Q_{33} = m^2n^2(C_{11} + C_{22} - 2C_{12}) - 2mn(m^2 - n^2)(C_{22} - C_{33}) + (m^2 - n^2)^2C_{33}$$

$$Q_{34} = \underline{(mC_{34} + nC_{35})(m^2 - n^2) + m^2n(C_{14} - C_{24}) + mn^2(C_{15} - C_{25})}$$

$$Q_{35} = \underline{(mC_{35} - nC_{34})(m^2 - n^2) + m^2n(C_{15} - C_{25}) + mn^2(C_{24} - C_{14})}$$

$$Q_{44} = m^2C_{44} + \underline{2mnC_{45}} + n^2C_{55}$$

$$Q_{45} = \underline{(m^2 - n^2)C_{45}} - mn(C_{44} - C_{55})$$

$$Q_{55} = m^2C_{55} - \underline{2mnC_{45}} + n^2C_{44}$$

The underscored terms are due to material nonlinearity for an orthotropic material. Also note that the constitutive matrix is no longer orthotropic.

APPENDIX II

Stiffness Coefficients

$$[K^{11}] = A_{11}[S^{11}] + A_{16}([S^{12}] + [S^{21}]) + A_{66}[S^{22}]$$
$$+ C_o(B_{16}[S^{12}] + [S^{21}]) + 2B_{66}[S^{22}] + C_iD_{66}[S^{22}]) + \frac{A_{55}}{R_1^2}[S^{00}]$$
$$- \frac{1}{R_1}(A_{15}([S^{10}]+[S^{01}])+A_{56}([S^{20}]+[S^{02}])-C_oB_{56}([S^{20}]+[S^{02}])$$

$$[K^{12}] = A_{12}[S^{12}] + A_{16}[S^{11}] + A_{26}[S^{22}] + A_{66}[S^{21}]$$
$$+ C_o(B_{26}[S^{22}] - B_{16}[S^{11}] - C_oD_{66}[S^{21}]) + \frac{A_{45}}{R_1R_2}[S^{00}]$$
$$- \frac{1}{R_2}(A_{14}[S^{10}] + A_{46}[S^{20}] + C_oB_{46}[S^{20}])$$
$$- \frac{1}{R_1}(A_{25}[S^{02}] + A_{56}[S^{01}] - C_oB_{56}[S^{01}])$$

$$[K^{13}] = \frac{1}{R_1}(A_{11}[S^{10}] + A_{16}[S^{20}]) + \frac{1}{R_2}(A_{12}[S^{10}] + A_{26}[S^{20}]) +$$
$$C_o(\frac{B_{16}}{R_1}[S^{20}] + \frac{B_{26}}{R_2}[S^{20}] - \frac{1}{R_1}(A_{45}[S^{02}] + A_{55}[S^{01}])$$
$$+ A_{14}[S^{12}] + A_{15}([S^{11}] - \frac{[S^{00}]}{R_1^2}) + A_{46}[S^{22}]$$
$$+ A_{56}[S^{21}] + C_o[B_{46}[S^{22}] + B_{56}[S^{21}]) - A_{25}\frac{[S^{00}]}{R_1R_2}$$

$$[K^{14}] = B_{11}[S^{11}] + B_{16}([S^{12}] + [S^{21}]) + B_{66}[S^{22}] +$$
$$C_o(D_{16}[S^{21}] + D_{66}[S^{22}]) - \frac{1}{R_1}A_{55}[S^{00}]$$
$$+ A_{15}[S^{10}] + A_{56}[S^{20}] - \frac{1}{R_1}(B_{15}[S^{01}] + B_{56}[S^{02}])$$
$$+ C_oB_{56}[S^{20}]$$

C-2

$$[K^{15}] = B_{12}[S^{12}] + B_{16}[S^{11}] + B_{26}[S^{22}] + B_{66}[S^{21}]$$
$$+ C_o(D_{26}[S^{22}] + D_{66}[S^{21}]) - \frac{1}{R_1} A_{45}[S^{oo}]$$
$$+ A_{14}[S^{10}] + A_{46}[S^{20}] - \frac{1}{R_1} (B_{25}[S^{02}] + B_{56}[S^{01}])$$
$$+ C_oB_{46}[S^{20}]$$

$$[K^{21}] = [K^{12}]^T$$

$$[K^{22}] = A_{22}[S^{22}] + A_{26}([S^{12}] + [S^{21}]) + A_{66}[S^{11}] - 2C_oB_{66}[S^{11}]$$
$$- C_o(B_{26}([S^{12}] + [S^{21}]) - C_oD_{66}[S^{11}]) - \frac{A_{44}}{R_2^2} [S^{oo}]$$
$$- \frac{1}{R_2} (A_{24}([S^{20}] + [S^{02}]) + A_{46}([S^{10}] + [S^{01}] + C_o[S^{10}])$$
$$- C_oB_{46}[S^{10}])$$

$$[K^{23}] = \frac{1}{R_1} (A_{12}[S^{20}] + A_{16}[S^{10}]) + \frac{1}{R_2} (A_{22}[S^{20}] + A_{26}[S^{10}])$$
$$-C_o(\frac{B_{16}}{R_1} + \frac{B_{26}}{R_2}) [S^{10}] - \frac{1}{R_2} (A_{44}[S^{02}] + A_{45}[S^{01}])$$
$$+ A_{24}([S^{22}] - \frac{1}{R_2^2} [S^{oo}]) + A_{25}[S^{21}] + A_{46}[S^{12}]$$
$$+ A_{56}[S^{11}] - \frac{A_{14}}{R_1R_2} [S^{oo}] - C_oB_{46}[S^{12}] - C_oB_{56}[S^{11}]$$

$$[K^{24}] = B_{12}[S^{21}] + B_{26}[S^{22}] + B_{16}[S^{11}] + B_{66}[S^{12}]$$
$$- C_o(D_{16}[S^{11}] + D_{66}[S^{12}]) - \frac{1}{R_2} A_{45}[S^{oo}]$$
$$+ A_{25}[S^{20}] + A_{56}[S^{10}] - \frac{1}{R_2} (B_{14}[S^{01}] + B_{46}[S^{02}])$$

$$- C_o B_{56}[S^{10}]$$

$$[K^{25}] = B_{22}[S^{22}] + B_{26}([S^{21}] + [S^{12}]) + B_{66}[S^{11}]$$
$$- C_o(D_{26}[S^{12}] + D_{66}[S^{11}]) - \frac{1}{R_2} A_{44}[S^{00}]$$
$$+ A_{24}[S^{20}] + A_{46}[S^{10}] - \frac{1}{R_2}(B_{24}[S^{02}] + B_{46}[S^{01}])$$
$$- C_o B_{46}[S^{10}]$$

$$[K^{31}] = [K^{13}]^T$$

$$[K^{32}] = [K^{23}]^T$$

$$[K^{33}] = A_{45}[S^{12}] + A_{55}[S^{11}] + A_{44}[S^{22}] + A_{45}[S^{21}]$$
$$+ [S^{00}]\left(\frac{1}{R_1}\left(\frac{A_{11}}{R_1} + \frac{A_{12}}{R_2}\right) + \frac{1}{R_2}\left(\frac{A_{12}}{R_1} + \frac{A_{22}}{R_2}\right)\right)$$
$$+ \frac{A_{14}}{R_1}([S^{02}] + [S^{20}]) + \frac{A_{15}}{R_1}([S^{01}] + [S^{10}])$$
$$+ \frac{A_{24}}{R_2}([S^{02}] + [S^{20}]) + \frac{A_{25}}{R_2}([S^{01}] + [S^{10}])$$
$$+ \frac{A_{24}}{R_2}([S^{02}] + [S^{20}]) + \frac{A_{25}}{R_2}([S^{01}] + [S^{10}])$$

$$[K^{34}] = A_{55}[S^{10}] + A_{45}[S^{20}]$$
$$+ \left(\frac{B_{11}}{R_1} + \frac{B_{12}}{R_2}\right)[S^{01}] + \left(\frac{B_{16}}{R_1} + \frac{B_{26}}{R_2}\right)[S^{02}]$$
$$+ \left(\frac{A_{15}}{R_1} + \frac{A_{25}}{R_2}\right)[S^{00}] + B_{14}[S^{21}] + B_{46}[S^{22}]$$
$$+ B_{15}[S^{11}] + B_{56}[S^{12}]$$

$$[K^{35}] = A_{45}[S^{10}] + A_{44}[S^{20}]$$
$$+ (\frac{B_{16}}{R_1} + \frac{B_{26}}{R_2})[S^{01}] + (\frac{B_{12}}{R_1} + \frac{B_{22}}{R_2})[S^{02}]$$
$$+ (\frac{A_{14}}{R_1} + \frac{A_{24}}{R_2})[S^{00}] + B_{24}[S^{22}] + B_{46}[S^{21}]$$
$$+ B_{25}[S^{12}] + B_{56}[S^{11}]$$

$$[K^{41}] = [K^{14}]^T$$

$$[K^{42}] = [K^{24}]^T$$

$$[K^{43}] = [K^{34}]^T$$

$$[K^{44}] = D_{11}[S^{11}] + D_{16}([S^{12}] + [S^{21}]) + D_{66}[S^{22}] + A_{55}[S^{00}]$$
$$+ B_{15}([S^{10}] + [S^{01}]) + B_{56}([S^{20}] + [S^{02}])$$

$$[K^{45}] = D_{12}[S^{12}] + D_{16}[S^{11}] + D_{26}[S^{22}] + D_{66}[S^{21}] + A_{45}[S^{00}]$$
$$+ B_{14}[S^{10}] + B_{46}[S^{20}] + B_{25}[S^{02}] + B_{56}[S^{01}]$$

$$[K^{51}] = [K^{15}]^T$$

$$[K^{52}] = [K^{25}]^T$$

$$[K^{53}] = [K^{35}]^T$$

$$[K^{54}] = [K^{45}]^T$$

$$[K^{55}] = D_{22}[S^{22}] + D_{26}([S^{12}] + [S^{21}]) + D_{66}[S^{11}] + A_{44}[S^{00}]$$
$$+ B_{24}([S^{20}] + [S^{02}]) + B_{46}([S^{10}] + [S^{01}])$$

where

$$S_{ij}^{\alpha\beta} = \int_{\Omega^e} \frac{\partial \psi_i}{\partial x_\alpha} \frac{\partial \psi_j}{\partial x_\beta} \, dx_1 dx_2 \quad , \quad S_{ij}^{oo} = \int_{\Omega^e} \psi_i \psi_j dx_1 dx_2$$

and the underscored terms are due to material nonlinearity.

REPORT DOCUMENTATION PAGE

Form Approved
OMB No. 0704-0188

Public reporting burden for this collection of information is estimated to average 1 hour per response, including the time for reviewing instructions, searching existing data sources, gathering and maintaining the data needed, and completing and reviewing the collection of information. Send comments regarding this burden estimate or any other aspect of this collection of information, including suggestions for reducing this burden, to Washington Headquarters Services, Directorate for information Operations and Reports, 1215 Jefferson Davis Highway, Suite 1204, Arlington, VA 22202-4302, and to the Office of Management and Budget, Paperwork Reduction Project (0704-0188), Washington, DC 20503.

1. AGENCY USE ONLY (*Leave blank*)	2. REPORT DATE	3. REPORT TYPE AND DATES COVERED
	January 1993	Final Contractor Report

4. TITLE AND SUBTITLE
Geometrically Nonlinear Analysis of Laminated Elastic Structures

5. FUNDING NUMBERS
WU-505-63-53
NAG3-208

6. AUTHOR(S)
J.N. Reddy, K. Chandrashekhara, and W.C. Chao

7. PERFORMING ORGANIZATION NAME(S) AND ADDRESS(ES)

8. PERFORMING ORGANIZATION REPORT NUMBER
E-7533

9. SPONSORING/MONITORING AGENCY NAMES(S) AND ADDRESS(ES)
National Aeronautics and Space Administration
Lewis Research Center
Cleveland, Ohio 44135-3191

10. SPONSORING/MONITORING AGENCY REPORT NUMBER
NASA CR-191055

11. SUPPLEMENTARY NOTES
Project Manager, C.C. Chamis, Structures Division, NASA Lewis Research Center, (216) 433-3252.

12a. DISTRIBUTION/AVAILABILITY STATEMENT
Unclassified - Unlimited
Subject Category 24

12b. DISTRIBUTION CODE

13. ABSTRACT (*Maximum 200 words*)

This final technical report contains three parts: Part 1 deals with the 2-D shell theory and its element formulation and applications. Part 2 deals with the 3-D degenerated element. These two parts constitute the two major tasks that were completed under the grant. Another related topic that was initiated during the present investigation is the development of a nonlinear material model. This topic is briefly discussed in Part 3. To make each part self-contained, conclusions and references are included in each part. In the interest of brevity, the discussions presented here are relatively brief. The details and additional topics are described in the references cited.

14. SUBJECT TERMS
Shell theory; 2-D finite elements; 3-D finite element; Nonlinear material

15. NUMBER OF PAGES
100

16. PRICE CODE
A05

17. SECURITY CLASSIFICATION OF REPORT	18. SECURITY CLASSIFICATION OF THIS PAGE	19. SECURITY CLASSIFICATION OF ABSTRACT	20. LIMITATION OF ABSTRACT
Unclassified	Unclassified	Unclassified	

National Aeronautics and
Space Administration

Lewis Research Center
Cleveland, Ohio 44135
Chamis 49-8
Official Business
Penalty for Private Use $300

FOURTH CLASS MAIL

ADDRESS CORRECTION REQUESTED

NASA S&T Information Fac.
Attn: Acquisition Div.
P.O. Box 8757
Baltimore-Washington
Int. Airport, MD 21240

NASA